DESIGN AND DEVELOPMENT OF WIDE BAND PRINTED MONOPOLE ANTENNAS FOR AIRBORNE APPLICATIONS

Thesis submitted to the

COCHIN UNIVERSITY OF SCIENCE AND TECHNOLOGY

in partial fulfilment of the requirements for the degree of

DOCTOR OF PHILOSOPHY

Under the Faculty of Technology

by

MARY RANI ABRAHAM

(Reg. No. 4952)

NAVAL PHYSICAL AND OCEANOGRAPHIC LABORATORY

Defence Research and Development Organisation

Kochi, Kerala, India, 682021

OCTOBER 2018

DESIGN AND DEVELOPMENT OF WIDE BAND PRINTED MONOPOLE ANTENNAS FOR AIRBORNE APPLICATIONS

Ph.D. Thesis under the Faculty of Technology

Author
Mary Rani Abraham
Research Scholar,
Naval Physical and Oceanographic Laboratory,
Defence Research and Development Organisation,
Thrikkakara, Kochi.
Email: maryraniabraham@gmail.com

Supervising Guide
Dr. Sona O. Kundukulam
Scientist 'E'
Naval Physical and Oceanographic Laboratory,
Defence Research and Development Organisation,
Thrikkakara, Kochi.
Email: sonalitto@yahoo.com

Research Center
Naval Physical and Oceanographic Laboratory,
Defence Research and Development Organisation,
Thrikkakara, Kochi.

October 2018

Dedicated to the Almighty,
my family and dear ones

CERTIFICATE

This is to certify that the research work presented in the thesis entitled "DESIGN AND DEVELOPMENT OF WIDE BAND PRINTED MONOPOLE ANTENNAS FOR AIRBORNE APPLICATIONS" is an authentic record of research work carried out by Smt. Mary Rani Abraham, under my supervision and guidance at Naval Physical & Oceanographic Laboratory, Kochi – 21, in partial fulfilment of the requirements for the award of Ph.D. degree of the Cochin University of Science and Technology and no part of it has previously formed the basis for the award of any degree in any university. I further certify that the corrections and modifications suggested by the audience during the pre-synopsis seminar and recommended by the Doctoral Committee of Ms. Mary Rani Abraham are incorporated in the thesis.

Kochi-21   Dr. Sona O. Kundukulam
29th October 2018   (Research Guide)
                                                                        Scientist 'E'
                                       Naval Physical and Oceanographic Laboratory
                                                                          Kochi- 21

DECLARATION

I, hereby, declare that the work presented in the thesis entitled DESIGN AND DEVELOPMENT OF WIDE BAND PRINTED MONOPOLE ANTENNAS FOR AIRBORNE APPLICATIONS is based on the original work done by me under the guidance and supervision of Dr. Sona O. Kundukulam, in Naval Physical and Oceanographic Laboratory, Thrikkakara, Kochi, India and has not been included in any other thesis submitted previously for the award of any other degree.

Cochin- 21   Mary Rani Abraham

29th October 2018

ABSTRACT

Major challenges faced by airborne VHF monopole antennas are to achieve wideband characteristics in permissible antenna height and to find the apt location for mounting, so as to satisfy sufficient ground plane around its feed point. The increased applications of electromagnetic spectrum result in a large number of antennas competing in the limited space available on platform. The deficient ground plane can deteriorate the radiation characteristics of antenna. Printed monopole antennas can overcome this deficiency, as the ground plane of these antennas are implemented in the same plane of that of the radiating element.

Hence, the present work deals with the development and analysis of two novel wideband printed monopole antennas in VHF band for mounting on airborne platforms. The radiation characteristics of these antennas were evaluated for free standing condition and also for mounted on standard ground plane condition. The performance of the presented printed monopole antennas are comparable to the VHF airborne blade monopole antennas operating in the same frequency band with the added advantage of requiring nil ground plane. The thesis also proposes empirical relations to calculate the resonant frequency of the antennas in terms of its geometrical parameters.

Acknowledgements

CONTENTS

1. Introduction

Antennas are indispensable component of any wireless communication device. An antenna is a transducer between the transmitter and the free space waves and vice versa. They efficiently transfer electromagnetic energy from a transmission line into free space.

The history of antenna starts with Hertz when he proved Maxwell's theoretical prediction of electromagnetic waves by the classical experiments in 1880s. Guglielmo Marconi transmitted wireless radio signals across the Atlantic Ocean on December 12, 1901 and is credited as the father and inventor of the radio. Prior to the 1920s, the radio was primarily used to contact ships, which were out at sea. With the First World War, importance of the radio became apparent as it was used for sending and receiving messages to the armed forces. At the end of World War II, antenna theory was mature to a level that made the analysis possible of, many antennas like freestanding dipole, horn and reflector antennas, monopole antennas, slots in waveguides and arrays. Microstrip antennas were developed in 1953, which was then followed by the theoretical and experimental research on microstrip and printed antennas. This lead to the development of many modern antennas, which are the derivative of basic antennas, like inverted F antenna, printed monopole antennas, etc.

Traditional aircraft communications are mainly based on Very High Frequency (VHF) or High Frequency (HF) radio waves for signal interception, direction finding, navigation, terrestrial communication, etc. [1]. Monopole antennas are the commonly used antennas in airborne systems for these applications [2].

1.1. AN OVERVIEW ON MONOPOLE ANTENNAS

Monopole antennas is a class of linear wire antennas, that consists of a conducting rod or wire mounted perpendicularly on infinite perfect conducting sheet called ground plane.

A monopole antenna is one-half of a corresponding double-length center-fed linear dipole antenna [3]. The ground structure serves as the other $\lambda/4$ half of the

antenna (Fig 1.1). If the ground plane is infinitely sized and conductive, the performance of the ground plane is equivalent to a vertically mounted dipole.
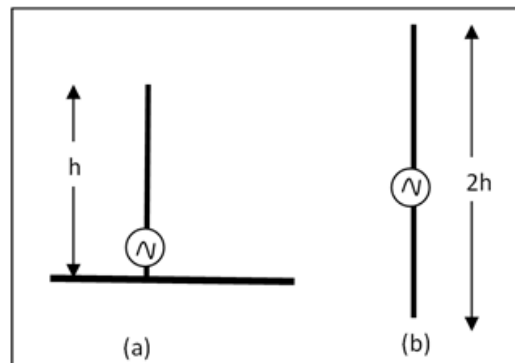
Fig 1.1. (a) Monopole antenna (b) Equivalent dipole antenna.

For the idealized case of a ground plane of infinite extent and of infinite conductivity, the input impedance of a $\lambda/4$ monopole above a ground plane is one half that of an isolated $\lambda/2$ dipole. Thus referred to the current maximum, the input impedance of the monopole Z_{im} is $(36.5 + j21.25 \ \Omega)$. The reason for this is that only half the voltage is required to drive a monopole antenna to the same current as a dipole ($Z_{im} = V/I$).

Together with the image, the monopole antenna appears to be a center-fed dipole for the upper half-space. There is negligible penetration of fields into the high conductivity ground for a monopole antenna, and all that radiation is directed into the upper half-space creating a power density that is twice as high as that for a dipole radiating the same amount of power. This makes the directivity or gain of the monopole antenna twice than that for the double-length dipole. Fig 1.2 shows the radiation pattern of a quarter wave monopole antenna.
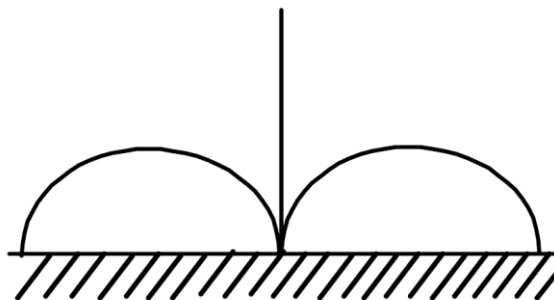
Fig 1.2. Radiation pattern of quarter wave monopole antenna.

The drawback of monopole antennas is their narrow bandwidth. The impedance bandwidth of a wire monopole antenna can be improved by increasing its diameter. Such antennas, where the wire element is replaced by flat square plate or circular disc, are called planar monopole antennas (Fig 1.3). The reason for wide bandwidth of these antennas with broadening the arms of monopole is the nature of current distribution which no longer remains sinusoidal. The modified current distribution does not alter the radiation pattern of the antenna appreciably but it significantly effects the input impedance [4]. The radiation pattern of these antennas is omnidirectional. The planar monopole antennas whose shape has been modified for aerodynamic purpose are called blade monopole antennas. Broadband blade monopole antennas are the commonly used antennas in airborne systems for signal interception, direction finding and monitoring applications [2].
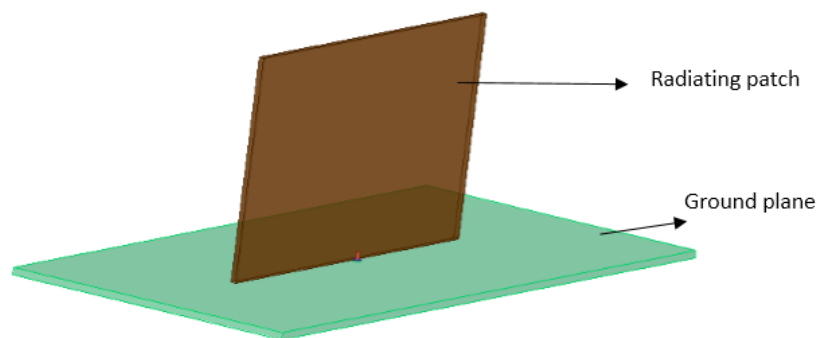
Fig 1.3. Planar monopole antenna.

1.2. APPLICATIONS OF MONOPOLE ANTENNAS

Monopole antennas are widely used in cellular communication, UWB applications, wireless LAN, software defined radio and reconfigurable radio network. Planar monopole antennas owing to its simple structure, wide impedance bandwidth and omnidirectional pattern find immense applications in various areas of communication. They are also the most preferred antennas for vehicular and airborne applications.

1.3. MONOPOLE ANTENNAS FOR AIRBORNE APPLICATIONS

Planar monopole antennas are simple with compact size, light weight and are easy to build in aerodynamic shape causing a minimum drag. These antennas possess

wideband characteristics with omnidirectional radiation pattern. Owing to these qualities, they are preferred for airborne applications. The planar monopole antennas whose shape has been modified for aerodynamic purpose are called blade monopole antennas. Broadband blade monopole antennas are the commonly used antennas in airborne systems for signal interception, direction finding and monitoring applications [2].

Electrically, a blade monopole antenna is a $\lambda/4$ length, end-fed antenna with an impedance of 50Ω. The antenna is encased in radome, thus strengthened to protect it from damage from birds, hail or other hazards.

Airborne monopole antennas are usually mounted vertically on the platform. Hence, in this scenario, the length of the monopole antenna can also be denoted as its height.

1.4 LIMITATIONS OF AIRBORNE BLADE MONOPOLE ANTENNAS

The electrical properties of blade monopole antennas depends on both the geometry of the monopole element and the ground plane used. The electrical length of a monopole antenna should be equal to the quarter wavelength at the resonating frequency and the ground plane should spread out at least a quarter wavelength or more, around the feed-point of the antenna.

For HF/VHF applications, the electrical length of monopole antenna extends to a few meters. The height of the antenna for airborne applications needs to be small to ensure minimum air drag. Hence size reduction techniques need to be employed.

Apart from size constraints, these antennas suffer from ground plane limitations also. Airborne monopole antennas utilize the skin of the airborne platform as its ground plane. The task of finding a suitable mounting location on platform is difficult when many systems are competing in limited surface area. The space constraints in the specific mounting location for the monopole antenna on the airborne platform result in an insufficient ground plane for these antennas on platform. This deteriorates radiation performance of antenna [5-6]. The asymmetries and curved surfaces on the platform as well as the limited size of the available ground plane influence the performance of monopole antenna significantly [7].

Also, nowadays, the skin of the airborne platform is made up of a mixture of composite materials whose conductivity may not be fairly good. Composite materials are used for aircraft skin owing to their weight savings over aluminium parts with high strength and corrosion resistance. Just as a non-infinite ground plane can affect the antenna performance, ground planes with non-infinite conductivity can move antenna operation away from ideal behavior. Hence reduced ground plane monopole antennas are a requirement for airborne applications.

1.5. PRINTED MONOPOLE ANTENNAS

Printed monopole antennas are microstrip antennas where the radiating patch and the ground plane are etched either on the same side of substrate or on opposite sides of substrate, depending on the feeding method chosen. This type of antenna was first presented in 1997. The term printed refers to the printed circuit technology used in the fabrication of these antennas. Almost all printed antennas are developed based on microstrip configuration or its modifications.

Fig 1.3 shows the printed monopole antenna configuration in which the patch is excited via 50Ω microstrip line. Both the patch and microstrip line are lying on one side of the substrate and the ground plane on the other side.
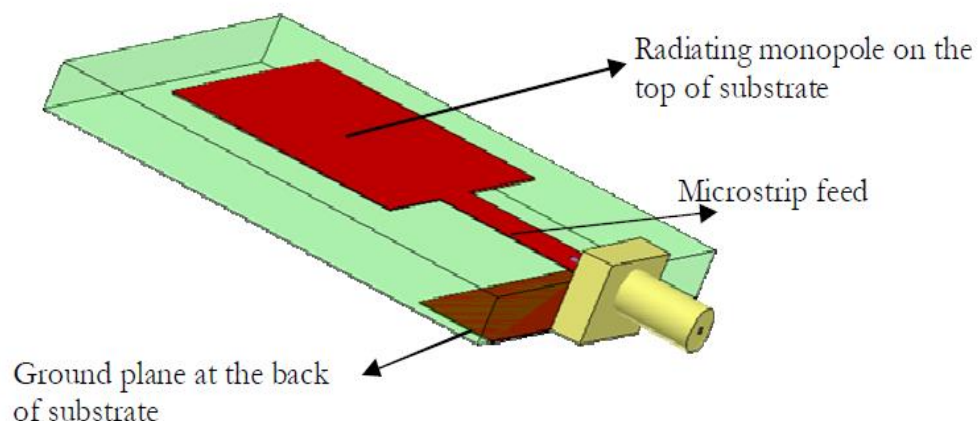
Fig 1.3. A printed rectangular monopole antenna

A printed monopole antenna can be considered as an asymmetrically driven dipole antenna, in which the radiating patch form one arm of the dipole and the

ground plane form the other arm [8]. It can be further realized as combination of two grounded monopole antennas one monopole is the radiating patch and the other is the ground plane. The radiation field of printed monopole antennas, is found by considering the contribution of both the patch and the ground plane.

Radiating patch of printed monopole antennas can be of any shape. Substrate is of low loss dielectric material to enhance the radiation performance. Commonly used dielectric materials are FR4, RT Duroid, Alumina etc.

The practical advantages of printed monopole antenna is the flat structure, the radiating monopole element is in the same plane as that of the ground plane. The other advantages of printed monopole antennas are low profile, conformal configuration, omni directional radiation coverage, wide bandwidth and simple design.

The other characteristics like low profile, conformable to planar and non-planar surfaces, simple, and inexpensive to manufacture using printed circuit technology, mechanically robust when mounted on rigid surfaces, compatible with MMIC designs make it suitable for aircraft, spacecraft, satellite and missile applications and for commercial applications like mobile and wireless applications.

1.6. MOTIVATION OF THE PRESENT WORK: THESIS OBJECTIVE

Although blade monopole antennas are good candidate for airborne application, the requirement of large ground plane on platform may results in deteriorated radiation characteristics in space constrained situations. Some reduced ground plane monopole antennas has been reported in the literature that achieve this characteristics by altering the ground plane geometry. Since the skin of the platform acts as ground plane for airborne antennas, alteration in the ground plane geometry is impracticable.

Here comes the advantage of printed monopole antennas as these antennas does not require a backing ground plane. The ground plane are etched either on the same side of substrate or on opposite sides of substrate, depending on the feeding method chosen.

Several configurations of printed monopole antennas have been reported for wireless communications in L-S-C-X bands but, only very few configuration of these antennas has been reported for VHF/UHF band. Printed monopole antennas incorporating wide bandwidth and size miniaturization concurrently have not been reported in the VHF band. Hence, the main aim of the research presented in this thesis is to design and develop wideband printed monopole antennas operating in VHF band, those require minimum mounting ground plane, for airborne applications.

During the period of work, two wideband printed VHF monopole antennas were developed for ground plane constrained airborne applications. The first antenna discussed is a bifolded printed bent monopole antenna with L shaped ground plane. The second antenna is a RL loaded meandered top loaded printed monopole antenna which incorporates meandering and top loading on the radiating patch as well as on ground plane for achieving the compactness. The theoretical investigations are carried out on theses antennas. The empirical relations are developed for predicting the resonant frequency easily.

1.7 REVIEW OF LITERATURE

Literature study was carried out mainly in following categories –

1. A brief survey of monopole antennas.

2. The effect of ground plane on the performance of monopole antennas.

3. Survey of printed monopole antennas.

Later, in this section, the literature referred in designing the printed monopole antennas proposed in this thesis are also described.

1.7.1. A brief survey of monopole antennas

1.7.1.1 Monopole antennas

The monopole antenna was invented in 1895 by Gugleimo Marconi during his first experiments in radio communication. He began by using Hertzian dipole antennas consisting of two identical horizontal wires ending in metal plates. He then

proved experimentally that a longer distance transmission is possible by grounding one end of this transmitter wire [9].

For low frequency (LF), High Frequency (HF) applications like radio broadcasting, the variants of monopole antenna -T antenna and Umbrella antenna are implemented by using the actual earth as ground plane. But for VHF and UHF frequencies, the size of the ground plane needed is smaller when compared to LF/HF antennas. Hence, artificial ground planes, which is a conducting sheet of radius greater than λ/4 were used as ground plane.

The most common type of monopole antenna used at VHF/UHF frequencies is quarter-wave whip antenna with a conductive ground plane placed perpendicularly at its base. Whip antenna is a narrowband antenna with height equal to λ/4. Several investigations were carried out on the size and shape of monopole antennas to reduce its resonant length and also to increase the bandwidth. These include loading of monopole antenna (base loading, top loading), making the monopole radiator in planar shape etc.

Disk loaded and plate loaded (top hat) monopole antennas has been reported in 1949 as a measure to reduce the resonant length [10]. Monopole antenna with helical top loading has been demonstrated in 1961 [11] and with umbrella top loading in 1965 for achieving compactness and wide bandwidth [12]. A top loaded monopole antenna using peano curves was reported by John McVay et.al in 2007 [13].

Monopole antenna with inductive loading at the base and also in series with the antenna conductor has been reported in 1963 [14]. The use of high permittivity substrate resonator material as monopole for antenna height reduction was reported in 1993 [15]. A magneto-dielectric material of high permittivity and high permeability has been demonstrated as a loading element on a standard quarter wavelength monopole antenna to achieve reduction in the resonant frequency in 2016 [16].

The bandwidth of thin wire monopole can be increased by increasing the diameter of wire. This thick wire can be replaced by a planar element. Monopole antennas with planar radiating elements were first outlined by Meinke and Gundlach in 1968 who described them as a variant of cylindrical and conical monopole [17-18].

Following this, monopole radiators with different shapes were developed, printed on dielectric substrate and mounted perpendicularly on ground plane for achieving height reduction and wide bandwidth.

Planar monopole antenna with one step change of the width, planar triangular monopole and linear + triangular cap monopole - were presented for size reduction by H. Lebbar et.al. in 1994 [19]. Wire radiators shaped into planar elements in the shape of circular, elliptical, hexagonal disc for broad bandwidth is reported in 1998 [20]. Planar trapezoidal and pentagonal monopoles were reported by J.A Evans and M.J. Ammann in 1999 [21]. Discone monopoles, Inverted hat monopoles, conical monopoles, elliptical monopole etc. are some of the other configurations of monopole antennas presented for broadband performance [22-24]. Square shaped planar monopole, corrugated square shaped planar monopole, sleeved monopole, monopoles with parasitic elements, annular planar monopole and other similar planar monopole antennas of various shapes were also reported for broadband performance [25-29].

1.7.1.2 Airborne blade monopole antennas

Planar monopole antennas whose shape has been modified for aerodynamic purpose are called blade monopole antennas. These antennas typically have a tapered airfoil cross section to minimize drag. The techniques used to transform a narrow band monopole antenna to a broadband blade monopole antenna are by keeping low length to diameter ratio (L/D), defining the antenna structure by angle (angular concept), matching networks or by a combination of these [30].

A blade conical monopole antenna with impedance matching circuit operating in the frequency range of 100-2000MHz was presented in 2009 [31].

A tapered planar blade monopole antenna with sleeved coaxial feed that operates in the frequency range of 200-850 MHz was reported in 2009 [32].

A blade monopole antenna with an oblique edge operating in 30-600 MHz is presented in 2013 [29]). A broadband impedance matching circuit was also used in this design to decrease VSWR in the frequencies less than 150 MHz.

A blade monopole antenna that uses exponentially shaped radiating profile working in the frequency range 500-2500 MHz is presented in 2015 [33]. Here, the radiator is fed by a capacitively coupled balun through a coaxial-to stripline transition.

A meander line blade shaped monopole antenna loaded with lumped elements operating in the frequency band of 30MHz – 500MHz is presented by Davood Basaery et.al. in 2015 [34].

An ultra-wideband blade monopole antenna that implement Giuseppe - Peano fractal structure in its radiating element is presented in 2016 [35].

A planar blade monopole antenna operating in the frequency range of 1.2 - 6GHz is presented in 2016 for airborne application [36]. The antenna design comprises of a hexagonal structure with slant tapered edges.

A wideband blade shaped monopole antenna with a horizontally mounted aluminium tube on top of the blade, covering 135-175MHz frequency band is presented in 2017 [37]. The blade is pentagon shaped and a matching network is also incorporated in the design near the feed for achieving wide bandwidth.

A number of modifications were made to the planar monopole antenna to provide a wider bandwidth, lower profile and improved omnidirectional radiation pattern. As discussed above, the modifications include altering the geometry, modifying the shapes by cutting tapered sections or folding the elements, and changing the electrical characteristics by lumped element loading or employing a matching circuit between the monopole and ground plane. However, all the above stated planar monopoles require a backing ground plane of λ/4 radius to mount on. For monopole antenna applications with ground plane constraints, these antennas are less suitable.

1.7.2. The effect of ground plane on the performance of monopole antennas

1.7.2.1 Significance of ground plane for monopole antennas

The studies on the importance of ground plane on monopole antenna performance started from early 1940's.

Meier and Summers in 1949 performed an experimental study to analyse the impedance characteristics of vertical antennas mounted on finite ground planes [38]. Leitner and Spence in 1950 confirmed some of these experimental results through the theoretical study of a quarter-wavelength monopole on a finite, circular-disc ground plane [39]. The study showed that there is a marked dependence of the antenna radiation resistance upon the diameter of the disc employed. In 1951, Storer obtained the expression for the dependence of the antenna impedance on the ground plane diameter [40].

An experimental and theoretical study of a monopole antenna mounted on a finite ground plane located above an infinite ground was conducted by Rhee in 1967. The results of this investigation shows that the radiation resistance of an electrically short antenna can be increased by locating it on a small ground plane above the infinite ground rather than directly on infinite ground [41].

Keico Iizuka in 1968 did an experimental study of monopole on a hemisphere shaped ground plane, which has possible applications on spacecraft antennas [42]. Marked differences in the admittances were observed for antennas mounted on the ground plane and on the hemisphere.

M. S. Smith and G. De Prunele in 1981 studied the cross polarized radiation of monopole antennas due to limited ground planes [43]. He explained that the limited ground plane size modifies the vertical polarization of the radiation and also some horizontally polarized radiation could occur, depending on the shape of the finite ground plane.

Weiner in 1987 analyzed a monopole element at the center of a circular ground plane of small radius and of large but finite radius [44]. When the ground plane size of a monopole antenna is reduced from infinity to zero, the monopole eventually becomes an end-fed dipole. In going from one extreme to the other, the resonant frequency doubles and the peak directivity is reduced by approximately 3dB. The radiation resistance with ground planes of zero extent is approximately one-half that with ground planes of large extent. Therefore, a small ground plane results in a very large mismatch loss at the original frequency of intended operation.

He also found that, for a monopole element mounted on a ground plane of finite extent, the outer edge of the ground plane diffracts incident radiation in all directions and consequently modifies the currents on the ground plane. It was observed that this edge diffraction can alter the input impedance by more than 100 percent and directive gain in the plane of the ground plane by more than 6 dB from the values for a ground plane of infinite extent.

Steven R. Best in 2006 demonstrated the performance characteristics of the small antenna with small finite ground plane and it was found that their performance characteristics are defined by the antenna element, the ground plane size as well as location of the antenna on the ground plane [45]. It was found that the operating bandwidth decreases with decreasing ground plane size.

An analysis in 2008 illustrated that the sensitivity of the antennas to ground plane length reduces significantly when its width is larger than half wavelength and length is equal or less than quarter wavelength at the lowest resonant frequency due to the sufficient coupling between the antenna and the ground plane [46].

S.R Best in 2009 presented a detailed study and demonstrated the significance of ground plane size and antenna mounting location as primary factors in establishing the performance of ground plane dependent antennas [47]. The time-varying current on the ground plane is the primary source of radiation that determines both the antenna's impedance and radiation-pattern properties. The location of the antenna and its feeding point on the ground plane, alters the current distribution on the ground plane thus affecting the antenna's performance in terms of its impedance, bandwidth, and radiation mode.

It was also shown that the finite ground plane has a significant impact on the monopole's radiation pattern. The radiation pattern of the monopole on the finite ground plane exhibited degraded omnidirectionality; pattern's peak was elevated well above the ground plane's horizon.

Hatem Rmili et.al. in 2010 analyzed the radiation resistance of a short planar monopole antenna on a small rectangular ground plane [48]. They investigated the radiation resistance of monopole antenna on small ground plane with two

configurations – on too long and other too wide. It was found that the radiation resistance is low as long as the dimension is less than 0.6λ.

Lusekilo Kibona in 2013 studied the impact of rectangular ground plane on the radiation pattern of monopole antenna [49]. He concluded that the ground plane size affects the gain directivity and electric field intensity of monopole antenna.

Radial wire system is an alternate way for the ground plane of monopole antennas. Perfect ground plane has zero resistance and zero reactance. A large number of radial wires at the surface of ground or using a mesh reduce the ground resistance and make the impedance close to perfect ground. Studies on radial wire ground system – the effect of radial wire length, effect of number of radials, effect of angling of radials downward etc. were reported since 1937. The conclusions of these studies can be summarized as – the length of the radials must be λ/4 at lowest frequency of operation for optimum performance of antenna; the arrangement of radials must be symmetrical so as to cancel radiation in the horizontal plane; increased number of radials can increase the efficiency of antenna; angling the radials can change the feed point impedance [50-54].

It can be summarized from the above literature study, that the ground plane has a significant role in determining antenna radiation characteristics. Irrespective of using conductive sheet or radial wire ground system, the ground plane should spread at least λ/4 radius at lowest operating frequency around the feed point of antenna for optimum performance. The **resonant frequency** increases with the decrease in the size of ground plane causing large mismatch loss in the intended frequency band. The operating **bandwidth** decreases with decreasing ground plane size. The **radiation pattern** of the monopole on the limited ground plane exhibits degraded omni directionality; pattern's peak gets elevated well above the ground plane's horizon. The limited ground plane size modifies the vertical **polarization** of the radiation and also some horizontally polarized radiation could occur, depending on the shape of the finite ground plane. The **peak directivity** of the monopole antenna decreases by about 3 dB when the ground plane size is decreased from infinity to zero. The antenna **radiation resistance** shows a marked dependence on the diameter of ground plane. The **location of the antenna on the ground plane and its feeding point** are also

important factors in establishing the antenna's performance in terms of its impedance, bandwidth, and radiation mode.

1.7.2.2 Reduced ground plane monopole antennas

Insufficient ground plane degrades the radiation performance of conventional monopole antennas. To overcome this, some reduced ground plane monopole antennas were reported in the literature, which addresses the ground plane size constraints by modifying the geometry of the ground plane.

A reduced size folded ground plane which provides a highly effective choking action has been developed in 1999 for handheld radio applications [55]. Here the ground plane is folded in the shape of a radial waveguide. The top of the radial waveguide acts as the ground plane and the interior of the wave guide provide the chocking action preventing the field from spreading on the bottom of ground plane.

In 2005, S. Lim et.al proposed a reduced size ground plane using a set of spiral shaped radial [56]. The spiral ground plane serves to generate large inductance that shifts the resonant frequency downward.

The above mentioned methods of achieving reduced size ground plane require alteration in the ground plane geometry. Since the skin of the platform serves to ground plane for airborne monopoles, alteration in the ground plane geometry is impracticable.

1.7.3. Survey of printed monopole antennas

1.7.3.1 Printed Monopole Antennas

The printed monopole antenna that does not requires a backing ground plane was first presented in 1997. In 1997, J. Michael Johnson and Yahya Rahmat-Samii introduced a tab monopole, with the monopole patch and the ground plane printed on the same side of the substrate, which overcomes the disadvantage of planar monopoles requiring backing ground plane [57]. He introduced the name "tab monopole" to differentiate this antenna from the other planar and printed monopoles which require a backing ground plane to mount on.

Various configurations of printed monopole antennas were studied in the following several years, mainly on the geometries of the monopole and the ground plane. The wideband characteristics of printed monopole antennas were explored widely for UWB applications.

Printed strip monopole antenna is the basic configuration of printed monopole antenna. To reduce the height of the antenna and to achieve wideband performance, different modifications were implemented in the radiating patch geometry and various shapes of patches were explored.

A strip line fed printed monopole antenna with equilateral triangular shaped radiator was reported in 1997 for broadband operations [58].

A printed monopole antenna that consists of three printed strips forming an isosceles right-angle triangle has been reported for wideband applications in 2004 [59].

Choi et.al introduced a printed monopole antenna that contains a rectangular patch with two steps and a single slot on the patch for ultra-wideband applications [60].

A CPW fed arrow like printed monopole antenna was developed by Wei Wang et.al for wideband applications [61].

A printed circular monopole antenna was developed in 2005 [62], which achieves the impedance bandwidth ratio of 3.8:1 (2.69~10.16 GHz) with satisfactory omnidirectional radiation properties.

Other configurations of printed monopoles such as spline- shaped monopole [63], U-shaped monopole [64], knight's helm shape monopole [65] two steps circular monopole [66], square ring with T shaped strips [67], circular ring monopole [68], tulip shaped planar monopole [69], pentagonal monopole [70], planar inverted cone monopole [71], crescent shaped monopole [72], semi elliptic monopole [73], annular ring monopole [74], arc shaped monopole with a rectangular parasitic patch [75], hexagonal shaped monopole with ground extended vertically on two sides of the radiator [76], etc. were also proposed and studied for UWB applications.

The possibility of achieving wide bandwidth by modifying ground plane geometry were also investigated and reported in the literature.

Huang et al. [77] introduced an impedance matching technique of printed monopole antennas by cutting a notch at the ground plane, and demonstrated that the impedance bandwidth can be enhanced by suitable size and position of notch chosen.

Azim et al. [78] proposed that the impedance bandwidth of square shaped printed monopole antenna can be improved by cutting triangular shaped slots on the top edge of the ground plane. This antenna obtains a impedance bandwidth ratio of 5.5:1 (2.9~16GHz).

A circular monopole patch and a trapeziform ground plane with a tapered CPW feed [79], a heart-shaped monopole with a microstrip feed line and an elliptical curved ground plane [80] were also reported for UWB applications.

A printed elliptical monopole antenna with trapezoidal ground plane fed by a tapered CPW line is presented by Jianjun Liu et.al [81]. The wideband performance of this antenna was achieved by adding two feeding branches and optimizing the elliptical patch and ground plane shape.

Jihak Jung et.al presented a small wideband microstrip fed monopole antenna [82] in which the wideband characteristics was achieved by placing a pair of notches at two lower corners of the patch and embedding a notch structure in truncated ground plane.

Considering high concentration of currents in the corners of the patch and ground, Melo et al.[83] studied a rounded monopole patch with a rounded truncated ground plane that provides an impedance bandwidth ratio of larger than 4.7:1 (2.55 ~12 GHz).

A low-profile coplanar waveguide fed monopole antenna comprising of a straight strip, a parasitic circular-hat patch, and a slotted CPW ground was presented for broadband operation by W. C. Liu et.al [84].

A compact microstrip-fed printed dual band antenna for Bluetooth and UWB applications with WLAN band-notched characteristics is proposed in 2011 [85]. The

antenna comprises of a fork shaped radiating patch, with two L-shaped slots and two symmetrical step slots etched on the rectangular ground plane.

A fractal monopole antenna with band rejection characteristics was proposed by Krishnan Shambavi et.al for UWB applications [86].

A microstrip monopole antenna with switchable band notch function is presented by Tasouji et.al for ultra-wideband applications [87]. The antenna comprises of an elliptical radiator and a half circular shape ground plane with arc shaped slots, which excites new resonances to achieve enhanced bandwidth.

A modified printed rectangular monopole antenna was reported for UWB applications [88]. In this design, a printed rectangular monopole antenna was modified with round edge at the lower side of the rectangle and chamfering the two upper corners of the antenna-radiating element.

Although the profound application of printed monopole antenna found in literature is for UWB application, it was also developed for other applications like RFID [89], MIMO [90] and WLAN applications [91].

In 2003, a microstrip-fed dual-U-shaped printed monopole antenna, a double T monopole antenna that consists of two T-shaped monopoles of different sizes stacked one over other, and a printed L-shaped monopole antenna were reported for dual band applications centered in the frequency range of 2.4GHz and 5.2GHz [92-94].

A multiband printed monopole antenna suitable for GPS, WLAN, WiMAX applications was proposed in 2012 [95]. The radiating elements of this antenna consist of three branches and the defected ground located on the backside of the dielectric substrate consists of two rectangular shaped slots. The slots on the ground plane improve the impedance matching.

A planar monopole antenna with two frequency tunable bands was developed by XL Sun et.al for Wi-Max wireless devices [96]. The antenna had a short stem with two radiating branches, one a folded branch and other a meandered branch.

An inverted L shaped monopole antenna with parasitic inverted F element in ground plane for dual band application was proposed by Sudhanshu Verma et.al [97].

Printed monopole antenna was primarily investigated for applications especially for wireless mobile communications in L-S-C-X bands. This is because, together with the partial ground plane, the overall size of the antenna is in the order of 0.5λ. A very few printed monopole antennas were reported in the literature for VHF/UHF band by incorporating different techniques for reducing antenna size.

1.7.3.2 Printed Monopole Antennas in VHF/UHF band

A compact printed monopole antenna that comprises of a square ring monopole fed by a microstrip line and a tapered ground plane was reported for RFID application [98]. To improve the impedance matching of the antenna, a parasitic square ring structure was added to the tapered ground plane also.

An ultra-wideband printed monopole antenna has been reported for partial discharge detection in 2014 [99]. In this design, both the radiating element and the ground plane are bevelled in order to ensure a smooth transition in the impedance between the adjacent resonances. The drawback of this antenna is the larger size, 0.3λ at 120MHz.

A dual-band printed monopole antenna for wireless M-Bus and M2M applications with operation in the VHF and lower UHF bands was presented by A. Loutridis et.al in 2015 [100]. The miniaturization of this compact antenna is based on a double-sided meandering structure.

A printed monopole antenna with C shaped ground system operating in the frequency range of 220-860MHz was reported in 2016 [101]. The antenna has a physical dimension of 0.3λ.

The above mentioned printed monopole antennas either lack wideband characteristics or compactness. The wideband printed monopole antennas presented above has a physical length of 0.3λ. For airborne application, we require the antenna to be very compact in order to reduce air drag along with wide bandwidth. Hence in this thesis, two compact (~0.1λ at lowest frequency of operation), wideband (~32%) printed monopole antennas operating in VHF band are presented for airborne applications.

The first antenna presented in this thesis is a bifolded printed bent monopole antenna. This antenna applies folding technique in to the bent monopole configuration to achieve height reduction. The second antenna is a meandered top loaded printed monopole antenna. This antenna uses both meandering and top loading techniques in the radiating patch and ground plane for achieving height reduction. The literature referred for developing these antenna structures is briefed below.

1.7.3.3 Printed Bent Monopole Antenna – A brief survey

The bent monopole or inverted L monopole antenna is a short monopole with the addition of a horizontal segment of wire at the top. The bending of the monopole results in a reduced size and low profile. These antennas were first designed for missile applications in 1960 [102]. Later in 1974 a class of bent monopole antenna was proposed by Richard W. Adler and Eugene G. Neely [103].

Various configurations of bent monopole antennas were developed since 2003 for achieving different characteristics like compactness, multiband operation, and even wideband characteristics. It was seen that the bending technique was widely implemented in conventional planar monopoles as well as the printed monopole antennas. Some of the notable investigations on the printed bent monopole antenna are briefly surveyed.

A wideband dual frequency design of a double inverted-L printed rectangular monopole antenna with CPW feeding was presented in 2003 for WLAN application [104]. The dual-frequency operations was achieved by embedding the patch with an L-shaped slit, which comprises both the horizontal and vertical sections, to form two inverted L-shaped monopoles.

The observation of tilted radiation pattern of bent monopole antenna was used in the development of a reconfigurable antenna to achieve beam switching in 2004 [105].

An inverted L folded monopole antenna with a parasitic inverted L wire was proposed in 2004 for dual band application [106].

In 2005, a printed bent monopole antenna that implements folding technique to achieve height reduction and multiband operation was presented [107]. In this folded monopole, the vertical structure is folded back parallel to the side of the structure and is grounded.

A CPW fed tapered bent folded monopole antenna was also investigated in 2005 for dual band WLAN systems [108].

A bent folded printed monopole antenna with microstrip feeding that exhibits 6% bandwidth was presented in 2006 [109].

A CPW-fed monopole antenna with double inverted-L strips – one a long meandered inverted L and other a short inverted L - was presented by H.S. Choi *et.al* in 2006 for dual-band WLAN applications operating at 2.44GHz and 5GHz [110].

A microstrip fed printed monopole antenna with double inverted L structures was proposed for RFID application in 2009 [111].

A bent-folded-monopole antenna with chip inductor and chip-capacitor was proposed in 2010 for dual band operation [112].

Bandwidth enhancement of a bent monopole antenna by placing a conductive sheet close to the monopole was proposed in 2012 to operate in the UHF band from 470MHz to 770MHz [113].

A method for bandwidth enhancement of printed bent monopole antenna by improving the impedance matching by extending the ground plate to L shape was proposed in 2015 [114].

It can be inferred from the above literature study that, printed bent monopole antenna configuration can be used to achieve height reduction for developing a printed monopole antenna in VHF band. Reduced size of the antenna results in poor impedance matching. Impedance matching of the bent monopole antenna can be improved by modifying the partial ground plane.

1.7.3.4 Meander line printed monopole antennas – A brief survey

Meandering and top loading are considered as effective techniques for reducing the resonant length of antennas.

Meander line antennas are a class of antennas intended to reduce the resonant length of the antenna [115]. Each half section is formed when the wire is folded three times over its course and a complete section is made when two half sections are connected back to back.

Meander antennas were first investigated by J. Rashed and Chen-To Tai in 1982 [116]. Later in 1986, a wideband meander line dual zig-zag monopole antenna has been reported for spacecraft applications [117]. A dual meander sleeve monopole antenna based on this configuration was reported in 1995 for personal communication network operating in the frequency band of 850-1900MHz [118].

Printed meander line monopole antennas are constructed on a dielectric substrate by continuously folding a conventional printed monopole patch. Various configurations of meander line were investigated in printed monopole antennas for achieving size reduction.

A CPW fed rectangular meander line monopole antenna with an extended conductor line has been reported in 2002 for dual band operation [119].

A coplanar waveguide meandered feed line was introduced to a planar monopole antenna to obtain a broadband dual-frequency operation in [120]. The modified feeding technology results in good impedance matching in a wide dual-band covering 2.4-5.2 GHz WLAN operations.

A multiple meander strip monopole antenna was reported in 2005 for UWB application [121]. This antenna consists of four radiating meander lines each connected symmetrically to the end of the cross shape microstrip feed line.

A multi-band monopole antenna with wideband characteristic was proposed for DVB-H/DCS1800/PCS1900/IMT2000/Wibro/WLAN/ S-DMB applications in 2008 [122]. In this antenna, the wideband characteristic is achieved using a meander structure and tapered feeding line.

A compact coplanar waveguide (CPW) fed antenna with meandering in the ground plane operating at 2.4GHz with 300MHz 2:1 VSWR bandwidth is presented in 2011 [123].

A printed meander monopole antenna, which is able to generate four resonant frequencies just by adding a branch and a meander structure is presented for operating in GSM/DCS/PCS/UMTS/ISM bands [124].

A meander rectangular monopole antenna has been reported in 2015 for quadband operation [125].

A double sided meandered monopole antenna operating at 169 and 433 MHz for wireless M-Bus and M2M applications is presented in 2015 [100].

From the literature study on meander line printed monopole antenna, it was inferred that meander line on radiating patch can reduce the antenna height significantly. By implying meander line on feed line and ground plane improved impedance matching and wideband characteristics can be achieved. It can be concluded from literature study that by properly configuring the meander line printed monopole antenna, wideband and multiband characteristics can be achieved along with compactness.

1.7.3.5 Top loaded printed monopole antennas – A brief survey

Top loading has been introduced in order to reduce the antenna resonant height along with increased radiation resistance [126]. Top loading increases the capacitive reactance of the antenna, thereby increases the bandwidth.

Various types of top loadings has been introduced to monopole radiators in literature for increased bandwidth and height reduction – cap loading, helical top loading, umbrella top loading, etc. [11-12] [127-132].

The various configurations of printed monopole antenna – printed rectangular monopole antenna, printed circular monopole antenna, printed elliptical monopole antenna etc. can be considered as variants of printed strip monopole antenna top loaded with these rectangular, circular, elliptical etc. shapes.

Implementation of top loading on ground for ultra-wideband performance was reported in 2005 [133].

1.8 THESIS ORGANIZATION

The organization of the thesis is as follows.

Chapter 1 gives the introduction of the thesis. The motivation of the work is discussed in this chapter. This chapter also includes a detailed literature review on conventional, planar and blade monopole antennas, the significance of ground plane on the performance of monopole antennas and an exhaustive study on the printed monopole antenna design in L-S-C-X bands as well as in the VHF/UHF band. It also briefly reviews the past work in the field of printed bent monopole antennas, printed meander line monopole antennas and printed top loaded monopole antennas.

Chapter 2 starts with the methodology used for developing the antennas reported in this thesis. The methodology of research includes selection of suitable substrate, simulation tool used for the design and optimization of the antenna, antenna fabrication and the measurement method. Measurements in the frequency domain such as return loss, radiation pattern, gain are explained. This chapter also presents an overview on the theoretical study carried out on the antennas. Theoretical study includes the parametric analysis for studying the effect of each antenna dimensions on the radiation performance, the analysis on the variation in the distributed reactance with different dimensions, and deduction of design equation.

Chapters 3 & 4 concentrate on the printed monopole antennas proposed in this work. The design details of the antennas are discussed. The surface current & field distributions on the antenna at the resonant frequency are analyzed in detail. An intensive parametric analysis was carried out to study the effect of each dimension on the radiation performance of these antennas and is presented in these chapters. The performance of the antennas is evaluated with the antenna mounted over a ground plane as well as for the free standing antenna and the results are presented. The effect of the mounting ground plane on printed monopole antenna was found to be very less compared to conventional monopole antenna. The measured results of the fabricated antennas are then plotted with their corresponding simulated results which are found to conform well in all cases.

Chapter 3 presents the development of a bifolded printed bent monopole antenna with L shaped ground plane operating in the frequency range of 130MHz-180MHz. The antenna achieves 3:1 VSWR bandwidth of 32%. It also achieves a height reduction of 78% compared to a basic printed strip monopole antenna and 73% compared to conventional planar quarter wavelength monopole antenna at lowest frequency of operation.

The design and development of a RL loaded meandered top loaded printed monopole antenna is presented in chapter 4. The evolution of the antenna design is presented first followed by the detailed study of the proposed antenna. The proposed antenna exhibits a 3:1 VSWR bandwidth of 38%. The antenna achieves a height reduction of 67% compared to basic printed strip monopole antenna and 63% compared to conventional planar quarter wavelength monopole antenna at lowest frequency of operation.

The numerical analysis done on the antennas for obtaining more insight about the radiation mechanism is presented in chapter 5. Based on the parametric analysis carried out on both the antennas, the factors affecting the resonant frequency were identified. The results of the surface current analysis along with the parametric studies have enabled to deduce their design equations. The calculated values are compared with the simulated results and the error was found to be less than 5%.

Finally the thesis is concluded in Chapter 6, by compiling the overall work and their results along with a brief description on the scope for future study.

2. Methodology

The chapter deals with the techniques used for the design, fabrication and measurement of antennas reported in this thesis. The design and simulations are performed using the FEM based ANSYS High Frequency Structure Simulator (HFSS) software. The prototypes of the antennas were fabricated using photolithographic process and the antenna characterization was done using E5071C Vector Network Analyzer in the open field.

2.1 SOFTWARE SIMULATION AND MODELING - HFSS

The design and optimization studies of the antennas presented in this thesis are performed using the commercial software ANSYS High Frequency Structure Simulator (HFSS). HFSS is one of the globally accepted commercial Finite Element Method (FEM) solver for electromagnetic structures [134].

HFSS utilizes the 3D full-wave Finite Element Method (FEM) with adaptive meshing to compute the electrical behavior of high-frequency and high-speed components. Solving any arbitrary 3D geometry, even with complex shapes and curves, are possible by this software in minimum time.

One of the key features of HFSS is that, it provides various kinds of boundary and port schemes. Radiation, Perfect Electric Conductor and Lumped RLC boundaries available in this software are widely used in simulating the antennas mentioned in this thesis.

Perfect Electric Conductor (PEC) is used to model conducting boundary. It represents a lossless perfect conductor. Radiation boundary is used to create an electromagnetic model that allows electromagnetic energy to emanate or radiate away. It is applied to outer faces of the solution space. For antenna simulation, it is placed a quarter wavelength away from the radiating surface. Lumped RLC allows creation of ideal lumped components. It is used to model ideal lumped resistors, inductors or capacitors. Once the values of R, and/or L, and/or C is specified, HFSS determines the impedance per square of the lumped RLC boundary at each frequency, effectively converting the RLC boundary to an impedance boundary.

There are seven types of excitations in HFSS through which a user can specify the sources of fields, voltages, charges or currents for a given simulation. In this work, lumped port excitation scheme is used to excite the antenna. Lumped ports are ports that can be used in simulations where energy needs to be sourced internally to a model. Lumped ports yield S, Y, Z parameters and fields. A lumped port can be defined on any 2D object that has edges which contact two conducting objects.

2.1.1 Steps involved in HFSS simulation

The main steps involved in the HFSS simulation of the antenna mentioned in this thesis is described in this section. A flow chart showing the steps involved in HFSS simulation is shown in Fig 2.1.
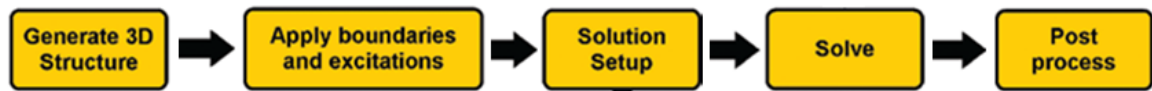
Fig 2.1. Steps involved in HFSS simulation.

Step 1. The first step in simulating an antenna in HFSS is to define the geometry of the system. To generate a 3D or 2D structure, user can either use modeler's DRAW command or draw 1D and 2D objects. Objects are drawn in the 3D Modeler window. After drawing the model, the user can assign material for each object.

On designing the printed monopole antenna, first, the substrate material was drawn by creating a 3D rectangular box with the required dimensions. Then the material FR4 was assigned to this structure by selecting the box, and selecting MODELER > Assign material > FR4. The base plate of the antenna was also drawn perpendicular to antenna substrate and was assigned aluminium material in the same manner. The patch is then drawn on the top and bottom of the substrate using Draw Rectangle and Unite tools.

Step 2: After drawing the antenna, the second step is to define the boundaries of the structure and to apply proper excitation.

After drawing the patches, perfect electric boundary was assigned to the patches by selecting them and using HFSS > Boundaries > Assign > Perfect E. To represent resistance and inductance loading, a rectangle is drawn on the patch, and the lumped component values are assigned by selecting the rectangle and choosing HFSS > Boundaries > Assign > Lumped RLC. The values of the RLC components are specified in the corresponding boxes. An integration line must also be specified.

A radiation boundary filled with air is then defined surrounding the structure. For this, a rectangular box of air material was drawn with the antenna substrate at

center of the box and by selecting this air box, radiation boundary is assigned by choosing HFSS > Boundaries > Assign > Radiation.

After the boundaries have been assigned, the suitable port excitation scheme is to be given. In our work, coaxial feed was used to excite antenna. For this coaxial feed connector of appropriate dimension was drawn at the base edge of the antenna, in a way that the base plate of the antenna holds the connector. At the base of the feed, lumped port excitation is given. When creating a lumped port, it is necessary to draw an integration line for the port. This integration line should be drawn between the center points of the edges that contact metal objects.

Step 3: Once boundaries and excitations have been created, the next step is to create a solution setup. During this step, the user will select a solution frequency, the desired convergence criteria, the maximum number of adaptive steps to perform, a frequency band over which solutions are desired, and what particular solution and frequency sweep methodology to use. For this user should select HFSS>Analysis Setup > Add Solution setup. After completing this, the frequency sweep can be given by selecting HFSS > Analysis setup > Add Frequency sweep.

Step 4: When the initial four steps have been completed, the model can be validated using HFSS > Validation Check. After saving the model, it can be analyzed by running the simulation using HFSS > Analyze all.

Step 5: Finally the simulation results such as scattering parameters, far field radiation pattern etc. are obtained by selecting the appropriate options from HFSS > Results. To plot the surface current distribution, the patch is selected. Then HFSS > Fields > Plot Fields > J is selected. A window will be opened in which, the solution, frequency and phase for plotting the surface current distribution is fed.

A CAD model of antenna simulated using HFSS is shown in Fig 2.2.
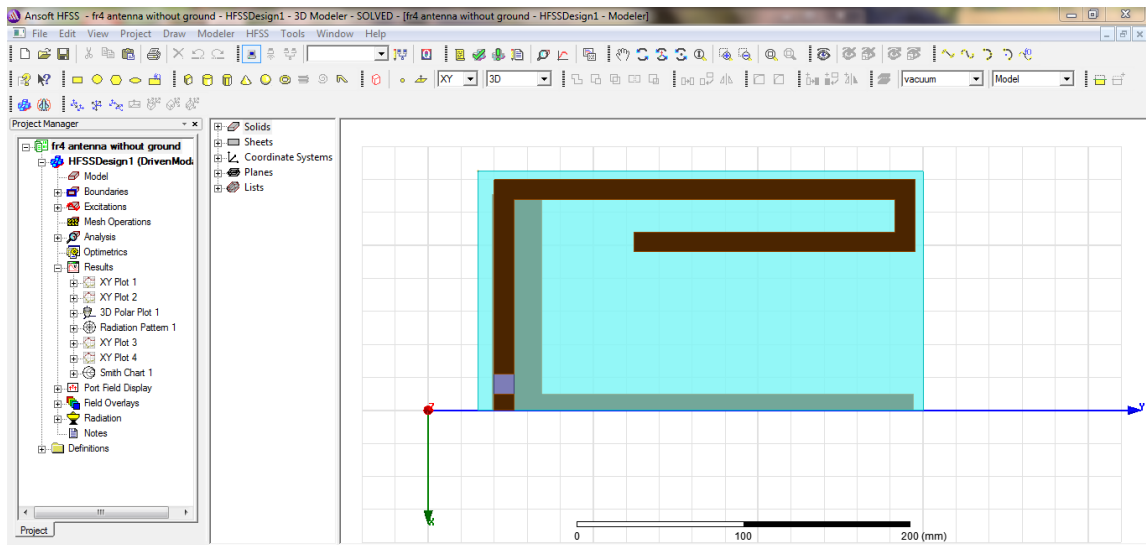
Fig 2.2. CAD model of antenna in HFSS.

2.2 SELECTION OF SUBSTRATE

The selection of a proper substrate material is the essential part in antenna design. The selection of the substrate depends on the application of the antenna and the required radiation characteristics. Properties like dielectric constant (ε) and loss tangent (tan δ) and their variation with temperature and frequency, dimensional stability, thickness uniformity of the substrate, thermal coefficient and temperature range must be involved in the considerations.

Dielectric constant of substrates affects the antenna performance. The substrate which has a low dielectric constant will give better performance than the substrate which has a high dielectric constant. The high dielectric material allows for a reduction of space but at the cost of higher moisture absorption level.

Loss tangent or dissipation factor also plays a part in antenna performance. Dielectric constant and loss tangent vary with operating temperature changes and levels of humidity. Loss tangent or Dissipation factor can change significantly with moisture absorption as little as 0.25% of dielectric weight. Thus moisture absorption should be as low as possible.

Dielectric materials cannot resist indefinite amount of voltage. Once current is forced through an insulating material, breakdown of that materials molecular structure will occur. Hence volume resistivity and surface resistivity should be good. After breakdown, the material may or may not behave as an insulator any more, the

molecular structure having been altered by the breach. Hence, the breakdown voltage should be high.

The antennas reported in this thesis were developed for VHF communication with omnidirectional radiation coverage in the azimuth plane and are designed for mounting on airborne platforms.

Microstrip antenna on being fixed on aircraft surface are subjected to unfavorable conditions such as intense heat, physical damage, very low temperatures and plasma environment. Hence, these antennas need to be rugged enough to withstand vibration and ought to be operated at extreme temperatures. It is coated with a dielectric cover layer also for proper shielding.

Prototypes of the antennas for this thesis have been realized on FR4 Glass Epoxy. "FR" stands for flame/fire retardant. FR-4 glass epoxy is famous and flexible high-pressure thermoset plastic laminate material with high strength to weight ratios. The material is of low cost and has excellent mechanical properties, making it ideal for a wide range of electronic equipment. It is also suitable for the use at RF and microwave frequencies for the design of microstrip and printed antennas. The substrate can be preferred based on the desired material characteristics for optimal performance over the specific frequency range. Dielectric constant, thickness and loss tangent are the commonly used parameters. The material properties of FR4 Epoxy are given in the Table 2.1 below.

Table 2.1 Material properties of FR4 Epoxy.

Dielectric constant	4.4
Dissipation factor	0.025
Temperature tolerance	High (0°C to 55°C)
Coefficient of thermal expansion	Low (11microns/m/^{o} C)
Humidity tolerance	High (0-90% non-condensing)
Moisture absorption	Less (0.15%)
Tensile strength	High (45000psi)
Breakdown voltage	High (65KV)

2.3. ANTENNA FABRICATION

For the fabrication of microstrip antennas, photolithographic technique or fast fabrication process can be employed. In the work presented here, photolithographic technique is used as it is reasonably more accurate.

Photolithography is the process of transferring geometrical shapes from a photo-mask to a surface. The step involved in the fabrication of antenna using this technique is depicted in Fig 2.3.

The CAD drawing of the antenna is printed on a high quality butter paper with a high resolution laser printer (mask). The copper clad of suitable dimension is cleaned with a suitable chemical like acetone to remove any impurities. A thin layer of negative photo resist solution (1:1 mix of negative photo resist solution and thinner) is coated using spinning technique on copper surfaces and is dried. The antenna mask is carefully aligned over the photo resist coated clad and exposed to UV light. The layer of photoresist material in the exposed portions hardens, while the unexposed region remains unaffected and it can be removed by carefully rinsing with a suitable developer solution. The board is then washed in water. After this, the unwanted copper portions are etched off using Ferric Chloride ($FeCl_3$) solution to get the required antenna geometry on the substrate. The etched board is rinsed in running water to remove any etchant. $FeCl_3$ dissolves the copper parts except underneath the hardened photo resist layer after few minutes. The laminate is then cleaned carefully to remove the hardened photo resist using acetone solution. A photograph of the fabricated antenna is shown in Fig 2.4.
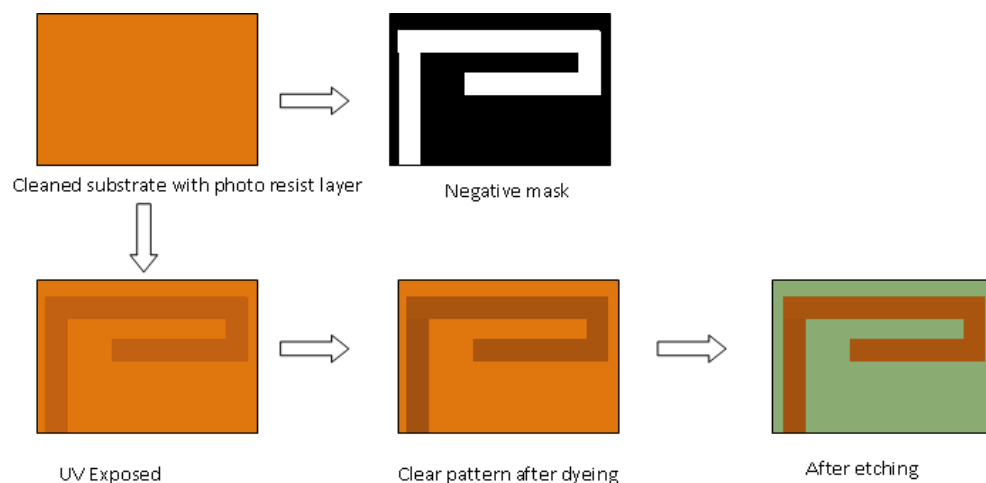
Fig 2.3 Steps in photolithography process.

Fig 2.4. Photograph of a fabricated antenna.

2.4. ANTENNA MEASUREMENT SETUP

The antennas reported in this thesis were measured for its electrical characteristics like resonant frequency, impedance bandwidth, radiation pattern and gain in the open field. The test facilities available include Network Analyzers (E5071C) and automated antenna positioner. The transmitting antenna used was a wideband Log Periodic Dipole Antenna (LPDA) radiating in the frequency range of 100 to 550MHz with an average gain of 9dB. The antenna under test is used as the receiver.

The E5071C from Keysight, is a 4 input network analyzer [135]. The model measures a frequency range from 0.3 to 20000 MHz and a maximum dynamic range of 123 dBm. The E5071C's maximum output power is 10 dBm. It is an integrated network analyzer with a four-port S-parameter test set, a synthesized RF source, a 10.4-inch color LCD, and a hard disk drive. The Network Analyzer is calibrated using the calibration kit, which includes standards such as open, short and load, before performing the measurements. A turntable assembly consists of a microcontroller based antenna positioner, interfaced with the PC for the radiation pattern measurement.
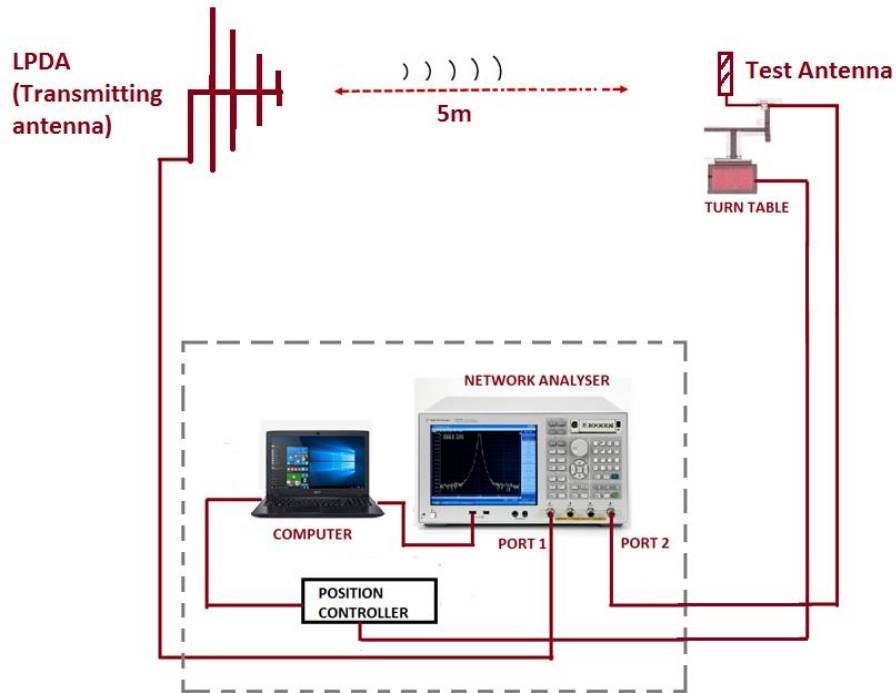
Fig 2.5 Antenna measurement setup.

Schematic of the setup used for measuring antenna radiation pattern and gain is shown in Fig 2.5.Transmitting antenna is fixed in a position and the antenna under test is mounted over the turntable assembly which rotates by 360° in azimuth. Both antennas are connected to a vector network analyzer. The turntable and measurement data from the vector network analyzer are gathered, processed and plotted in a PC using software which controls both devices. The measured radiation patterns are obtained in far field conditions.

2.5 ANTENNA CHARACTERIZATION

The major antenna characterization procedures are depicted in the following sessions.

2.5.1 Return loss Measurement

When there is an impedance mismatch between the antenna and the source line, a part of the incident energy is reflected back to the source. The ratio of the reflected voltage (or current) to the incident voltage (or current) is termed as the input reflection coefficient (Γ). S_{11} is the reflection coefficient expressed in dB.

$$S_{11} = 20 \log 10(|\Gamma|)$$

The level of mismatch is also defined in terms of the Voltage Standing Wave Ratio (VSWR). VSWR is defined as the ratio of the voltage maximum to minimum of the standing wave existing on the antenna input terminal.

In order to measure the return loss characteristics of the antenna under test, the test antenna is connected to any one of the network analyzer ports and the VNA is operated in the S_{11} or S_{22} mode. The specific port of the analyzer should be calibrated for the frequency range of interest using the standard open, short and matched load, prior to the measurement. The S_{11} values of the antenna in the entire frequency band are then stored in a computer in Comma Separated Variable, "CSV", format. The frequency at which the return loss value is lowest is taken as the resonant frequency of the antenna.

The range of frequencies for which the return loss value is within the -6dB points is usually treated as the 3:1 VSWR bandwidth of the antenna. Basically the bandwidth is defined more concisely as a percentage calculated using the formulae

$$\% \text{ bandwidth} = (f_2\text{-}f_1)/f_0$$

Where, f_2 and f_1 represent the upper and lower edge of the frequency band respectively and f_0 represents the center frequency of the band.

2.5.2 Radiation Pattern Measurement

Radiation pattern of an antenna is the graphical representation of its radiation properties as a function of the space co-ordinates. Generally, far field patterns are specified for an antenna where the pattern is measured at a distance, $d > 2D^2/\lambda$, where D is the largest dimension of the antenna and λ is the operating wavelength.

The radiation pattern measurement is carried out in the open field with the help of E5071C Vector Network Analyzer. The antenna under test is mounted on a turn table and connected to one port of the network analyzer configured in the receiver mode. The other port of the network analyzer is connected to the transmitting antenna. The height and polarization of both antennas are aligned for maximum transmission (S_{21}) between them. The network analyzer and the turntable controller are interfaced to a computer which runs the measurement automation software. *The*

measurement band, *start angle*, *stop angle, angular step size* and *file name* are input to the measurement automation software. The system automatically undergoes THRU calibration prior to the measurement and performs the transmission measurement for each step angle and records the angular transmission characteristics in a data file. This is used to plot the 2-D radiation pattern at the required frequency.

2.5.3 Antenna Gain Measurement

Gain is the ratio of the intensity of an antenna's radiation in the direction of strongest radiation to that of a reference antenna, when both antennas are fed with the same input power. If the reference antenna is an isotropic antenna, the gain is expressed in units of dBi.

The gain transfer method using a standard gain antenna is employed to determine the absolute gain of the antenna under test [136]. The experimental setup for determining the gain is similar to the radiation pattern measurement setup. The gain of the antenna under test is measured relative to the power levels detected by a standard gain antenna. Here, for the gain measurement of the antennas mentioned in this thesis, tuned monopole antenna of 2dB gain is used as the standard antenna. Initially, the standard antenna is positioned for bore-sight radiation and the transmission coefficient $\left| S_{21ref} \right|$ (dB) is read on the analyzer display. A THRU calibration is performed and the data is stored in the analyzer. This is the reference gain for the antenna under test. Now the test antenna replaces the reference antenna and the transmission coefficient $\left| S_{21} \right|_{test}$ (dB) is recorded, which gives the relative gain. The absolute gain can then be calculated as

$$G \text{ (dBi)} = G_{ref} \text{ (dBi)} \pm \left| S_{21} \right|_{test}$$

2.6. ANALYSIS OF ANTENNAS

Analysis of antennas are done to get a good physical insight of the antenna. The analysis may be based on theoretical approach and/or experimental measurements [137].

The theoretical analysis has the following advantages:

- It can reduce the number of costly tests on prototypes by supporting the design process.

- It can ascertain the advantages as well as limitations of a configuration by carrying out parametric studies.
- It can provide an understanding of the operating principles that could be useful for a new design, for modification of an existing design, and for the development of new configurations.

The analysis of antennas described in this thesis is based on parametric studies and surface current analysis of structure using FEM based HFSS software. Based on these studies the empirical formulae for calculating the resonant frequency of the structures is derived.

2.6.1 Parametric analysis:

The effect of various dimensions of the antenna structure and substrate parameters on the radiation characteristics of the antenna are analyzed using parametric analysis technique available in HFSS software. A parametric setup specifies all of the design variations that optometric drives HFSS to solve. A parametric setup is made up of one or more variable sweep definitions, which are a set of variable values within a range that HFSS need to solve when the parametric setup is run.

The parameter which is to be analyzed is varied over a range keeping all other parameters constant. The effect of this dimension on the frequency response of the antenna is obtained from the return loss characteristics. The effect of this parameter on radiation pattern and gain of the antenna is obtained from radiation pattern plot and gain plot respectively.

2.6.2 Surface current analysis:

The analysis of surface current distribution over antenna surface enable us to determine the mode of resonance. HFSS provides Field overlays option for plotting the field distribution on a surface or object. The distribution of current on the radiating patch and ground patch is obtained from surface current analysis (J_{surf}), which come under Field overlays option. For this, the patch under consideration is selected and the surface current distribution at a particular frequency is selected. The analysis gives the magnitude and direction variation of surface current distribution over the structure.

2.6.3. Extraction of distributed RLC parameters:

The variation in the frequency response of the antenna is analyzed by studying the variation of the distributed reactance with dimensions.

The antenna is considered as a resonant circuit with its own resonant frequency and bandwidth. Antennas can be approximated to series RLC networks with a specific resonant frequency and Q factor. The resonant frequency is a function of the capacitance and inductance present in that circuit while the Q factor is a function of all the three components [138]. By doing some simple mathematical calculations, the circuit parameters of the antenna can be extracted from their resonant frequency and bandwidth. These values of circuit parameters can be used to explain the resonance mechanism.

The algorithms included in the extraction of parameters of the circuit are given below.

- **Step 1:** Calculate the Bandwidth **BW** and the resonant frequency $\mathbf{f_r}$ from reflection co efficient

- **Step 2:** Calculate the resistance **R** of the circuit at resonance by solving the equation

$$\frac{R - Z_0}{R + Z_0} = 10^{S_{11}/20}$$

  Where, S_{11} is the return loss measured at resonant frequency and $Z_0 = 50\ \Omega$ is the characteristic impedance of the transmission line used to guide the energy into antenna. At resonance the circuit only offers resistance; the reactance will cancel each other.

- **Step 3:** Calculate Q by the relation $\mathbf{Q = f_r\ /BW.}$

- **Step 4:** Calculate inductance L by the formula $\mathbf{L = RQ/2\pi f_r}$.

- **Step 5:** Calculate capacitance C by the formula $\mathbf{C = 1/2\pi QRf_r}$.

2.6.4 Design Equation Formulation

In order to decrease the long-time processing, it would be convenient to start the design process by drawing an antenna with sizes close to its resonant frequency instead of using random initial sizes and then optimizing the antenna with cut and try methods. Thus, by having an initial geometrical configuration of the antenna, the design process would be quicker, as a good initial configuration can strongly affect the numerical convergence efficiency.

The design equations for a rectangular patch antenna based on cavity model is modified to derive the equation for the resonant frequency of the patches described in this thesis. The derivation of the design equation of rectangular microstrip patch antenna involves the computation of relation between resonant frequency and its patch dimensions.

The design equations for the resonant frequency of the printed monopole antennas mentioned in this thesis are derived using the same methodology as adopted for deriving the design equation of rectangular microstrip antenna. The steps involved in this process is described below.

- To determine the fundamental mode excited by the printed monopole antennas mentioned in this thesis, the surface current distribution on these structures are studied and analyzed. From this, we can determine the number of half wave variations occurred along the length of the patch.
- To determine the effective electrical length of the patch $L_{eff,}$ the dimensional factors affecting the resonant frequency are identified by executing exhaustive parametric study. Based on this parametric analysis, the effective length is determined by applying random coefficients to the dimensional factors using trial and error method.
- The effective dielectric constant, ε_{reff} of the antenna is then determined. For printed monopole antennas, the variation in the resonant frequencies of printed monopole antennas with the substrate dielectric constant is not by a factor of $\sqrt{\varepsilon_r}$ as observed in conventional microstrip antennas, but by a factor closer to unity [152]. Following this, the factor k, whose value closer to unity can be thought of as having similar significance as $\sqrt{\varepsilon_{reff}}$.

- The resonant frequency is then calculated using the relation $f_r = \dfrac{c}{\lambda \times k}$

Replace the wavelength λ, in terms of the effective electrical length (L_{eff}) of the patch.

2.7. CHAPTER SUMMARY

This chapter has discussed the methodology to simulate, optimize and fabricate the antennas mentioned in the following chapters of the thesis. Prefabrication studies are performed using ANSYS HFSS simulation software. Measurements in the frequency domain include return loss, radiation pattern and gain. The various methods used for the analysis of antennas and the algorithm for deriving the design equation is also discussed.

3. Bifolded Printed Bent Monopole Antenna

One of the main problems faced by airborne monopole antennas is the space constraints in the mounting platform; to achieve a $\lambda/4$ radius ground plane around the feed point of antenna. This problem can be overwhelmed with by using printed monopole antenna, as ground plane of these antennas are in the same plane as that of the radiating element. This chapter presents a wideband printed bent monopole antenna operating in VHF band for airborne applications. The compactness is achieved using folding technique and the wideband characteristics by resistance loading method. The ground plane of this antenna is L shaped for achieving improved impedance matching. The effect of patch and ground plane dimensions as well as the substrate parameters on the radiation characteristics of the antenna has been studied in detail and presented.

3.1. INTRODUCTION

Planar monopole antenna are the most widely used antennas for airborne communication due to simple design, planar shape, wide bandwidth and nearly omnidirectional radiation coverage. The conventional height of these antennas are in the order of $\lambda/4$ at lowest frequency of operation. Due to the mechanical limitations of airborne antennas, height reduction techniques are generally applied to planar monopole antennas while designing for VHF band. Another main handicap of these antennas is the requirement of $\lambda/4$ ground plane around the feed point of antenna. Airborne antennas utilize the skin of the platform as ground plane. Since airborne communications are mainly based on HF/VHF band, the limited space available on the platform constrains the ground plane size available for these antennas. This results in deteriorated radiation characteristics. Literature presents printed monopole antennas as a solution to the backing ground plane constrained monopole antenna applications [57].

A printed monopole antenna structure consists of a strip or a flat plate printed on a dielectric substrate and a ground plane printed either on same side or opposite side of substrate depending upon the feeding method chosen.

A standard microstrip-fed printed strip monopole antenna (PSMA) design is shown in Fig.3.1. In the figure, a 50Ω microstrip line of width 'w' and a strip monopole of length 'L_m' are printed on a dielectric substrate of relative permittivity 'ε_r' and height 'h'. A partial ground plane having a length, L_g and width W_g is printed on the other side of the substrate.
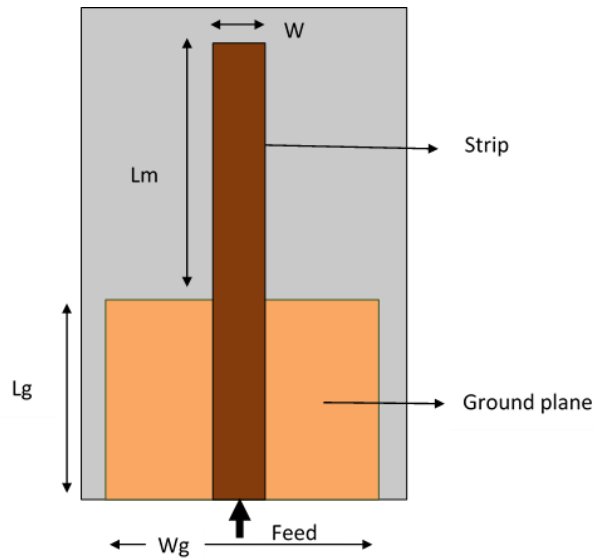
Fig 3.1. Printed strip monopole antenna.

According to [139], the optimum length of printed strip monopole L_m is 0.23λ. As per this, when a printed strip monopole antenna is designed for resonant frequency in VHF band, say for 150 MHz, on a substrate of FR4 dielectric with ε_r = 4.4 and height h = 0.16cm, the dimensions will be: L_m = 46cm and the total length of the antenna is 70cm. Since compactness is a major concern for airborne antennas, the dimension of printed strip monopole antenna is quite large.

To achieve compactness and impedance matching, the patch as well as the ground plane of printed strip monopole antenna has to be modified. Folding or bending technique is a common method used for reducing antenna dimension. In this chapter, a bifolded printed bent monopole antenna with resistance loading and L shaped ground plane operating in VHF band is presented for airborne applications.

3.2 BIFOLDED PRINTED BENT MONOPOLE ANTENNA

3.2.1. Antenna Evolution

Airborne monopole antennas has height restrictions in VHF band. In order to overcome this, one of the method used was folding or bending the radiating strip of monopole antenna into an inverted L shape (into bent monopole) (Antenna 1 in Fig 3.2) [102-103].

A single folding on the horizontal arm of the bent monopole antenna further reduced the antenna's height resulting in single folded printed bent monopole antenna (Antenna 2 in Fig 3.2).

A second folding again reduced the antenna's height and resulted in bifolded printed bent monopole antenna (Antenna 3 in Fig 3.2). Folding the radiating patch increases the effective length of surface current path, and decreases the resonant frequency. But, the height reduction achieved by second folding also decreased the impedance matching at desired resonant frequency. To improve the impedance matching, the ground plane of bifolded printed bent monopole antenna was modified to L shape.

Decreasing the height of the antenna by triple folding the horizontal arm of the bent monopole antenna resulted in two problems: 1). the impedance matching at the desired frequency decreased drastically and it became difficult to match the antenna. 2). the polarization of antenna changed and the null depth of the antenna became very less. Hence, the bifolded printed bent monopole antenna (Antenna 3) was selected as the optimum design.

The evolution of the antenna is shown in Fig 3.2. FR4 epoxy (ε_r = 4.4, tan δ = 0.02 and thickness 1.6mm) was used as substrate for the design of the antenna. The width of the substrate was chosen to be less than 30 cm for all archetypes. The return loss characteristics of these antennas are shown in Fig 3.3.

(a) Antenna 1   (b) Antenna 2   (c) Antenna 3
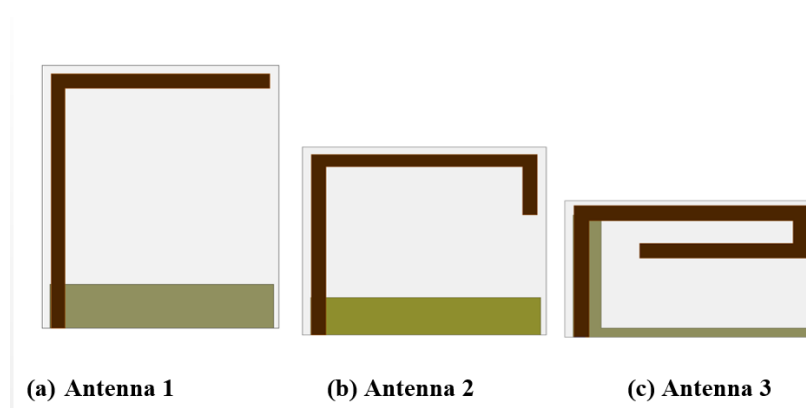
Fig 3.2. Antenna Evolution
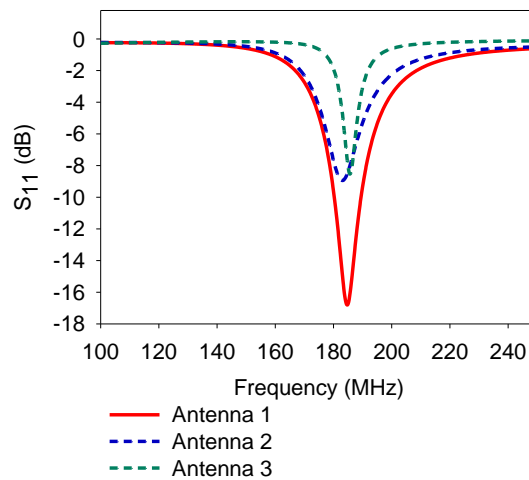
Fig 3.3 Simulated variation of return loss with frequency of the antennas in the design evolution of bifolded printed bent monopole antenna

3.2.2. Antenna Geometry

The antenna geometry is depicted in Fig 3.4. The radiating patch of the antenna consists of a bent monopole configuration which is folded twice in order to reduce antenna dimension for a lower resonant frequency.

The ground plane consists of L shaped patch. The partial ground plane of a standard printed monopole antenna is modified in this design into L shape. This shape was chosen for ground plane as it was found that the vertical length of 'L' improves the impedance matching [114].

Edge feeding of 50Ω is used to excite the antenna. An aluminium base plate of rectangular shape was used for mounting the antenna. The base plate holds the connector and serves as an interface between antenna and platform.
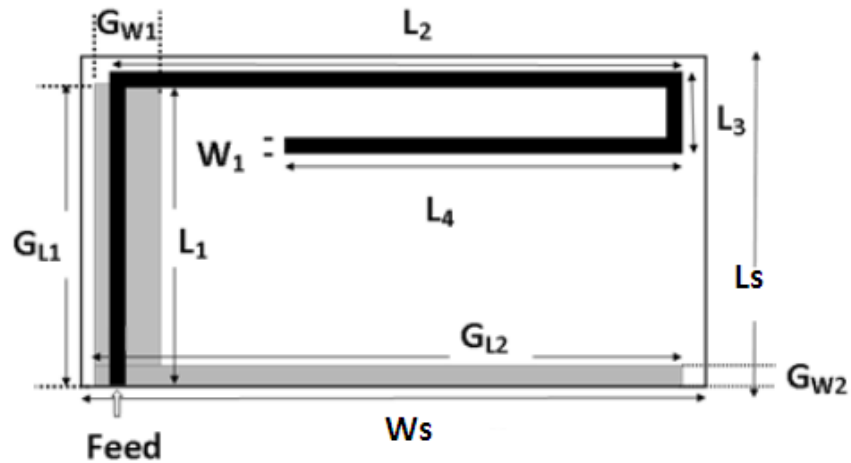
(a)
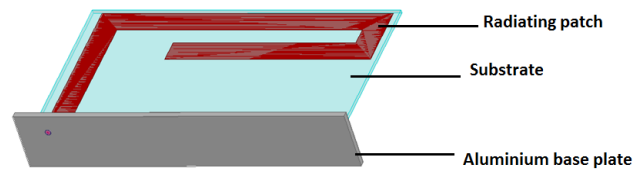
(b)

Fig 3.4. Geometry of bifolded printed bent monopole antenna

3.3. CHARACTERISTICS OF A TYPICAL STRUCTURE

Before going into a detailed study of the patch geometry, the basic characteristics of a typical patch is discussed. The substrate used is FR4 glass epoxy of dielectric constant ε_r=4.4 and thickness 0.32cm. The dimensions of the geometry are:

Table 3.1. Dimensions of the geometry

Parameters	L_s	W_s	L_1	L_2	L_3	L_4	W_1	G_{L1}	G_{L2}	G_{W1}	G_{W2}
Value (mm)	14.5	27	140	250	56	180	12	130	255	30	10

The dimensions of aluminium base plate used for mounting the antenna is 0.2cm X 29cm X 5cm.

3.3.1. Return loss

The reflection characteristics of this antenna is shown in Fig 3.5. The fundamental frequency of resonance of this structure is 181.3 MHz.
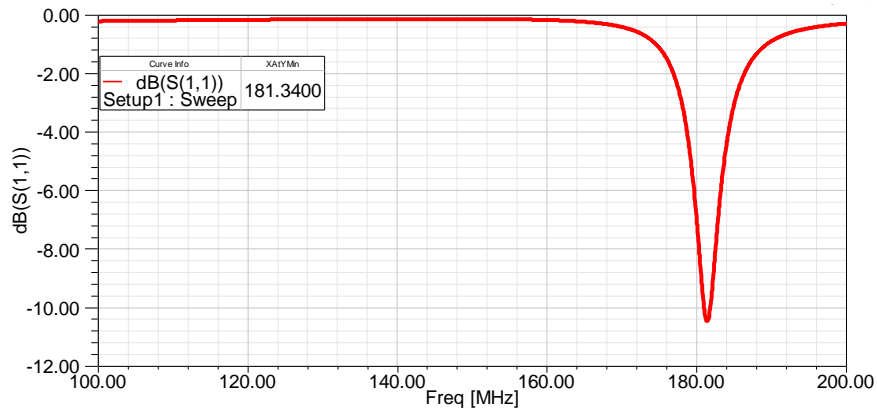
Fig 3.5 Simulated variation of return loss with frequency of bifolded printed bent monopole antenna

3.3.2 Surface current distribution

The surface current distribution of the antenna is a good tool for finding the resonant mechanism, polarization and hence the radiation characteristics. The surface current distribution along the radiating patch and the ground plane at resonant frequency is shown in Fig 3.6 (a) and (b) respectively. It is clearly evident from Fig.3.6 that there are a quarter wave current variations along the length of monopole strip. The contribution of ground plane towards resonance is very feeble.
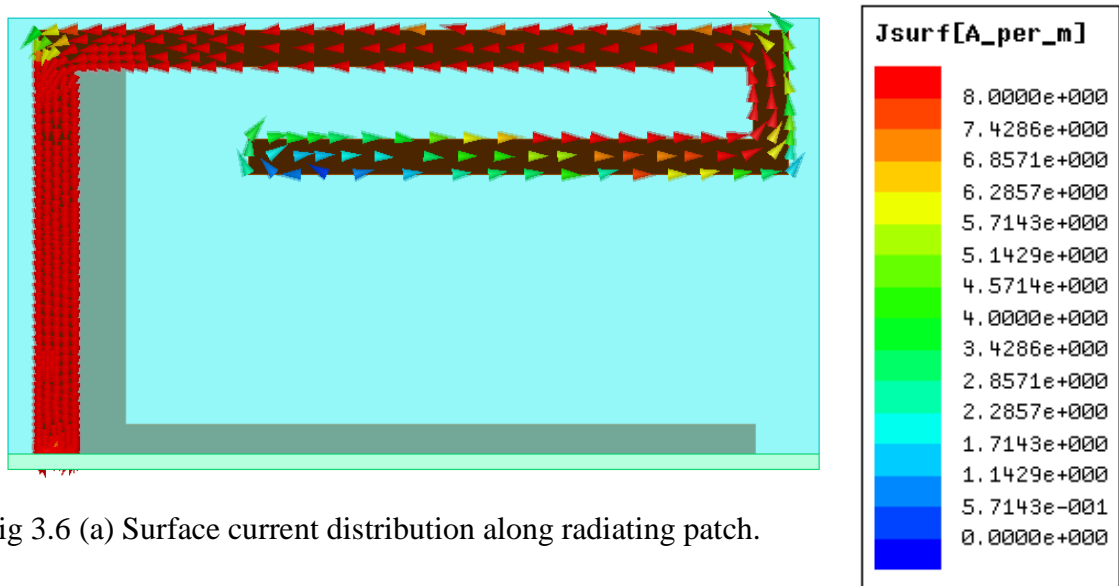
Fig 3.6 (a) Surface current distribution along radiating patch.
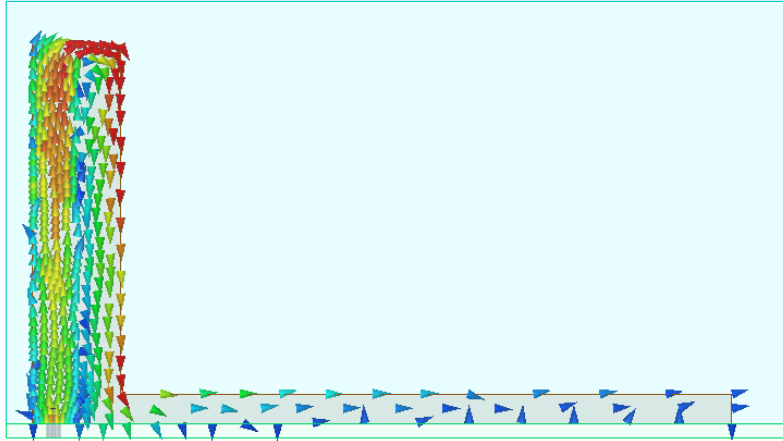
Fig 3.6 (b) Surface current distribution along ground plane.

3.3.3 Radiation pattern and gain

The simulated radiation pattern of the antenna (3D and 2D) at resonant frequency is shown in Fig 3.7 (a) and (b). The antenna shows omnidirectional radiation pattern in azimuth plane. It can be observed from the figure that the radiation pattern of the antenna is tilted and the null depth is less compared to conventional monopole antenna. The reason for this is the higher concentration of current on horizontal arms of the radiating patch, [105]. The simulated gain and efficiency of the antenna at resonant frequency is plotted in Fig 3.7 (c).

(a)

(b)
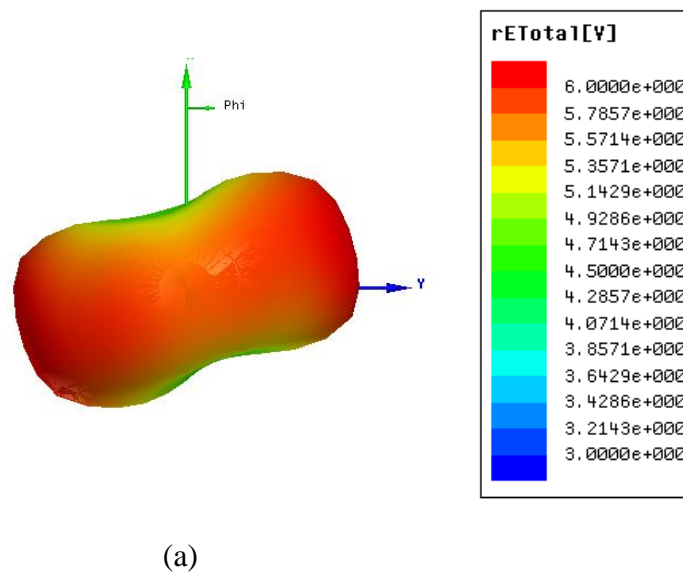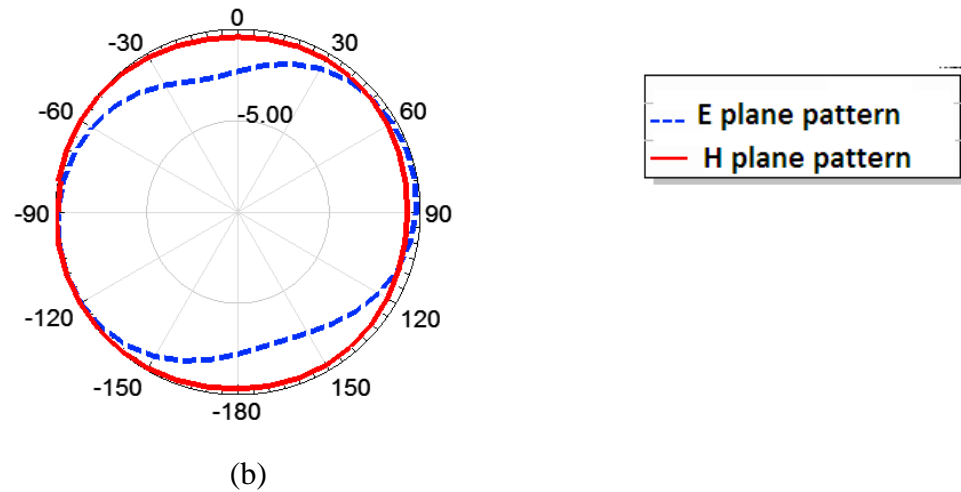
Fig 3.7. Simulated (a) 3D; (b) 2D radiation pattern of bifolded printed bent monopole antenna.

(C)
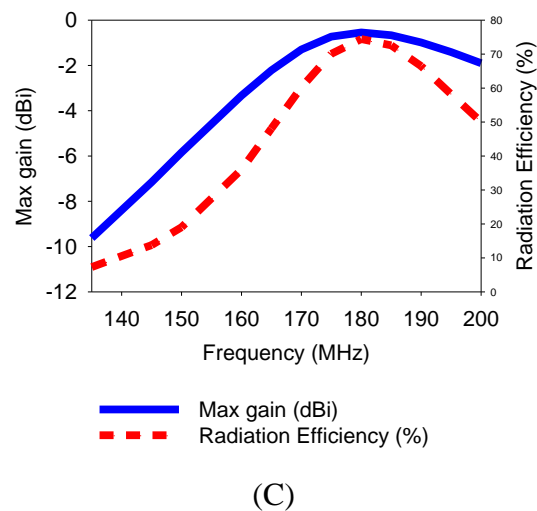
Fig 3.7. (c) Simulated variation of gain and efficiency with frequency of bifolded printed bent monopole antenna

3.4 BANDWIDTH ENHANCEMENT OF BIFOLDED PRINTED BENT MONOPOLE ANTENNA

The major design requirements of VHF airborne antennas are compact size and wide bandwidth. It is known that decreasing the length of radiator also decreases impedance and radiation resistance of antennas. It also results in narrow bandwidth. The bifolded printed bent monopole antenna with typical dimensions shown in Table 3.2 had a very compact size, but with 3:1 VSWR bandwidth of only 4MHz. Since airborne application demands wide bandwidth, the antenna required to operate over a wide frequency range.

The variation of impedance with frequency of the bifolded printed bent monopole antenna is plotted in Fig 3.8. It can be observed that the resistive part of the impedance is very low over a wide frequency range and also the reactive part of the impedance is highly capacitive. This makes the antenna very difficult to match to a source whose output impedance is on the order of 50ohms over a wideband.
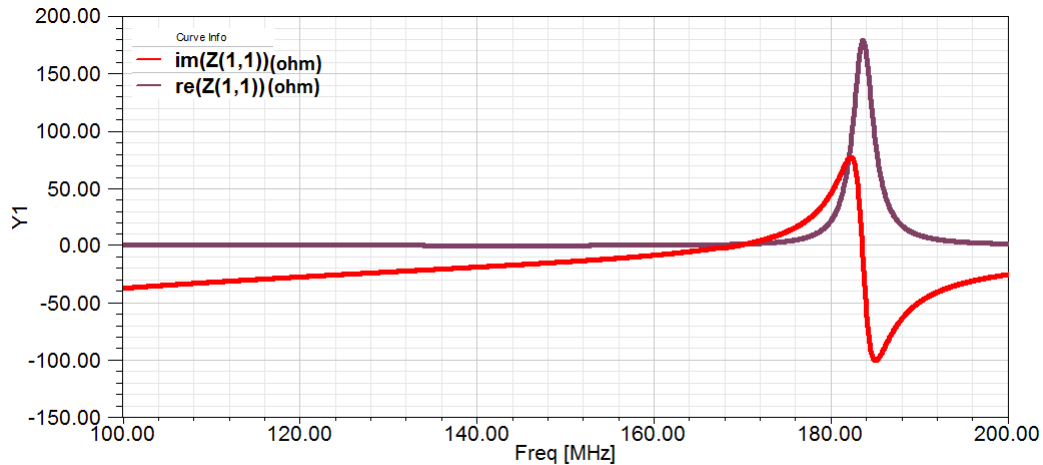
Fig 3.8 Variation of impedance with frequency of bifolded printed bent monopole antenna.

To increase the bandwidth of operation, the resistive component of the input impedance of the antenna has to be increased. The only practical way to execute this without compromising length or degradation of azimuthal radiation pattern is to incorporate resistive loading within the antenna [140-142]. Hence, resistance loading method was employed to the radiating patch. The inclusion of resistance within the antenna will increase the resistive component of input impedance over the entire band. The effect is most distinct when the resistance is located near the feed [143].

In order to fix the resistance value, a parametric analysis was carried out on the effect of resistance on the frequency response of the antenna. The effect of resistance on the return loss of the antenna is depicted in Fig 3.9. From the parametric analysis, a resistor value of 23.5Ω was selected as it gives required bandwidth.
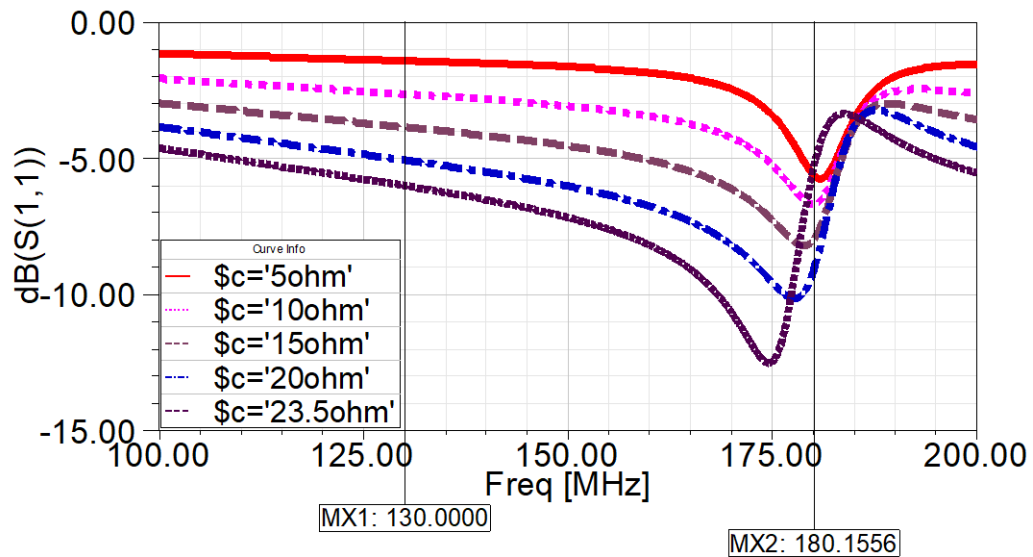
Fig 3.9. Effect of resistance loading on the return loss of the antenna

The effect of resistor on the radiation characteristics of the antenna is analyzed using HFSS simulation. The surface current distribution of the radiating patch and ground plane at center frequency 155 MHz is shown in Fig 3.10(a) & (b). By analyzing this figure and comparing it with Fig 3.6, it is evident that the intensity of the current distribution along the arms is decreased by the presence of the lumped resistor loading, due to the power loss in resistor.

(a)

```
Jsurf[A_per_m]

    8.0000e+000
    7.4286e+000
    6.8571e+000
    6.2857e+000
    5.7143e+000
    5.1429e+000
    4.5714e+000
    4.0000e+000
    3.4286e+000
    2.8571e+000
    2.2857e+000
    1.7143e+000
    1.1429e+000
    5.7143e-001
    0.0000e+000
```

(b)
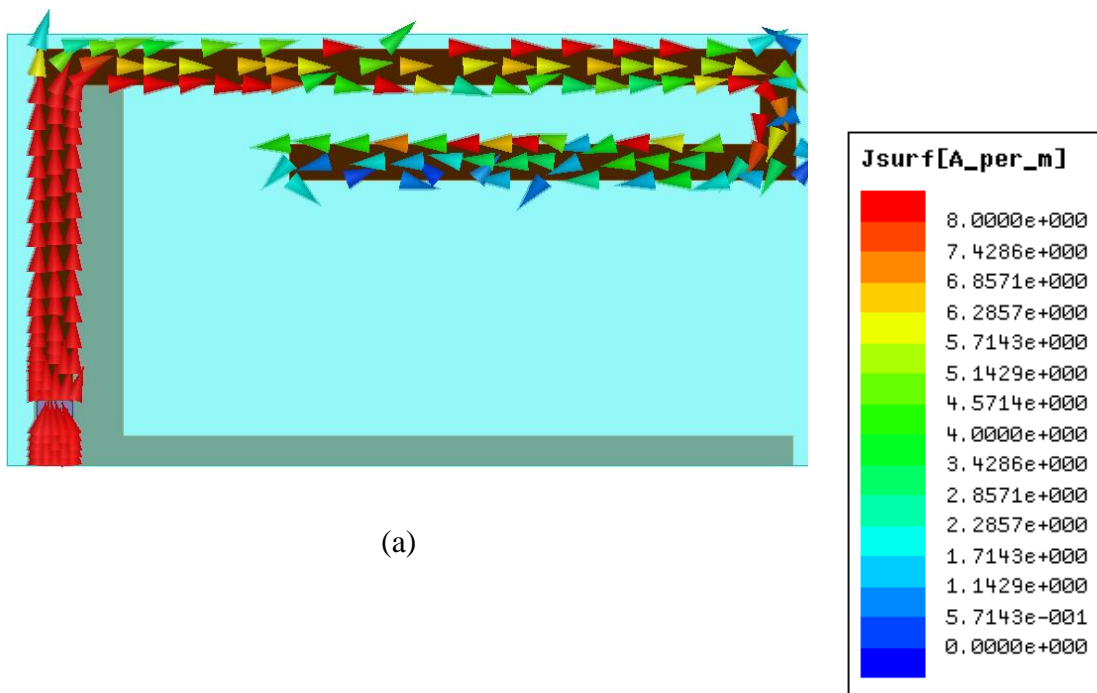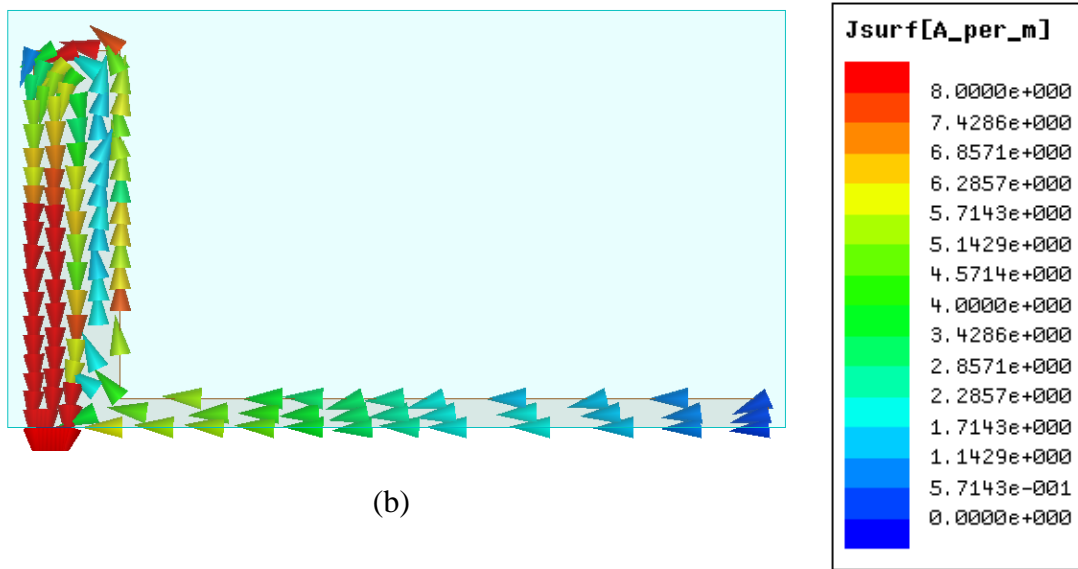
Fig 3.10 surface current distribution along (a) Radiating patch (b) Ground plane.

Fig 3.11 shows the 3D radiation pattern at center frequency 155 MHz. It can be observed that radiation pattern of the antenna is unaffected by the resistance loading.


```
rETotal[V]

    1.7902e+000
    1.6980e+000
    1.6059e+000
    1.5137e+000
    1.4216e+000
    1.3294e+000
    1.2373e+000
    1.1451e+000
    1.0529e+000
    9.6078e-001
    8.6863e-001
    7.7647e-001
    6.8431e-001
    5.9216e-001
    5.0000e-001
```
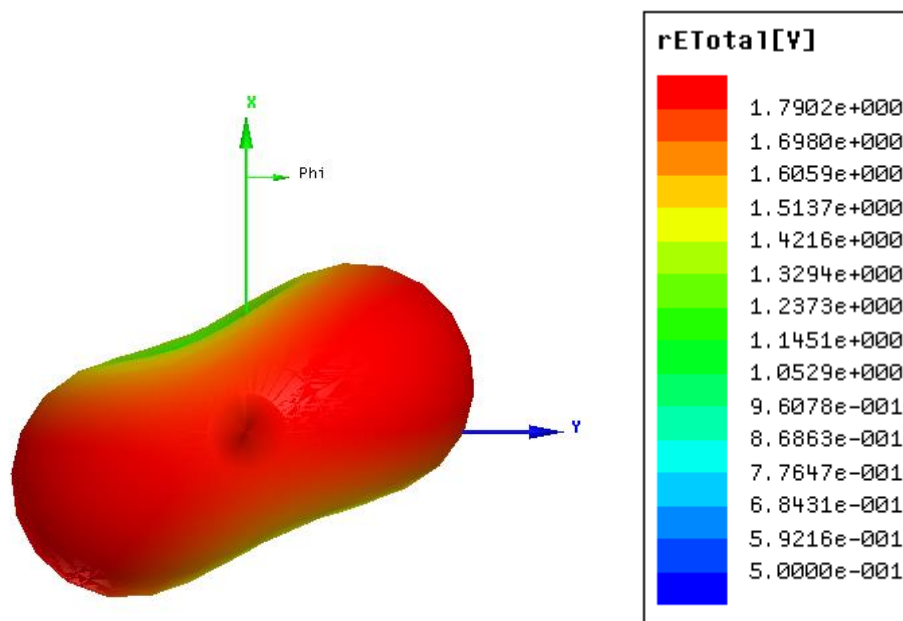
Fig 3.11. Simulated radiation pattern of bifolded printed bent monopole antenna with resistance loading.

The simulated variation in gain and efficiency of the antenna with frequency is shown in Fig 3.12.
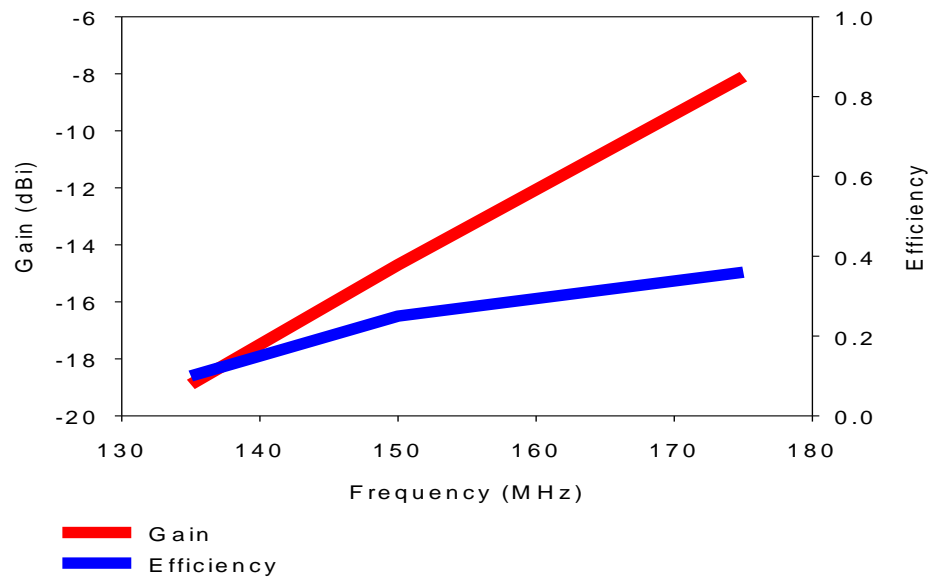
Fig 3.12 Variation of gain and efficiency with frequency of bifolded printed bent monopole antenna

The power gain and efficiency of the antenna is less, although it is comparable to the conventional airborne blade monopole antenna of same height. The reason for this reduced gain is the compact structure of the antenna and the resistance loading. It is known that the radiation resistance of short monopole antennas is very low and, hence, the power gain of these antennas is also low [144].

The resistance loading used for bandwidth enhancement also contributes to the gain reduction. It is because the resistances are placed nearer the feed. Most of the current is concentrated in the lower portion of the structure. Hence a resistor placed near the base of a short antenna will dissipate some amount of the power that would otherwise be radiated.

Simulated results shows that the radiation efficiency of the antenna is low due to the impact of resistance loading.

3.5. PARAMETRIC ANALYSIS

A parametric study on the proposed antenna design was carried out to investigate the influence of each antenna dimension on the antenna performance. One parameter is varied while the other parameters are kept constant, as shown in Table

3.1. The variation in the frequency response of the antenna is analyzed by studying the variation of the distributed reactance with dimensions. These values are calculated using the method explained in Section 2.6.3.

3.5.1 Effect of radiating patch dimensions

The length of the radiating element determines the resonating frequency. The decrease in the resonant frequency with the increase in the dimensions L_1, L_2, L_3 and L_4 is plotted in the figures Fig 3.13 (a-d). It was found that the resonant frequency is determined by the total length of the arms of the radiator. The contribution of L_1 towards resonant frequency is less as it acts as a microstrip feed line to couple RF power to radiator. The contribution of L_3 towards resonant frequency is found to be comparatively high.
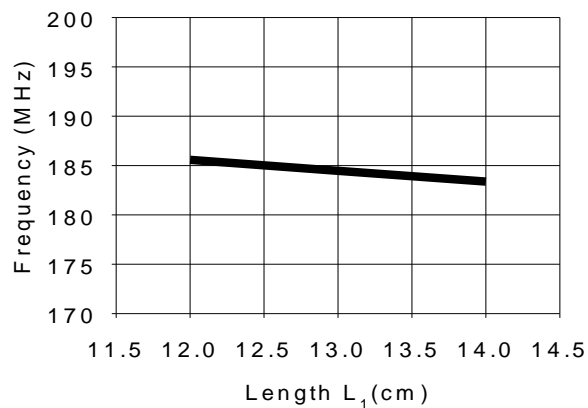
(a)
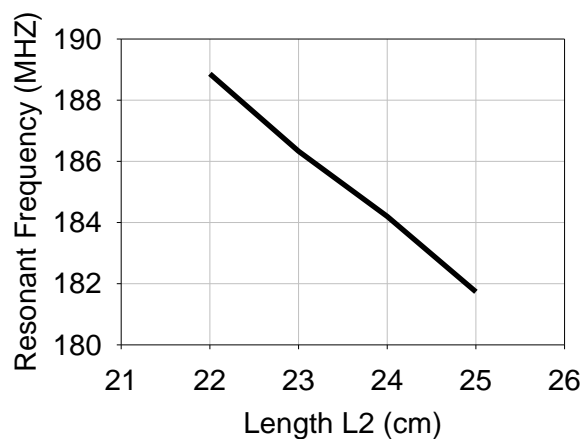
(b)
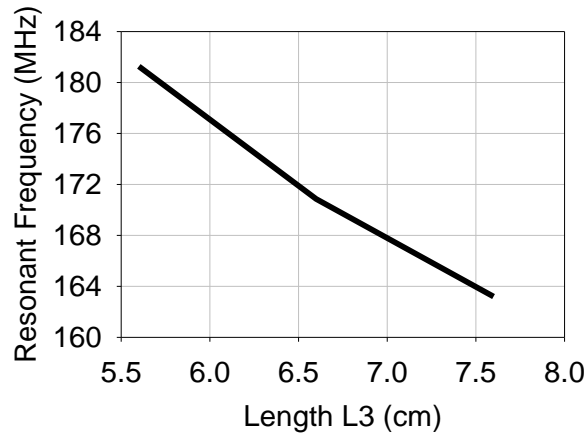
(c)
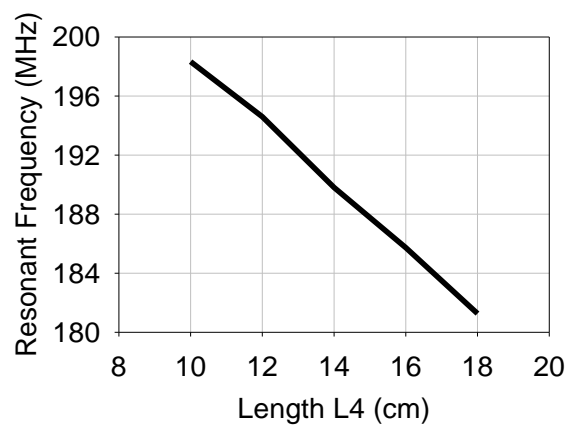
(d)

Fig 3.13 Effect of (a) L_1 (b) L_2 (c) L_3 (d) L_4 on resonant frequency.

The proposed antenna was simulated for various patch widths and the effect of this parameter on the return loss characteristics is shown in Fig 3.14. The radiating patch width (W_1) is varied from 2mm to 8mm in step of 2mm. It can be observed from the figure that 3:1 VSWR bandwidth (for return loss less than -6dB) of the antenna increases as the radiating patch width increases from 2mm to 8mm, where, the lower edge of the band remains almost constant and the upper edge of the band increases. It can be seen from Fig 3.15 that the increase in width W_1 increases the capacitive reactance which result in the increased bandwidth.
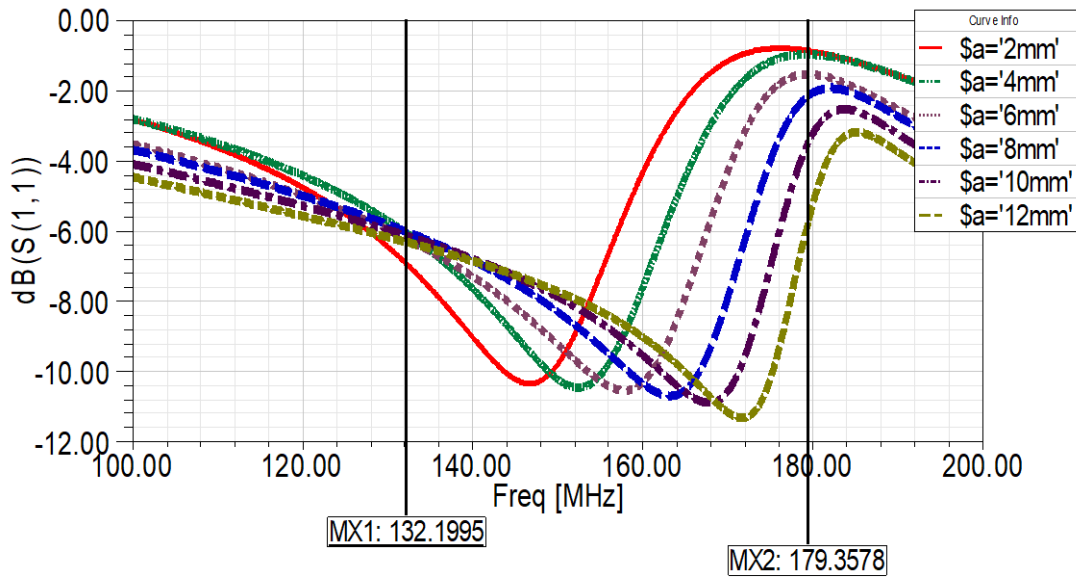
Fig 3.14. Effect of patch width W_1.
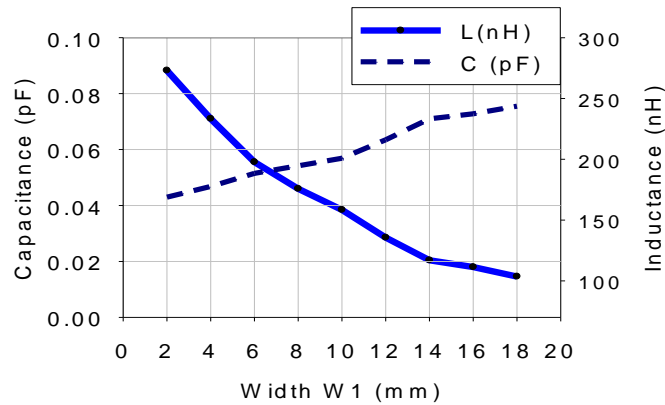
Fig 3.15 Effect of W_1 on the impedance of the antenna.

3.5.2 Effect of ground plane dimensions

The proposed antenna was simulated for various ground plane dimensions. The effect of G_{W1} on the return loss of antenna was studied by varying G_{W1} from 1cm to 4cm in step of 1cm and is plotted in Fig 3.16. The bandwidth of the antenna for S11< -6dB, increases with increase in G_{W1}. The lower edge of the band remains almost constant and the upper edge of the band increases. The effect of G_{W1} on the impedance of the antenna is plotted in Fig 3.17. It is evident from the figure that the increase in the bandwidth is due to the increase in the capacitive reactance of the antenna.

55
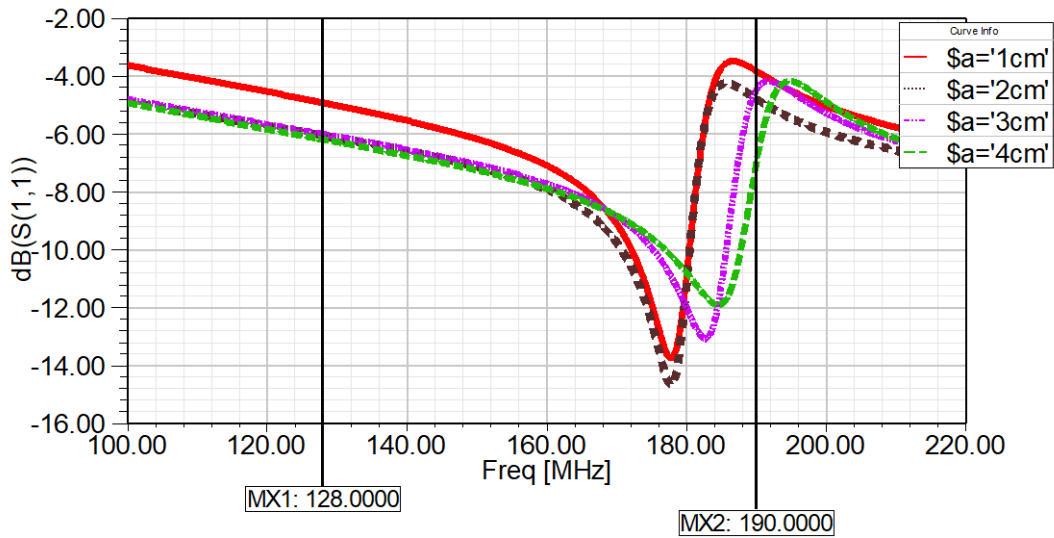
Fig 3.16. Effect of ground plane dimension G_{W1}.
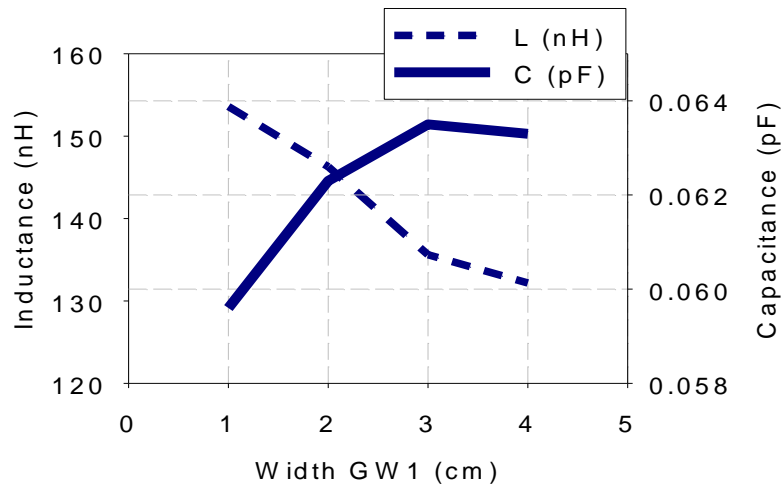
Fig 3.17 Effect of G_{W1} on the impedance of the antenna.

To study the effect of ground plane length G_{L1}, the parameter was varied from 5cm to 13cm in step of 3cm. The effect of G_{L1} on the return loss of the antenna is shown in Fig 3.18. It can be seen from figure that increase in G_{L1} improves the impedance matching of the antenna at lower frequency.
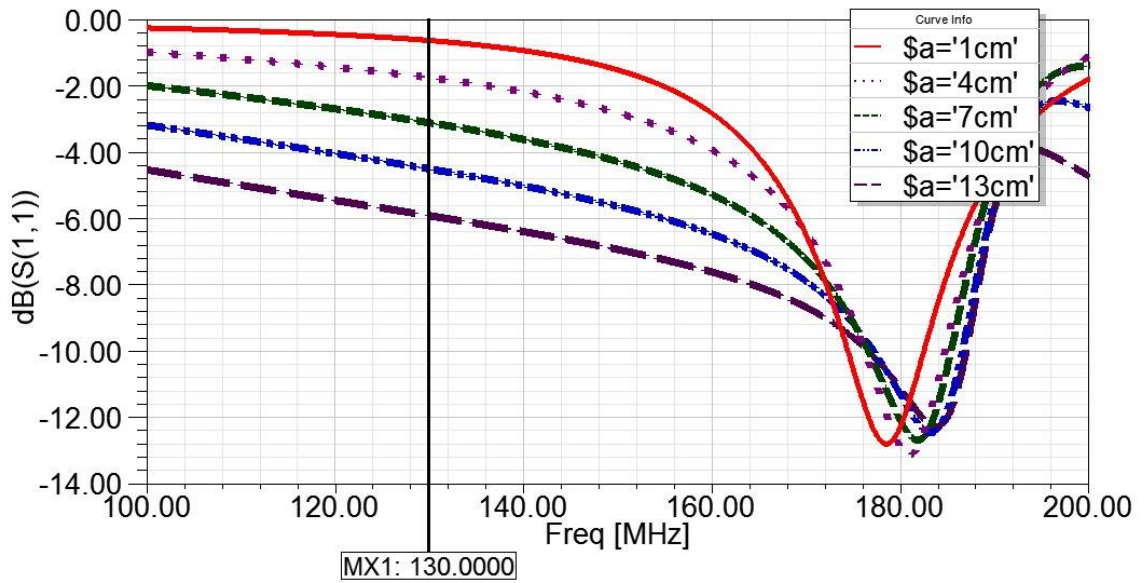
Fig 3.18. Effect of Ground plane dimension G_{L1}.

The effect of G_{L2} on the radiation characteristics of the antenna was studied by varying G_{L2} from 1cm to 25cm in step of 5cm. The effect of G_{L2} on the return loss of the antenna is shown in Fig 3.19. It was found that, the increase in G_{L2} decreases the resonant frequency, shifting the higher edge of the frequency band towards lower side. The lower edge frequency of the band remains almost constant with increase in G_{L2}. The bandwidth decreases with increase in G_{L2}.

The simulated elevation pattern of the antenna at three different values of G_{L2}, i.e. 3cm, 10cm and 25cm is plotted in Fig 3.20. It can be observed that the polarization of the antenna changes with increase in G_{L2}.
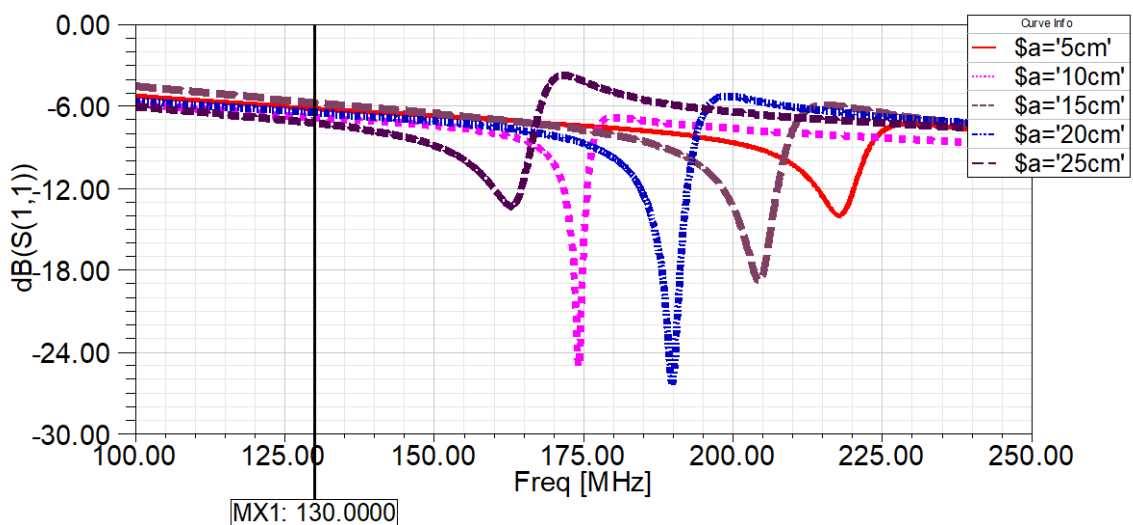
Fig 3.19. Effect of G_{L2} on return loss of the antenna.
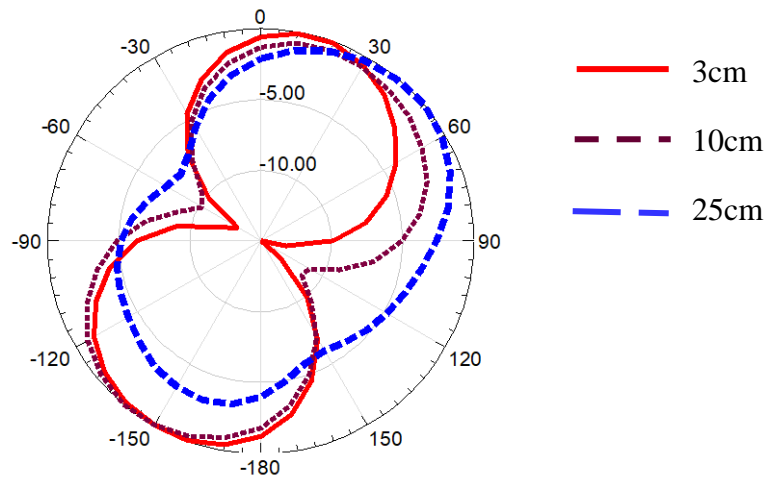
Fig 3.20. Effect of G_{L2} on the radiation pattern of the antenna.

The effect of G_{W2} on the return loss of the antenna was studied and is plotted in Fig 3.21. It can be seen that the increase in G_{W2} decreases the bandwidth of the antenna slightly by shifting the upper edge frequency of the band towards lower side.
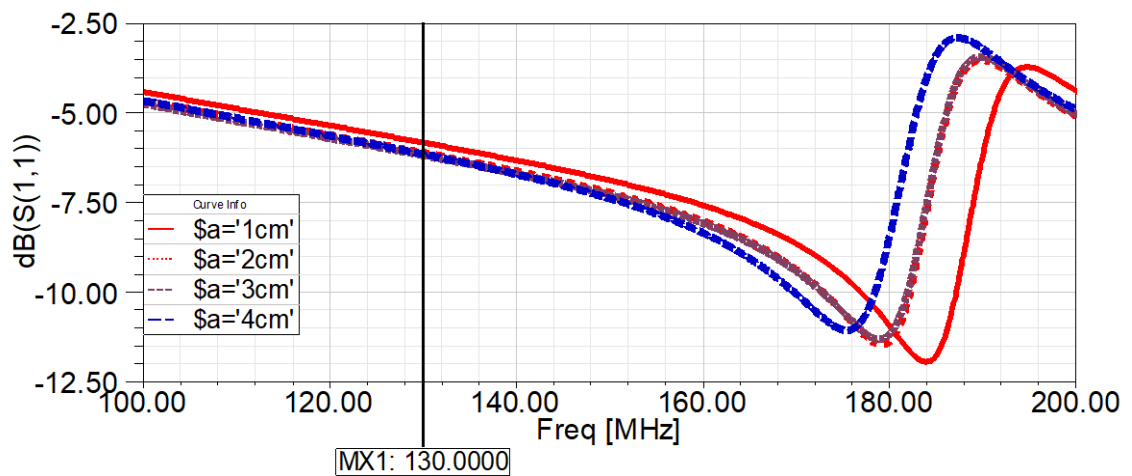
Fig 3.21. Effect of ground plane dimension G_{W2}.

3.5.3 Effect of substrate parameters

The effect of the thickness of the substrate on the impedance bandwidth and gain of the antenna is studied by varying the thickness from 1.6mm to 6.4mm in step of 1.6mm. Unlike microstrip patch antennas, increase in the thickness of the substrate decreases the antenna impedance bandwidth. However, the gain of the antenna increases with increase in the thickness of the substrate. The effect of substrate thickness on the impedance bandwidth of the proposed antenna is shown in Fig 3.22.

It can be observed from the figure that, the lower edge of the frequency band is nearly unaffected with increase in substrate thickness whereas the upper end decreases, resulting in a reduced impedance bandwidth. The variation in the gain of the antenna at frequencies 135, 150 and 175 MHz for various substrate thickness is tabulated in Table 3.2. The gain of the antenna for substrate thickness 3.2mm is greater than that for thickness 1.6mm as seen from Table 3.2. So, as a compromise, the thickness of the antenna was fixed to 3.2mm as it could give improved gain in the entire frequency band.
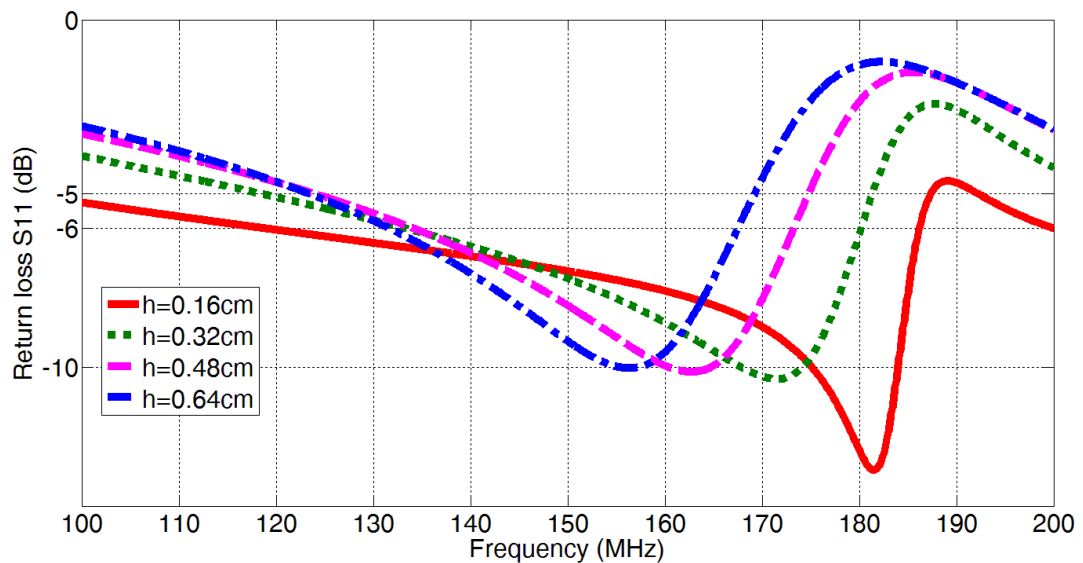
Fig 3.22 Effect of substrate thickness on the return loss of the antenna.

Table 3.2. Effect of substrate thickness on the gain of the antenna.

Frequency (MHz)	Simulated peak gain in dB for various substrate thickness			
	1.6mm	3.2mm	4.8mm	6.4mm
135	-29.89	-18.9	-16.6	-15.4
150	-24.25	-14.7	-12.5	-11.3
175	-14.96	-8.14	-7.03	-7.01

The effect of substrate dielectric constant on the antenna resonant frequency was studied by varying ε_r values from 1 to 10 and is plotted in Fig 3.23. It can be found that the effect of dielectric constant of the substrate on decreasing the resonant frequency of printed monopole antenna is not prominent as in other microstrip antennas. This is because printed monopole antennas can be considered as a monopole

antenna on a substrate above a very thick air dielectric substrate, that the effective permittivity is closer to unity [145].
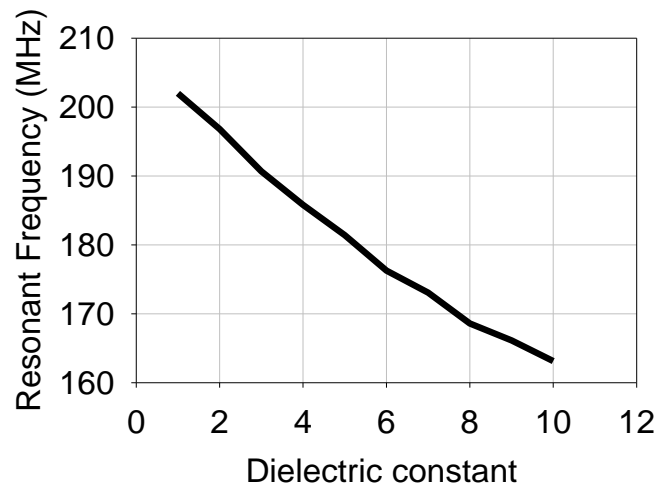
Fig 3.23 Effect of substrate dielectric constant on resonant frequency of bifolded printed bent monopole antenna.

3.5.4 Effect of the mounting ground plane

The bifolded printed bent monopole antenna was developed for airborne applications, where it is to be mounted on the skin of the platform. The effect of the size of mounting ground plane was analyzed using HFSS simulation. For this two conditions was considered: one for the free standing antenna and the other- antenna mounted on a ground plane of 1.2m diameter.

The return loss and gain of the antenna plotted in the above conditions is shown in Fig 3.24 (a) and (b) respectively. It can be observed from Fig 3.24 (a) that the frequency band shifts slightly towards lower region. But the effect of ground plane on this printed monopole antenna is very less compared to conventional monopole antenna. It can be noticed from Fig 3.24 (b) that the gain of the antenna is improved in the entire band when mounted on large ground plane.
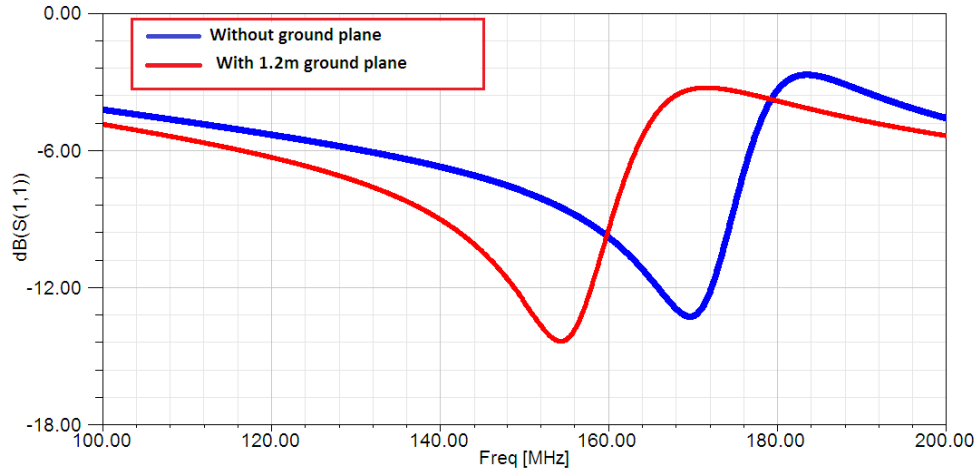
Fig 3.24 (a) Comparison on the return loss for antenna mounted on 1.2m diameter ground plane and for free standing condition.
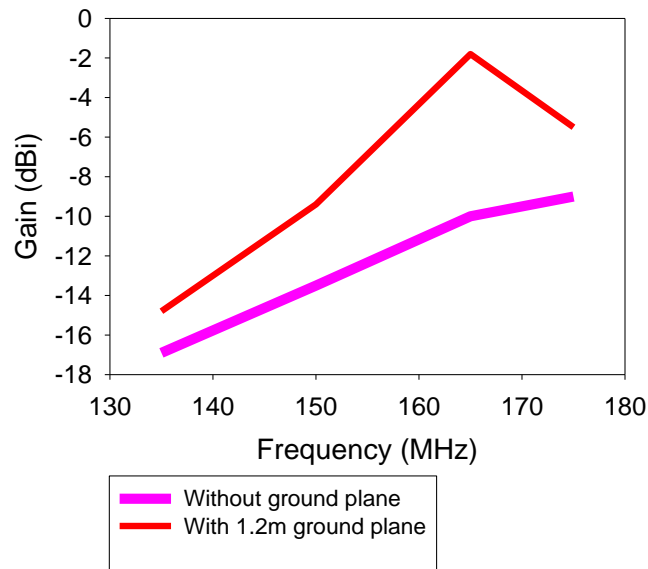
Fig 3.24 (b). Comparison on the gain of the antenna mounted on 1.2m diameter ground plane and for free standing condition.

3.6 ANTENNA FABRICATION

A bifolded printed bent monopole antenna shown in Fig 3.4 is fabricated on FR4 glass epoxy substrate of $\varepsilon_r = 4.4$ and loss tangent 0.02. The antenna has two layers of 1.6mm thick substrates, the top layer contains the radiating element and bottom layer contains the ground patch, placed back to back.

The dimensions of the antenna are as shown in Table 3.1.

A lumped resistor of 23.5Ω is inserted to the radiating patch near the feed of the antenna. An aluminium base plate of rectangular shape of dimensions 0.2cm X 29cm X 5cm was used for mounting the antenna. The aluminium base plate was used to hold the connector and provide interface to platform. A 50Ω TNC connector is used to excite the antenna. The center conductor is connected to the printed radiating element of the antenna and outer to the ground patch and to the aluminium base plate. A photograph of the fabricated antenna is shown in Fig 3.25.
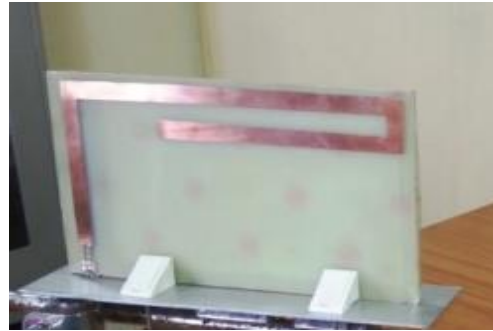
Fig 3.25. Photograph of fabricated antenna with base plate.

3.7   EXPERIMENTAL RESULTS

The performance of the antenna was evaluated using E5071C Vector Network Analyzer. The measured return loss of the antenna is found to be less than -6dB over the referred frequency band. The antenna exhibits a 3:1 VSWR bandwidth of 32% at the center frequency 155 MHz as shown in Fig 3.26. Measured result shows a good agreement with the simulated result. The slight discrepancy is due to the fabrication tolerance.
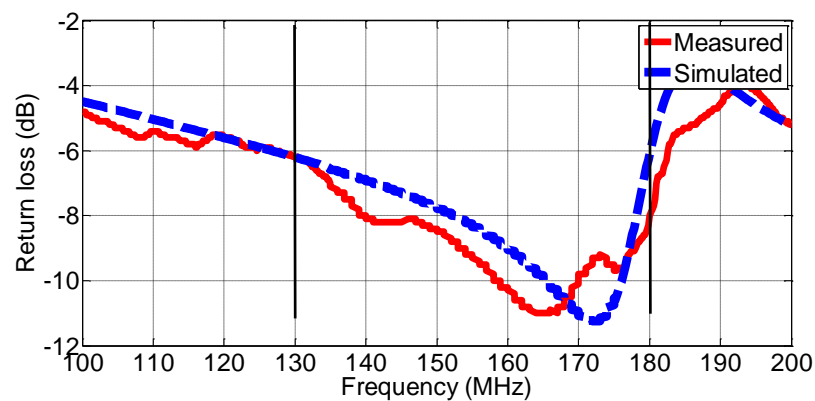
Fig 3.26. Measured return loss of bifolded printed bent monopole antenna with resistance loading.

The antenna was tested for its far field radiation characteristics in an open field. The measured H plane and E plane radiation patterns of the antenna at 135, 150 and 175 MHz is shown in Fig 3.27 (a) & (b). It can be seen that the H plane radiation pattern of the proposed antenna is nearly omnidirectional at all frequencies. As seen from Fig 3.27 (b), the radiation pattern is tilted and the null depth of these antennas is less for higher frequencies. The reason for this is the higher concentration of current on the horizontal arms of the radiating patch.

(a)

(b)
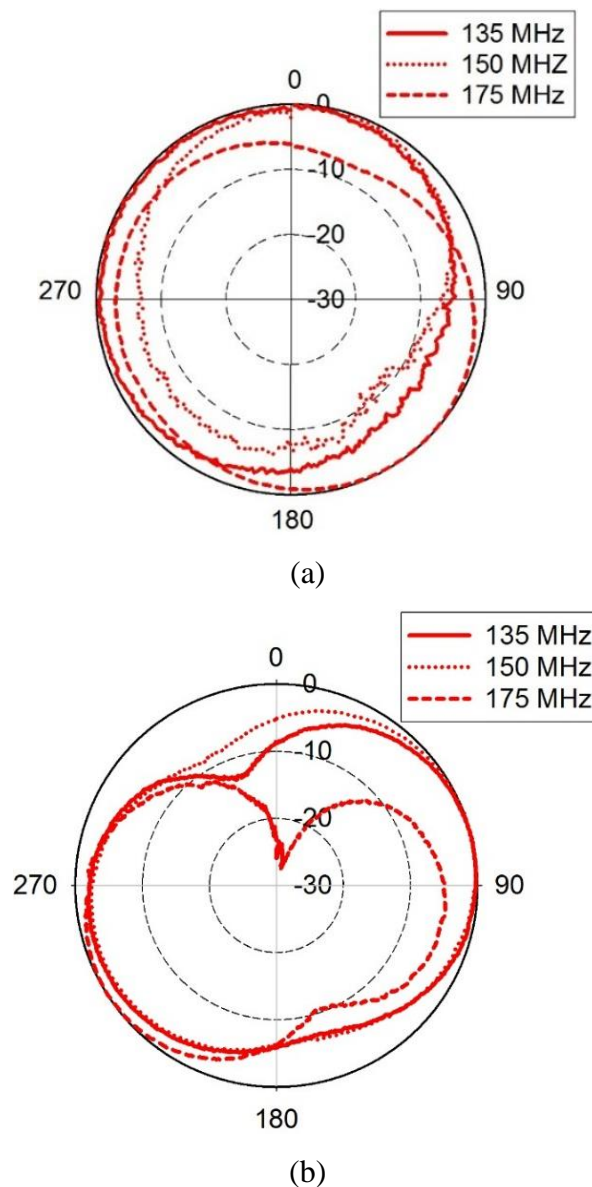
Fig 3.27 Measured Radiation pattern at (a) Azimuth plane (b) Elevation plane.

The boresight gain was measured using gain comparison method. The measured gain of the antenna at three discrete frequencies 135, 150 and 175 MHz is

shown in Fig 3.28. This measured gain is compared with the gain of an airborne blade monopole antenna operating in same frequency band reported in the literature [37] and is shown in Fig 3.28. The low gain value is expected as the loaded resistance absorbs a part of the energy. The decreased height and minimal mounting ground plane size of the bifolded printed bent monopole antenna compared to the conventional airborne blade monopole antenna [37] is the reason for the decreased gain of the referred antenna at the higher frequency side.
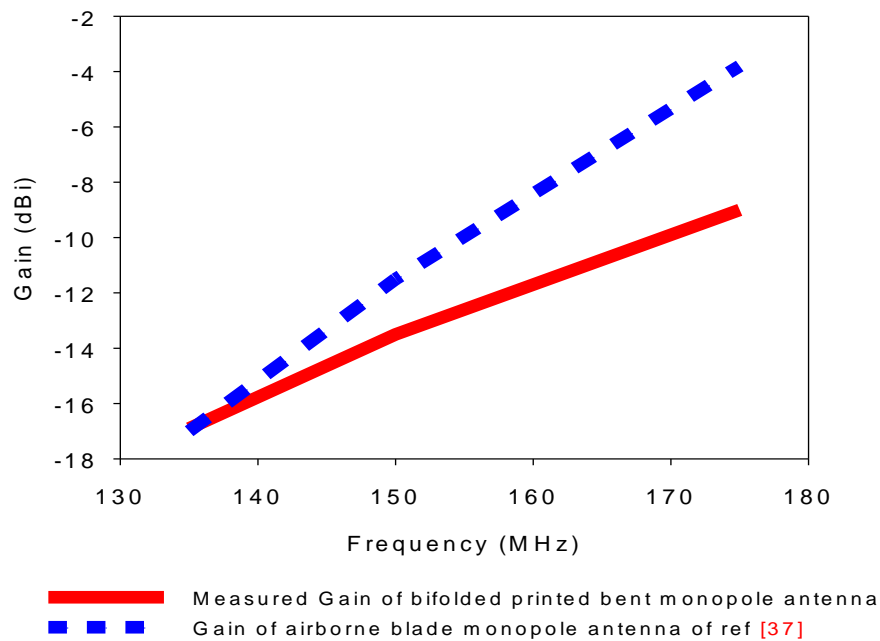
Fig 3.28 Measured gain.

3.8. SUITABILITY OF ANTENNA FOR AIRBORNE APPLICATIONS

Airborne antennas have stringent electrical and mechanical constraints. The physical constraints are its size, environmental factors, space constraints for optimum mounting location and the effects due to airframe [1,146]. The shape and size of the antennas used for airborne applications are restricted by the physical length, width and height of the aircraft and it is further restricted by the environment and aircraft operations. Applications like communication, navigation, telemetry, electronic warfare demands wideband monopole antennas with omnidirectional coverage in azimuth and near azimuth plane with linear polarization.

The main features of bifolded printed bent monopole antenna are: compactness, wide bandwidth and mounting ground plane independence.

The proposed antenna achieves a height reduction of 78% compared to basic printed strip monopole antenna (Fig 3.1) and 73% compared to conventional quarter wavelength planar monopole antenna. The height of the antenna is of the order of 0.065λ at lowest frequency of operation. This compact size make the antenna well suitable for mounting on aircrafts especially for mounting positions with less ground clearance like the belly of helicopter.

The antennas possess wide impedance bandwidth (32%) at VHF band, and possess omnidirectional radiation pattern with vertical polarization, thus satisfying the electrical requirements of airborne VHF monopoles for communication, navigation purposes.

Since the antenna belongs to the class of printed monopoles, they require minimal ground plane on platform, thus, the effect of airframe ground on this antennas is little. Thus they can overcome the degraded radiation performance of conventional blade monopoles due to the lack of sufficient ground plane on platform. The space constraints in the siting locations faced by the conventional blade monopole antennas requiring λ/4 ground plane are also overwhelmed.

The antenna is designed in planar configuration which makes it easily streamlined. Due to the compact size, the wind loads on these antennas due to drag is also less.

The antenna is fabricated using FR4 Epoxy material. The material properties of the antennas are discussed in chapter 2 (Table 2.1). The substrate can operate in a wide temperature range and pressure difference. The tensile strength of the substrate is very high making it suitable to operate for airborne applications.

A comparison of this antenna was carried out with the airborne blade monopole antenna reported in literature operating in the band of 135 MHz - 175 MHz and is tabulated in Table 3.3. It is obvious from the table that the antenna size and radiation performance is comparable to that of airborne blade monopole antenna with the added advantage of requiring minimal ground plane to mount on.

Table 3.3. Comparison of the antenna with the airborne antenna in literature.

Characteristics	Bifolded printed bent monopole antenna	Airborne blade monopole antenna of ref [37]
Height	15cm	18.8cm
Ground plane size	Minimal (antenna baseplate of size 0.2cm x 29cm x 5cm)	1.2m diameter around the feed
3:1 VSWR bandwidth	130-180 MHz	135-175 MHz
Minimum gain over the frequency band	-17dBi	-17dBi
Maximum gain over the frequency band	-9dBi	-4dBi
Radiation pattern	Omnidirectional	Omnidirectional

3.9 CHAPTER SUMMARY

A bifolded printed bent monopole antenna with resistance loading and L shaped ground plane has been investigated for operating over VHF band. The measured results shows that the antenna exhibits a 3:1 VSWR bandwidth of 32% and omnidirectional radiation pattern. The gain of the antenna varies from -17dB to -9dB within the operating band. Simulation studies shows that the radiation characteristics of the antenna is less effected when mounted on large ground plane, thus making this antenna highly suitable for mounting ground plane constrained monopole antenna applications. A parametric study was carried out to study the effect of the dimensions of the radiator as well as the ground plane on the antenna performance. The antenna achieves a height reduction of 78% compared to basic printed strip monopole antenna and 73% compared to conventional quarter wavelength planar monopole antenna at lowest frequency of operation.

4. R-L loaded Meandered Top Loaded Printed Monopole Antenna

This chapter presents RL loaded meandered top loaded printed monopole antenna for airborne applications. The evolution of antenna is discussed first which is followed by the design details of the proposed antenna. The antenna uses meandering and top loading technique for achieving compactness. The wideband characteristics is achieved by resistor inductor loading. The surface current distributions on the antenna and their radiation characteristics at the referred frequency band are analyzed in detail. A detailed parametric study is carried out on the effect of patch and ground plane dimensions as well as the substrate parameters on the radiation characteristics. The performance of the fabricated antenna is evaluated with the antenna mounted over a ground plane as well as for the free standing antenna and the results are presented.

Planar monopole antennas are the most preferred antennas for airborne communications owing to its simple design, wide bandwidth, and omnidirectional radiation pattern. Usually, these antennas are mounted vertically on the platform and the skin of the platform serves as its ground plane. Many of the aircraft communications use HF/VHF band of frequencies. At these frequencies, the requisite of optimum height of the monopole antenna as λ/4 at lowest operating frequency and the optimum ground plane radius around the feed point of the antenna as λ/4 are difficult to achieve on platform due to the mechanical constraints of airborne antennas and space limitations on mounting platform. To overcome the height constraints, various height reduction methods are considered and to overcome the inadequate ground plane on platform, printed monopole antennas are considered.

Hence, in this chapter a wideband printed monopole antenna in VHF band is presented for airborne applications. The antenna was evolved from the basic printed strip monopole antenna after undergoing step by step iterations for height reduction.

4.1 DESIGN EVOLUTION

The evolution of the antenna is shown in Fig.4.1. The simple printed strip monopole antenna (Fig. 4.1(a)) is chosen as the reference antenna. Then the height of the antenna is reduced by implementing top loading in the radiating patch and ground plane as shown in Fig. 4.1(b) (Antenna 1). Then meandering of the radiating strip and ground plane is introduced to further decrease the antenna height (Fig.4.1(c)) (Antenna 2). Finally, the horizontal length of the meander line is increased and resistor-inductor loading in introduced to achieve a compact wideband printed monopole antenna (Fig.4.1 (d)) (Antenna 3). The dark area in the figure shows the radiating patch and the grey area shows the ground patch at the bottom.

FR4 epoxy (Ɛr = 4.4, tan δ = 0.02 and thickness 1.6mm) was used as substrate for the design of the antenna. The width of the substrate was chosen to be less than 30cm for all archetypes.
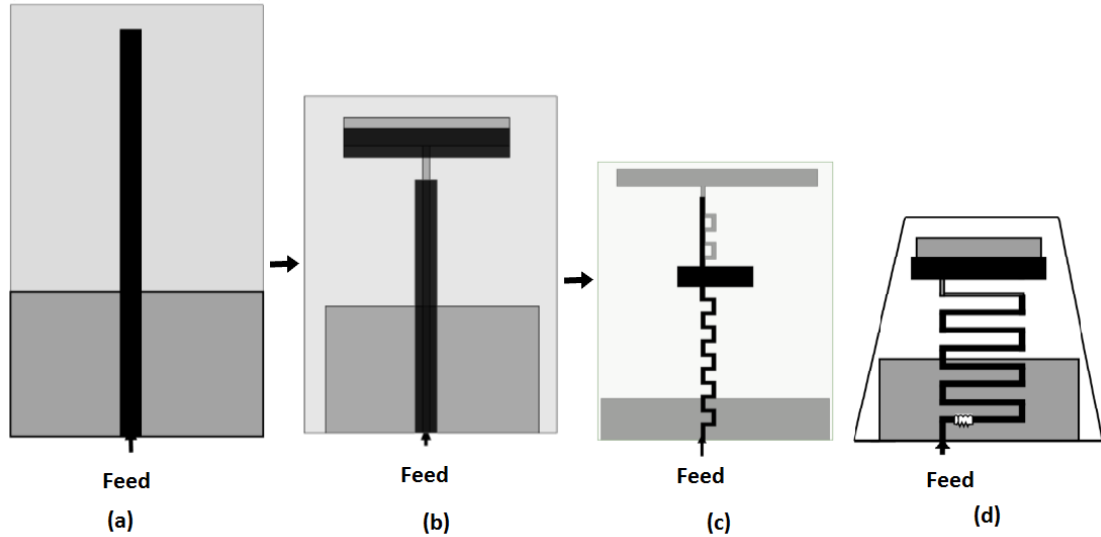
Fig 4.1. Antenna evolution.

4.1.1. PRINTED STRIP MONOPOLE ANTENNA (Reference antenna)

A microstrip fed Printed Strip Monopole Antenna (PSMA) is considered as reference antenna in the design evolution. A PSMA consists of a strip radiator on one side of the substrate and a partial ground plane on other side of the substrate. As shown in Fig 4.2 the length of the strip above ground plane is denoted by L_m and width by w. The dimensions L_g and width W_g denote the length and width of the partial ground plane.

In [139], optimum design of a printed strip monopole antenna is discussed. According to this study, the optimum length of the strip radiator above ground plane (L_m) is 0.23λ, where λ is the free space wavelength at lowest frequency of operation.

Consistent with [139], a printed strip monopole antenna is designed in VHF band as reference antenna for design evolution. The total height of this antenna is 71cm.
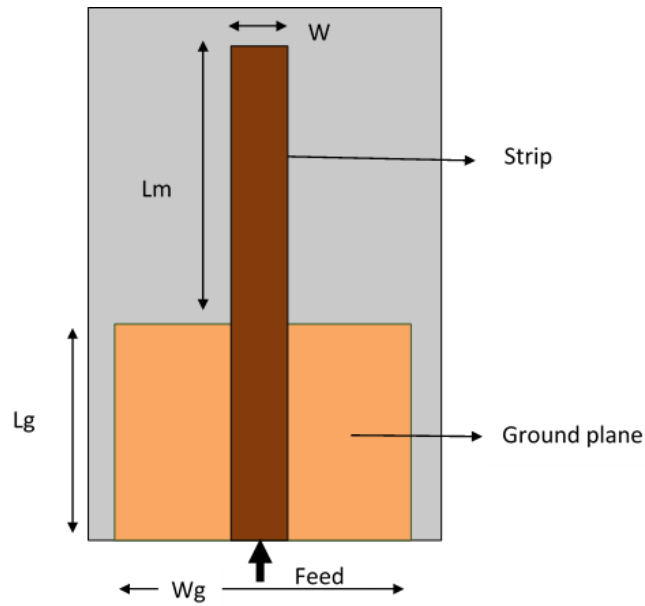
Fig 4.2 Geometry of reference antenna (L_m = 46cm; w = 0.2cm; L_g = 24cm; W_g = 29cm).

The reflection characteristics of this antenna is shown in Fig 4.3. The antenna shows a 3:1 VSWR bandwidth of 22%; i.e. 34 MHz ranging from 138 MHz to 172.5 MHz.
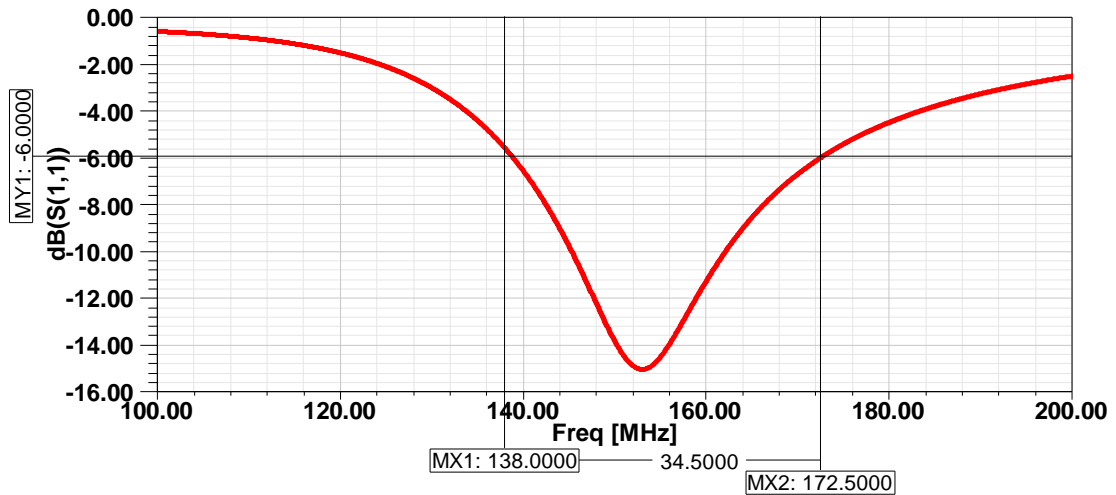
Fig 4.3. Reflection characteristics of reference antenna.

The surface current distribution along the radiating patch and the ground plane at center frequency f_0 =152 MHz is shown in Fig 4.4 (a). A quarter wave current density variation is found along the strip above the ground plane. The polarization of the antenna can be observed from the current density plot. By analyzing the plot, it is found that, the direction of the current throughout the strip is along the vertical axis

and hence it is vertically polarized. Since the intensity of current distribution along ground plane is uniform and feeble, its contribution towards resonance is insignificant. However, the ground plane play an important role in determining the bandwidth of the antenna.
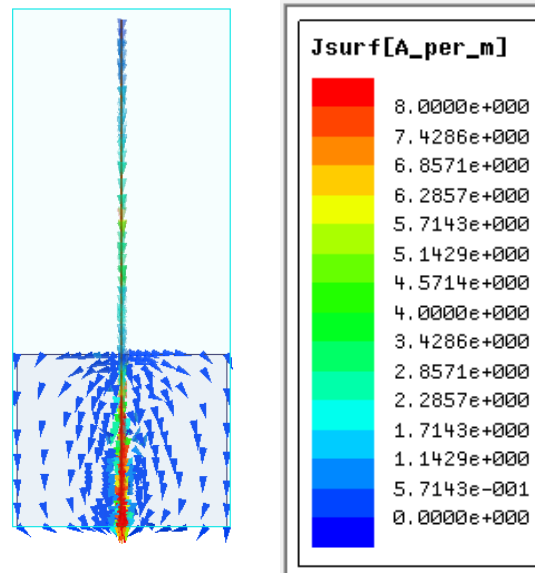
(a)

Fig 4.4. (a) Current distribution of reference antenna at center frequency f_0.

The simulated radiation pattern of the antenna at center frequency f_0 is plotted in Fig 4.4 (b). It can be observed that the radiation pattern of the antenna is omnidirectional. The simulated gain of the antenna is 2dBi for all frequencies within the band.
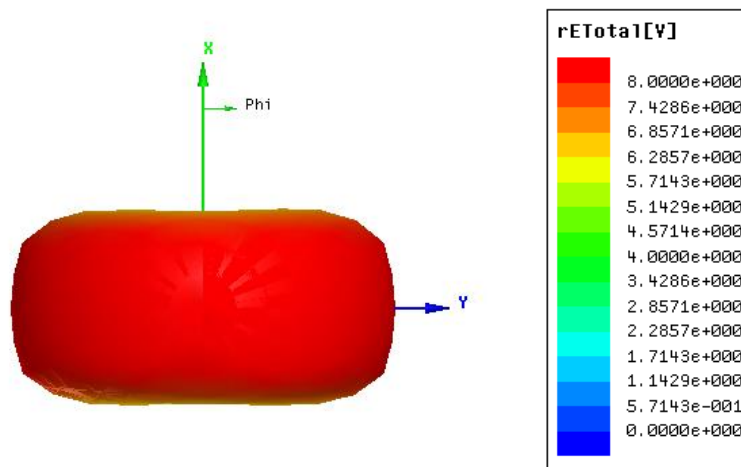
Fig 4.4 (b) Simulated radiation pattern of the reference antenna at frequency f_0

4.1.2. PRINTED TOPLOADED STRIP MONOPOLE ANTENNA(ANTENNA 1)

For airborne communications, compact height is a major concern. Hence height reduction methods has to be employed on reference antenna. Decreasing the height of the monopole radiator shifts the resonant frequency to higher side and the radiation resistance of the antenna at the intended frequency band decreases. This can be compensated by top loading. Top loading the antenna increases the length of surface current path within the reduced antenna dimension and thus decreases the resonant frequency. The current distribution does not terminate at the tip of the strip, else it gets distributed uniformly and thereby it increases the radiation resistance of the antenna. It also improves the capacitive reactance and thus increases the bandwidth [147]. Hence, top loading was introduced to reduce the height of reference antenna.

Fig 4.5 depicts the geometry of the antenna when the radiating patch is top loaded. The antenna has a dimension of 52cm X 29cm X 0.16cm. It achieves 25% height reduction compared to reference antenna.
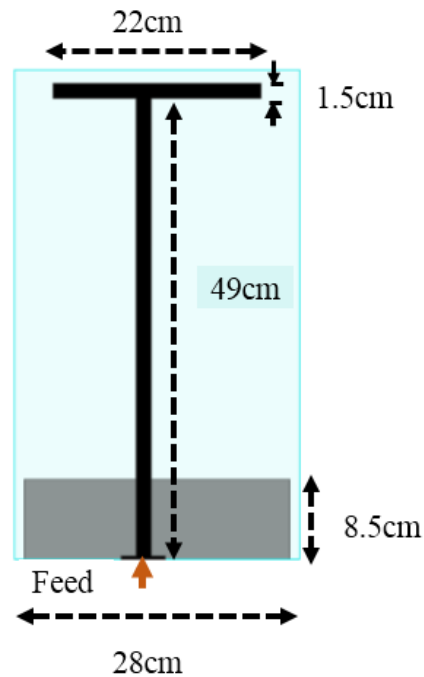
Fig 4.5 Geometry of Antenna 1 when only radiating strip is top loaded.

Fig 4.6 shows the return loss characteristics of the antenna. As seen from the figure, although top loading decreases the resonant frequency, the bandwidth of the antenna is only 9%.
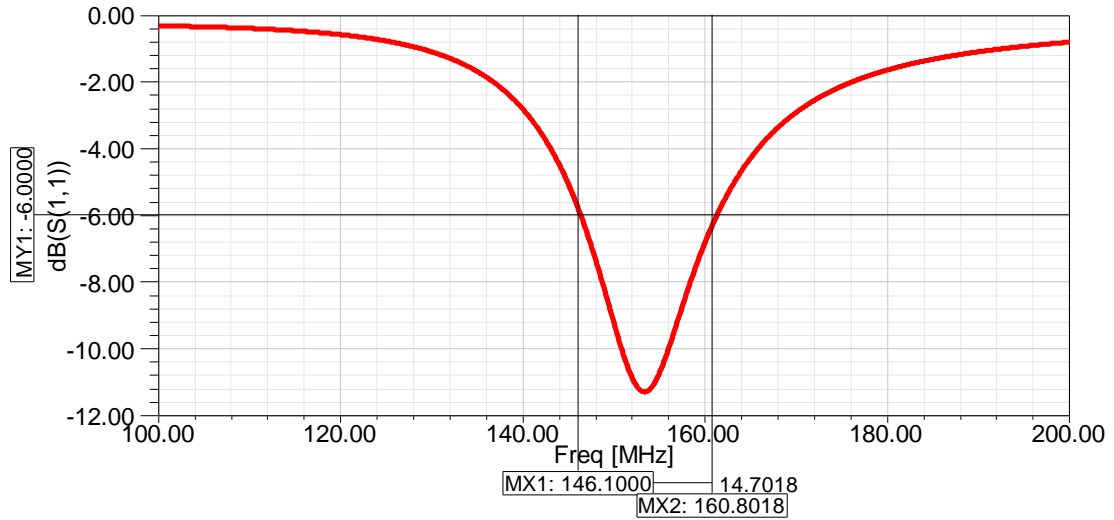
Fig 4.6 Return loss characteristics of Antenna 1 when radiating patch is top loaded.

As the size of the monopole antenna decreases, ground plane size plays a role in determining resonant frequency and bandwidth. In order to increase the bandwidth, a strip and a top loading were introduced in the ground plane and the patch top loading was gap coupled to the radiating strip for improved impedance matching.

The geometry of Antenna 1 is shown in Fig 4.7. It can be seen that a strip and top loading are implemented on the ground plane above the partial ground structure of Fig 4.5. The height of the antenna is not altered (52cm).
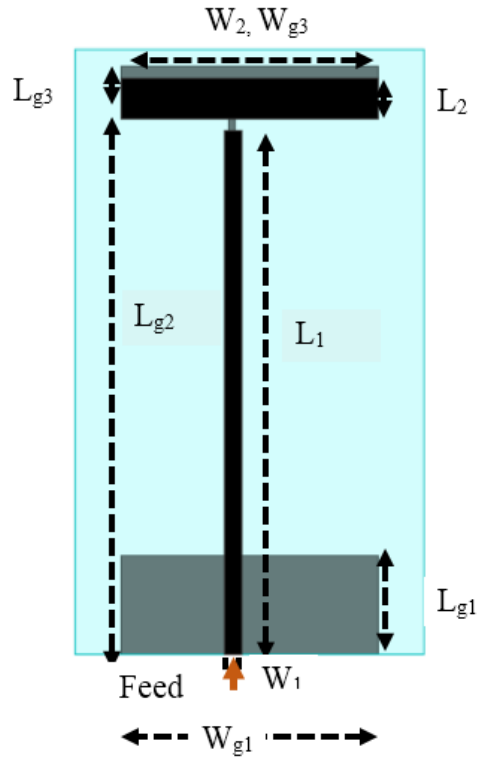
Fig 4.7. Geometry of Antenna 1 (L_1 = 45cm; W_1 = 1.5cm; G = 1cm; L_2 = 3.5cm; W_2 = 22cm; L_{g1} = 8.5cm; W_{g1} = 22cm; L_{g2} = 47cm; W_{g2} = 0.6cm; L_{g3} = 3.5cm; W_{g3} = 22cm).

The return loss characteristics of this antenna is plotted in Fig 4.8. It can be observed that by employing a strip and top loading in the ground plane, the impedance bandwidth of the antenna is increased from 9% to 27%.
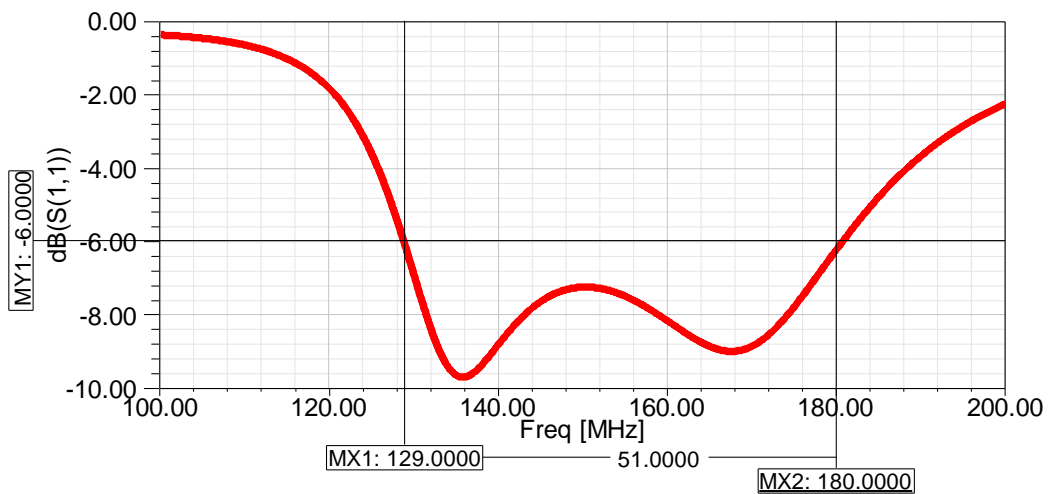
Fig 4.8 Return loss characteristics of Antenna 1.

The surface current distribution along the radiating patch and the ground plane at center frequency (f_0) 155 MHz is shown in Fig 4.10 (a) & (b) respectively. A quarter wave current density variation is found along the strip. It is also observed that the current distribution along the top loading of the antenna is uniform and it is minimum. The current distribution along the strip on the ground patch is intense which contributed to the increased bandwidth of the antenna.

(a)   (b)
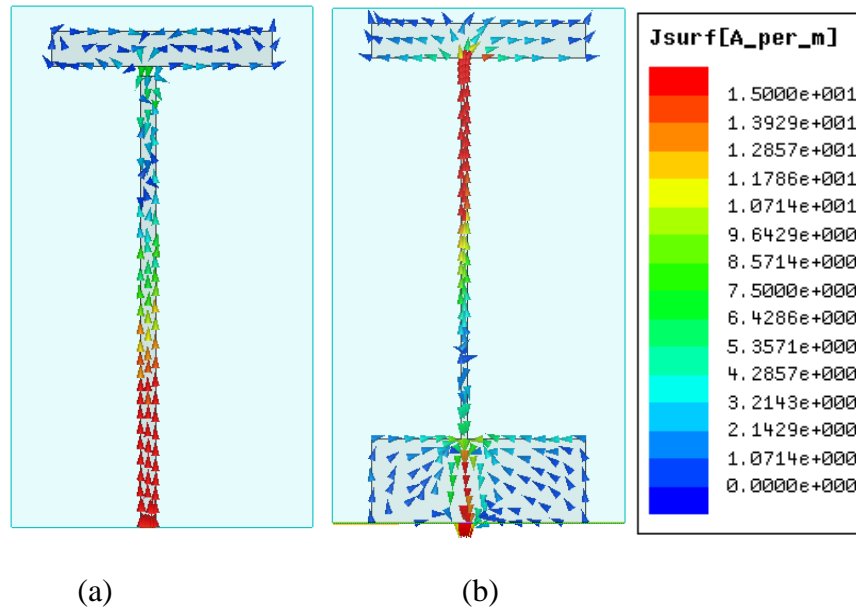
Fig 4.9 Surface current distribution at f_0 along (a) Front patch (b) Ground patch.

The simulated gain of the antenna is plotted in Fig 4.10 (a) and radiation pattern in Fig 4.10 (b). The simulated gain of the antenna is 1.8dBi. From Fig 4.10 (b), it can be observed that the antenna shows an omnidirectional radiation pattern.
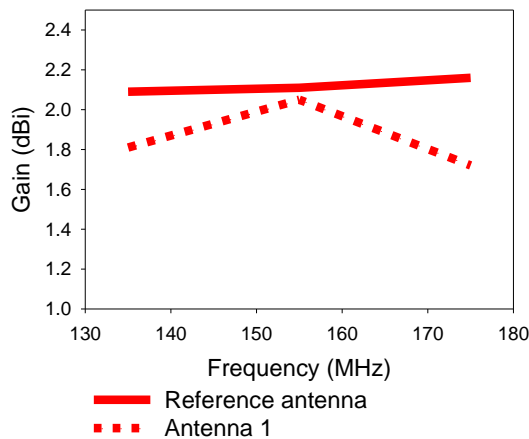
Fig 4.10 (a) Simulated Gain of Antenna 1.
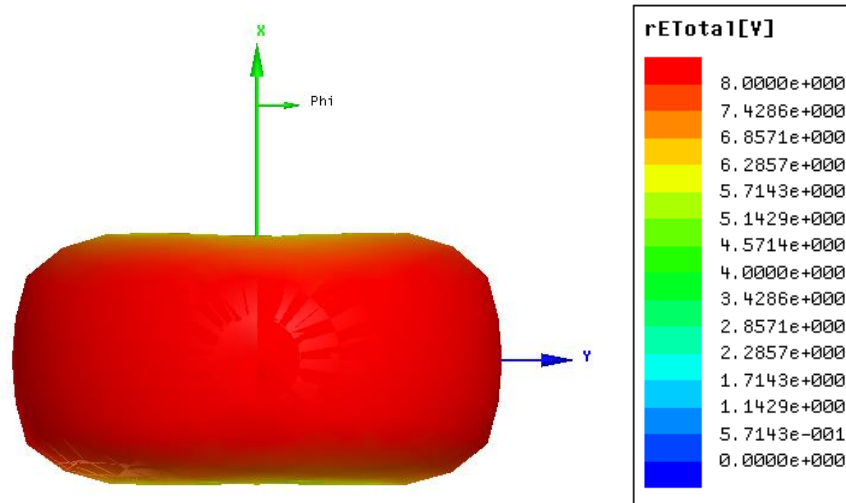
Fig 4.10 (b). Simulated 3D radiation pattern of Antenna 1 at f_0.

It was found that the ground top loading has significant effect on determining the bandwidth of the antenna. The width of ground top loading (W_{g3}) was analyzed by increasing it symmetrically to both sides of the central strip from 2cm to 11cm and is plotted in Fig 4.11. It can be observed that increasing W_{g3} decreases the resonant frequency and also increases the bandwidth.
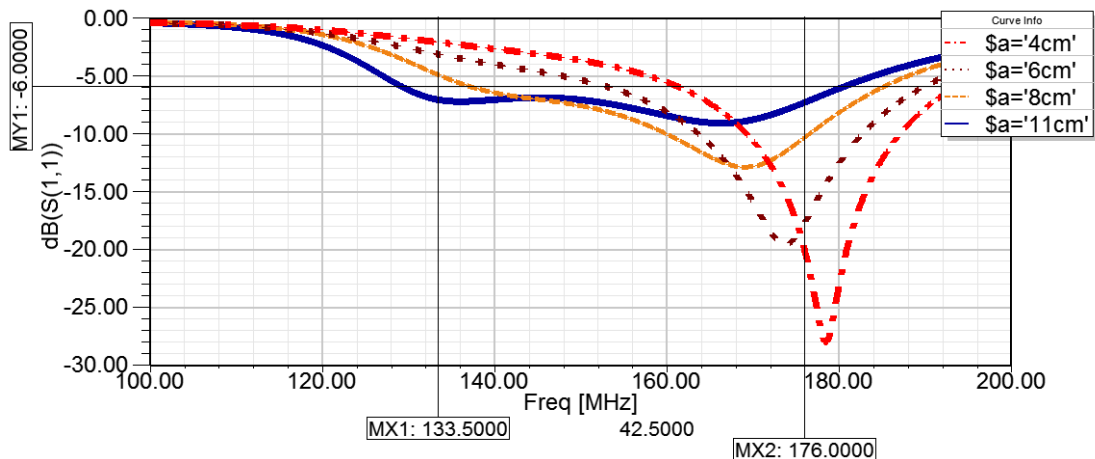
Fig 4.11 Effect of W_{g3} on return loss characteristics of Antenna 1.

4.1.3. MEANDERED TOP LOADED PRINTED MONOPOLE ANTENNA (ANTENNA 2)

Meander line antenna is an attractive candidate for a miniaturized antenna with omnidirectional radiation, considerable radiation efficiency and negligible cross polarization. Meandering the patch increases the path over which the surface current

flows and that eventually results in lowering of the resonant frequency. Hence meandering technique was considered to further reduce the height of Antenna 1. Printed meander line monopole antennas exhibit a narrow bandwidth which can be enhanced by various techniques [148-151].

In this section a wideband printed monopole antenna is discussed, in which the strip in Antenna 1 is meandered. The meandering and top loading implemented on the radiating patch as well as on the ground patch serves to increase the bandwidth.

The geometry of meandered top loaded printed monopole antenna is shown in Fig 4.12 and the dimensional values are detailed in Table 4.1. A meander line monopole antenna with equal vertical and horizontal sections was employed symmetrically in the radiating patch and the ground plane. The length of each vertical (L_1) and horizontal meander line (W_1) is 2cm and the width of each meander line (W) is 0.6 cm. The strip above the top loading on the radiating patch and the symmetrical arrangement of meander line on the radiating patch and ground serves to improve the impedance matching. Edge feeding is used to excite the antenna with port impedance 50Ω. The total height of the antenna is 39cm.
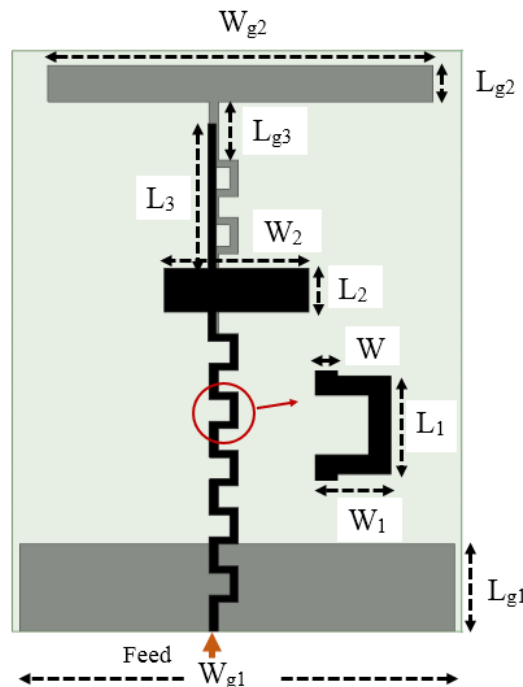
Fig 4.12 Geometry of Antenna 2.

Table 4.1 Dimensions of Antenna 3 in cm.

L_1	2.0	W_4	0.6
W_1	2.0	L_{g1}	6.0
L_2	3.0	W_{g1}	30.0
W_2	6.0	L_{g2}	2.5
L_3	9.0	W_{g2}	28
W	0.5	L_{g3}	3.0

The return loss characteristics of this antenna is plotted in Fig 4.13. The antenna shows a 3:1 VSWR bandwidth of 23%, i.e. 36 MHz ranging from 140 MHz to 176 MHz.
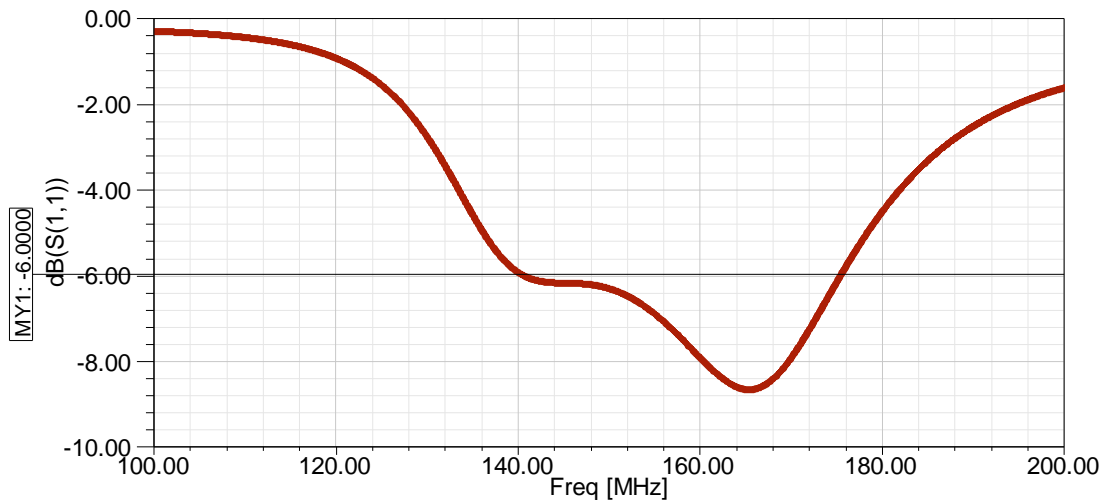
Fig 4.13 Reflection characteristics of Antenna 2.

The surface current distribution along radiating patch and ground plane at center frequency (f_0 =158 MHz) is shown in Fig 4.14. It can be observed that there is $\lambda/2$ variation along the meanders of ground plane and radiating patch. The current distribution along top loadings is uniform. Current along horizontal portions of meander are opposite in direction and hence cancels, yielding vertical polarization.

(a)   (b)
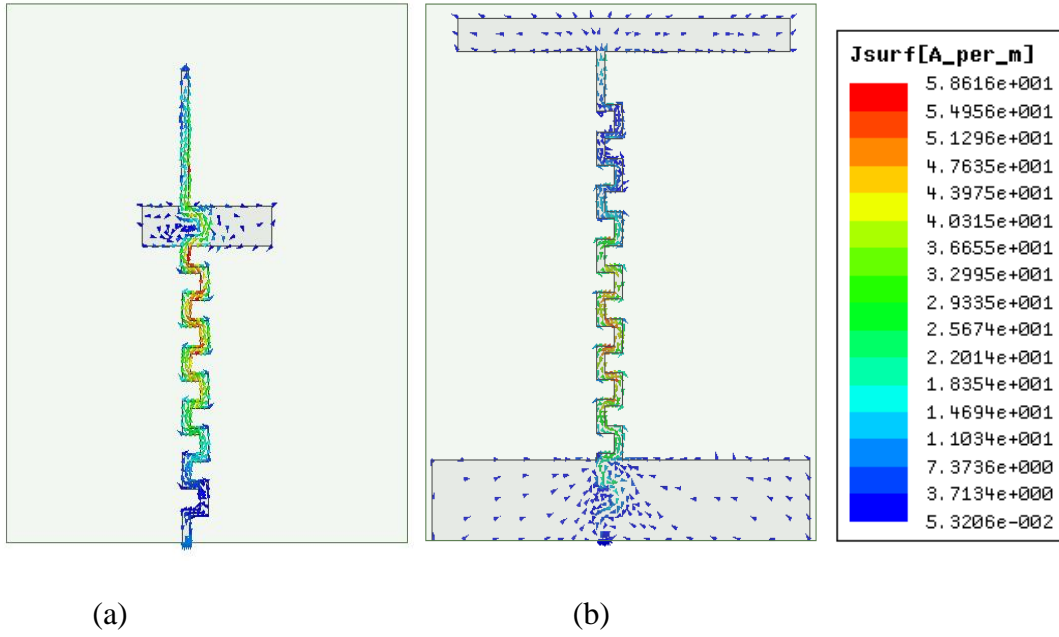
Fig 4.14 Surface current distribution on (a) radiating patch (b) ground of Antenna 2

The simulated gain and radiation pattern of this antenna is shown in Fig 4.15 (a) and (b) respectively. The simulated gain of the antenna varies from 0.8dBi to 1.8dBi. It can be observed from Fig 4.15 (b) that the antenna has omni directional radiation pattern.
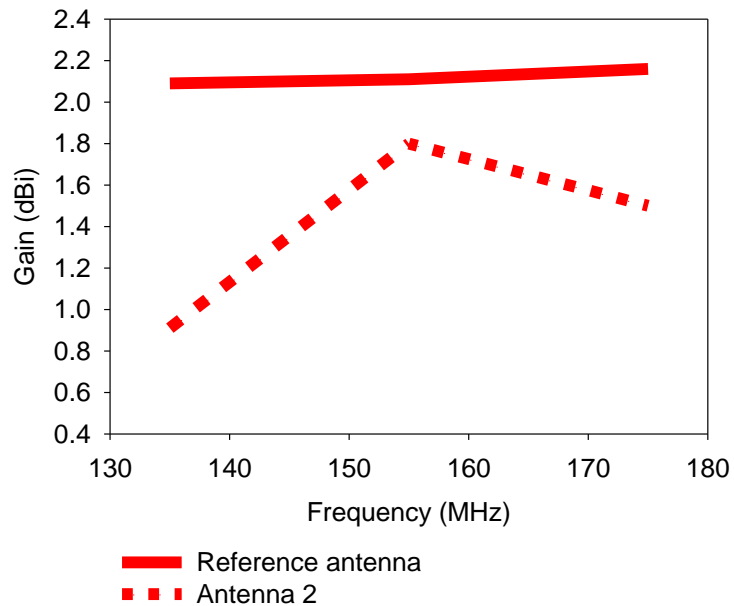
Fig 4.15 (a) Simulated gain of Antenna 2
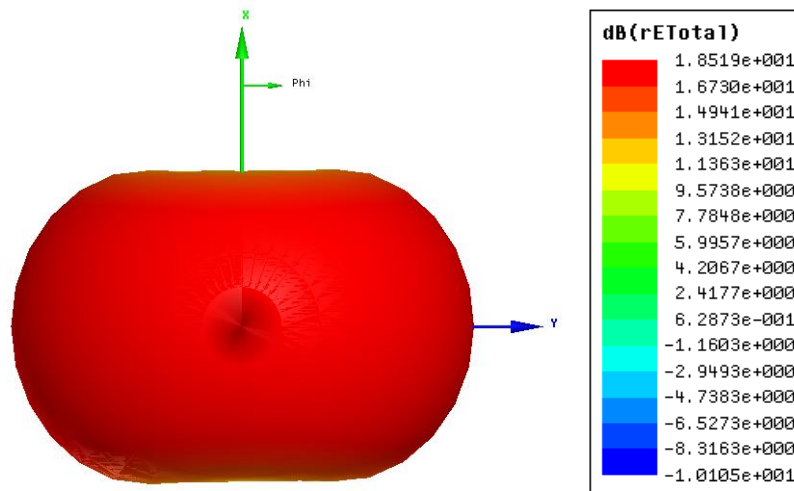
Fig 4.15 (b) 3D radiation pattern of Antenna 2

4.1.3.1 Parametric Study

A detailed parametric study has been carried out in this antenna to study the influence of each parameter on the radiation characteristics. The variations in the frequency response of the antenna is explained by analyzing the variations in the distributed reactive components (L & C). These values were calculated using the method explained in Section 2.6.3.

(a) Effect of radiating patch dimensions

The effect of L_2 was studied by varying it from 1 cm to 4 cm and is plotted in Fig 4.16 (a). The variation in distributed parameters with L_2 is plotted in Fig 4.16(b). As L_2 increases from 1 cm to 4 cm, the impedance matching of the antenna improves till 3 cm and then decreases. The bandwidth of the antenna increases with increase in L_2 due to the increase in capacitive reactance. Further increase in L_2 decreases the capacitive reactance resulting in decreased bandwidth.
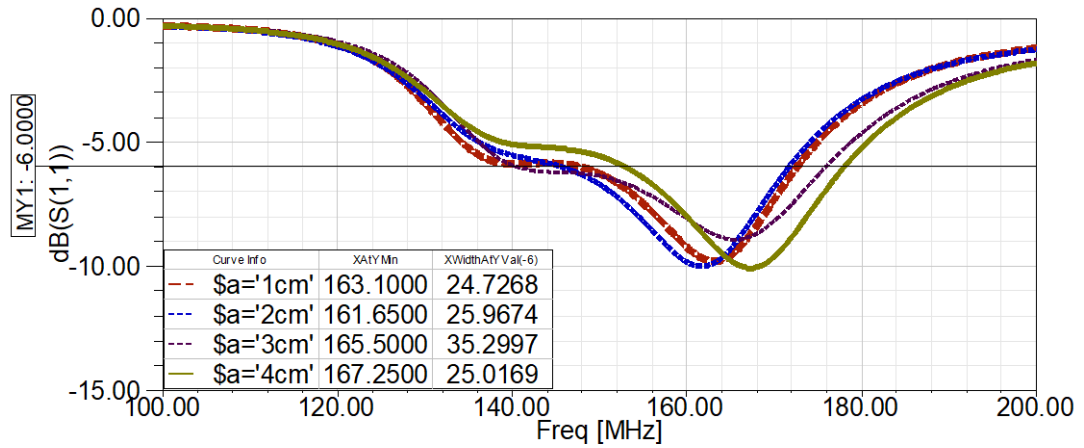
(a)
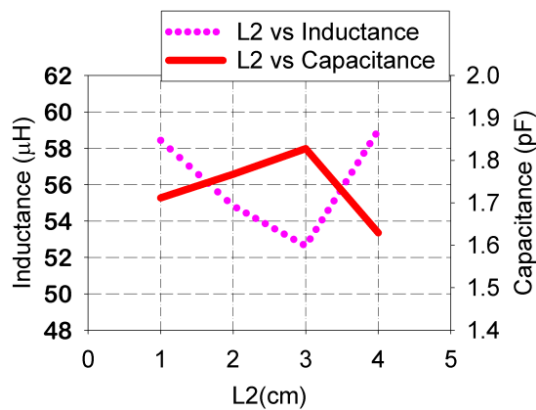
(b)

Fig 4.16 (a) Effect of L_2 on return loss of antenna. (b) Variation of reactive components with L_2.

Fig 4.17(a) shows the effect of variation of W_2 on return loss of the antenna and Fig 4.17 (b) plots the variation in distributed parameters with variation in W_2. As W_2 was increased symmetrically from 1 cm to 4 cm to both sides, the impedance matching is improved till 3 cm and further increase cause decrease in impedance matching at lower edge of the frequency band. The distributed capacitance increases as W_2 was increased from 1 cm to 3 cm and cause increase in bandwidth. Further increase in W_2 caused a decrease in capacitive reactance and increase in inductive reactance, thereby decreasing bandwidth.
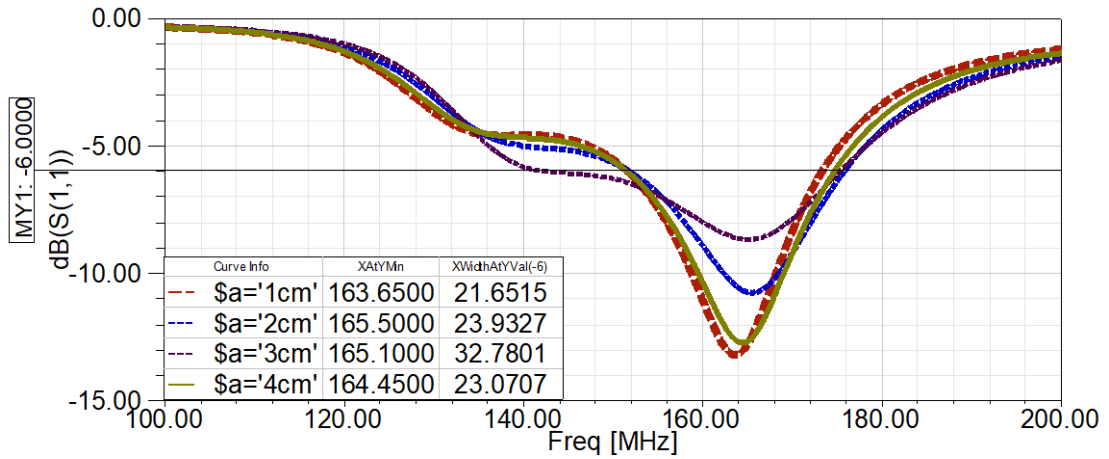
(a)
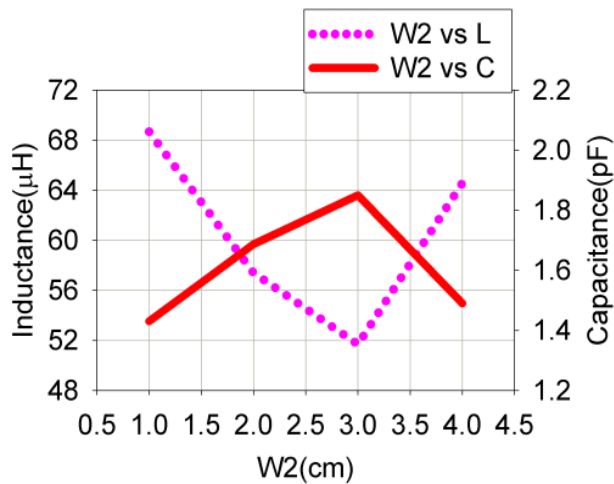
(b)

Fig 4.17 (a) Effect of W_2 on return loss of antenna. (b) Variation of reactive components with W_2.

The effect of L_3 on frequency response of antenna is plotted in Fig 4.18 (a). When dimension L_3 was varied from 1 cm to 9 cm, it could be observed from the smith chart (Fig 4.18 (b)) that the impedance became more capacitive and the bandwidth is increased. At $L_3 = 9$ cm, impedance matching at higher side of the band improves, and a wide bandwidth is observed at $L_3 = 11$cm. This mean that the coupling between the patch at the top and bottom played an important role in generating wide bandwidth. Hence $L_3 = 11$ cm was chosen as the optimum value as it has given maximum bandwidth.
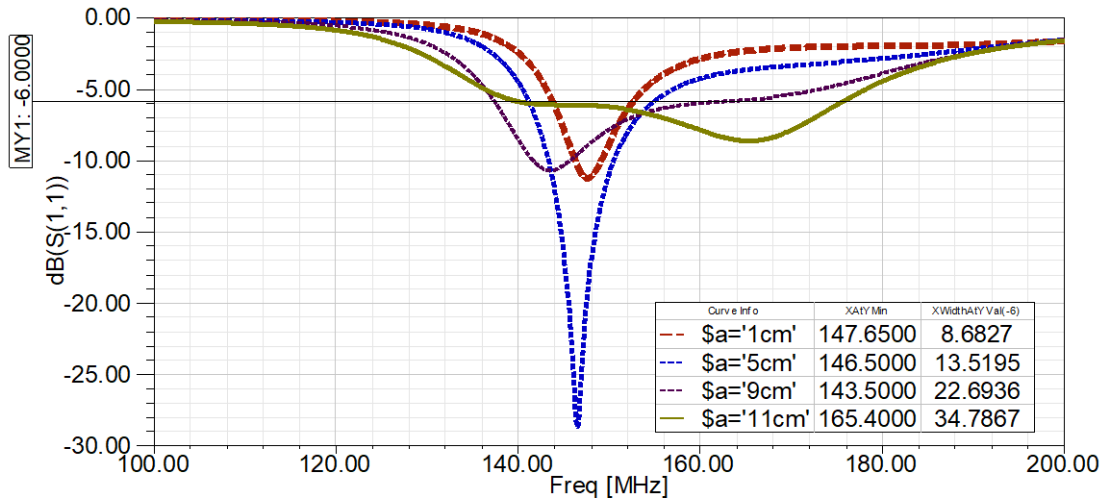
(a)
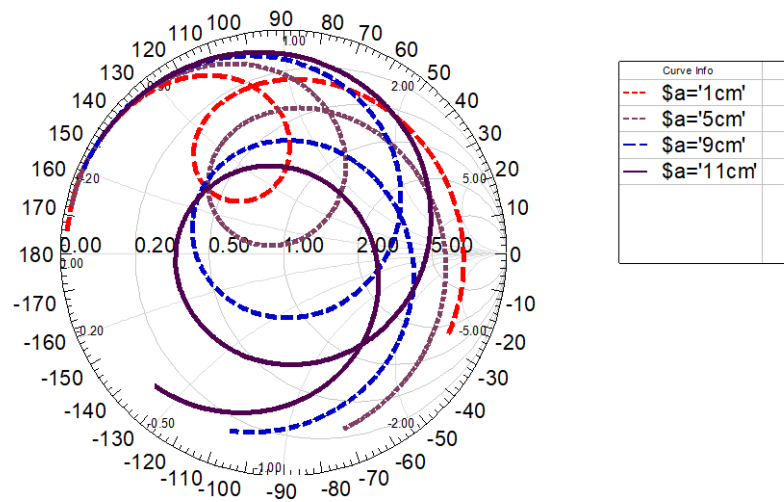
(b)

Fig 4.18 (a) Effect of L_3 on return loss of antenna. (b) Input impedance loci of antenna for various values of L_3.

(b) Effect of ground plane dimensions

The effect of ground plane dimension L_{g1} on the impedance bandwidth of the antenna was studied and is plotted in Fig 4.19(a). The variation in distributed parameters with variation in L_{g1} is plotted in Fig 4.19(b).

The bandwidth of the antenna was seen increasing on increase of L_{g1} from 2cm to 6cm, and on further increase of L_{g1}, a decrease in the bandwidth of the antenna is observed. This is due to the decrease in inductance and increase in capacitance as

L_{g1} increases from 2 cm to 6 cm. Further increase in L_{g1} decreases capacitance and bandwidth of the antenna decreases. Hence L_{g1}=6 cm was chosen as the optimum value.
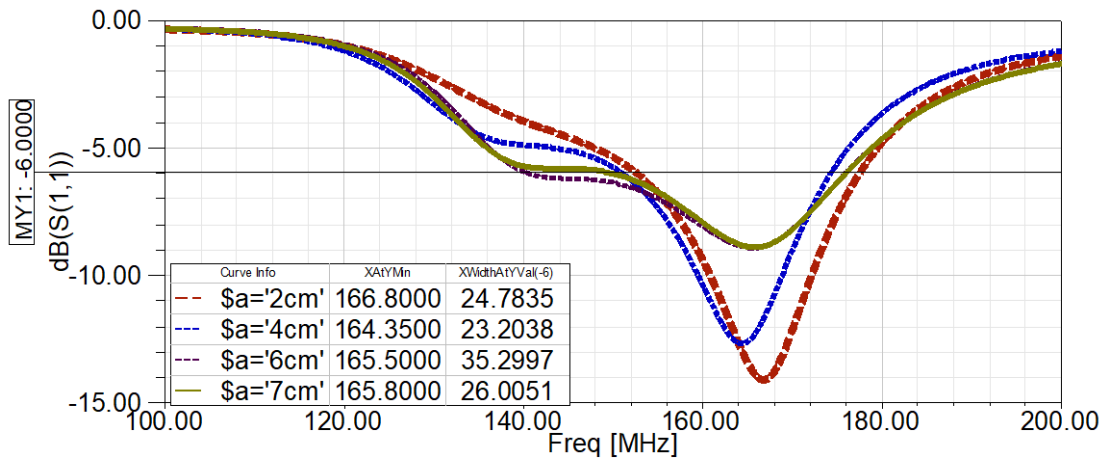
(a)
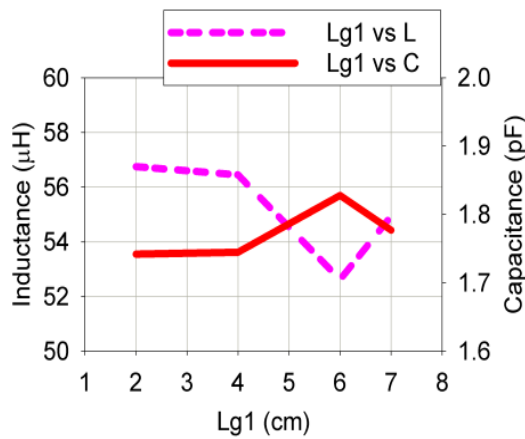
(b)

Figure 4.19 (a) Effect of L_{g1} on return loss of antenna. (b) Variation of reactive components with L_{g1}.

The effect of W_{g1} on frequency response of antenna was studied by varying it from 8 cm to 15 cm symmetrically to both sides from the center of antenna. As observed from Fig 4.20, W_{g1} is a frequency determining factor. The increase in W_{g1} shifts the frequency band to lower side. Also, the impedance matching at lower edge of the frequency band improves on increase of W_{g1}, increasing bandwidth.
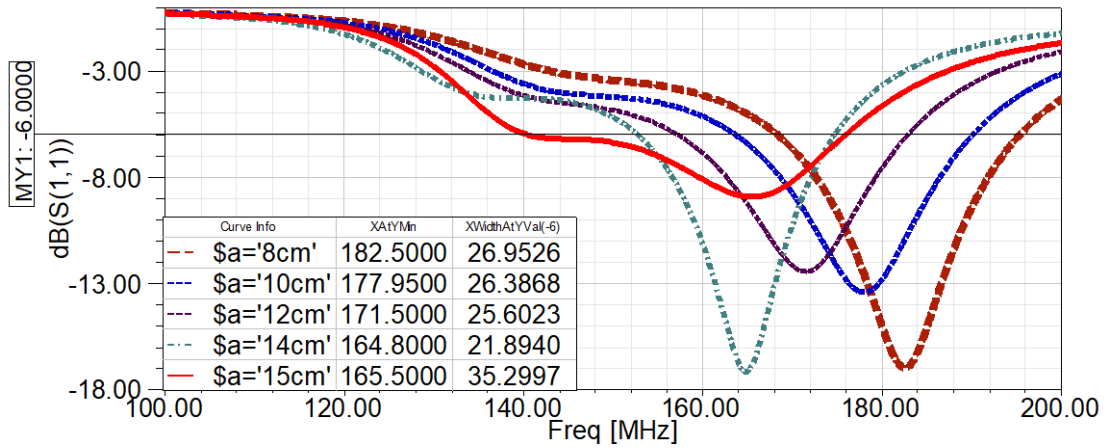
Fig 4.20. Effect of W_{g1} on return loss of antenna.

The effect of ground plane dimension L_{g2} was studied by varying it from 1 cm to 3 cm and its effect on the bandwidth is plotted in Fig 4.21 (a). It was found that as L_{g2} increases from 1 cm to 2.5 cm, the impedance matching at lower edge of the frequency band improves, increasing the bandwidth of antenna. It was evident from Fig 4.21(b) that increase in bandwidth is due to increase in distributed capacitance of antenna. Further increase in L_{g2} increases the inductive reactance, decreasing the bandwidth of antenna. Hence, $L_{g2} = 2.5$ cm was chosen as the optimum value.

(a)

(b)
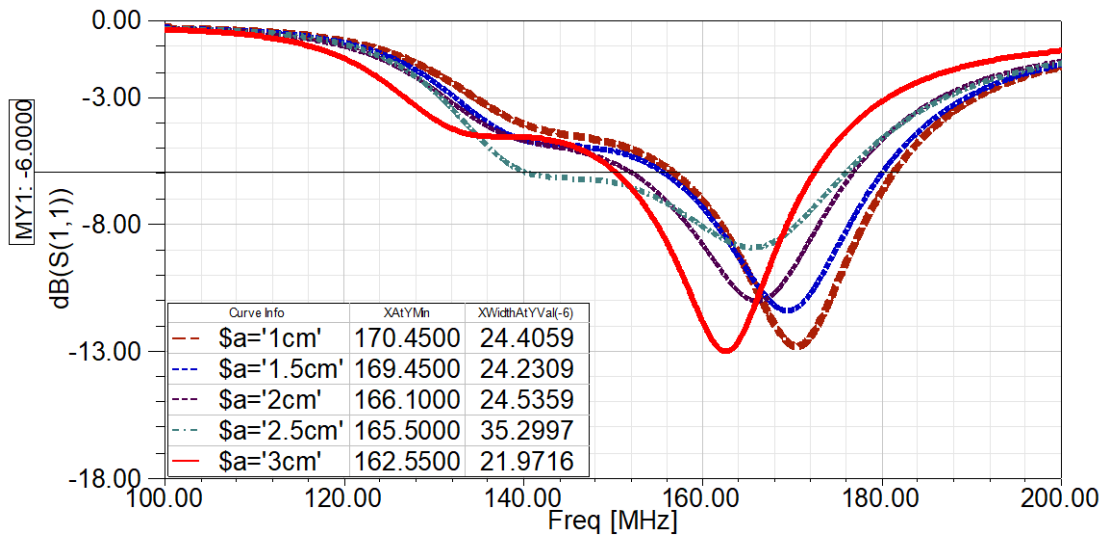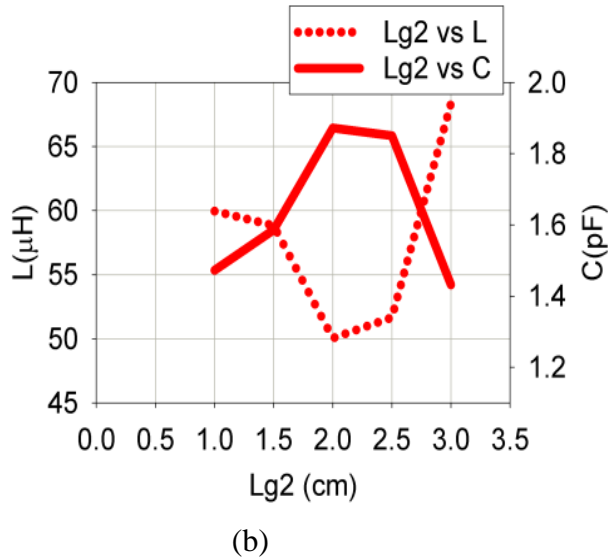
Fig 4.21 (a) Effect of L_{g2} on return loss of antenna. (b) Variation of reactive components with L_{g2}.

The frequency domain response of antenna with variations in W_{g2} was studied and is shown in Fig 4.22. It can be observed that, increase in W_{g2} from 7 cm to 14 cm symmetrically to both sides, leads to decrease in resonant frequency, and the impedance matching at lower frequency region improves.
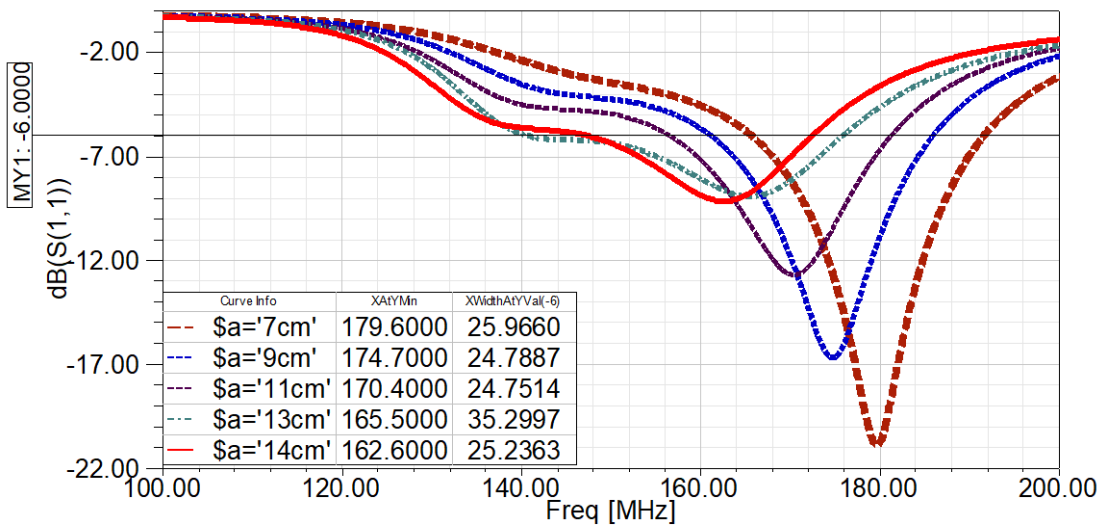
Fig 4.22. Effect of W_{g2} on the return loss of the antenna.

Fig 4.23 (a) shows the frequency response of the antenna with variations in L_{g3}. As L_{g3} increases, the resonant frequency decreases. Also as L_{g3} is increased, the impedance matching at lower edge of the frequency band increases causing increase in bandwidth. The variations in the distributed parameters with variation in L_{g3} is

shown in Fig 4.23 (b). The shift in resonant frequency was due to the predominance of variation in distributed inductance.
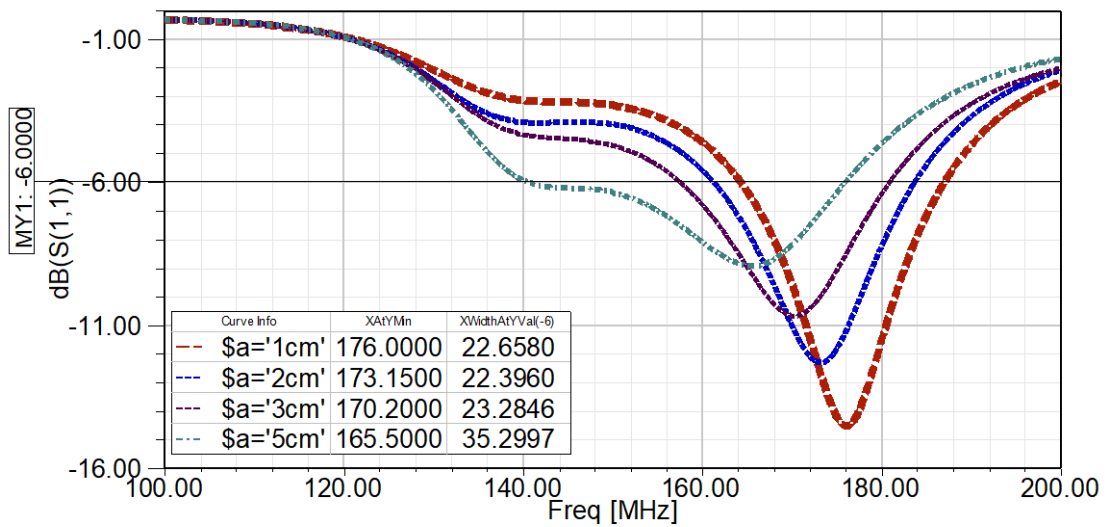
(a)
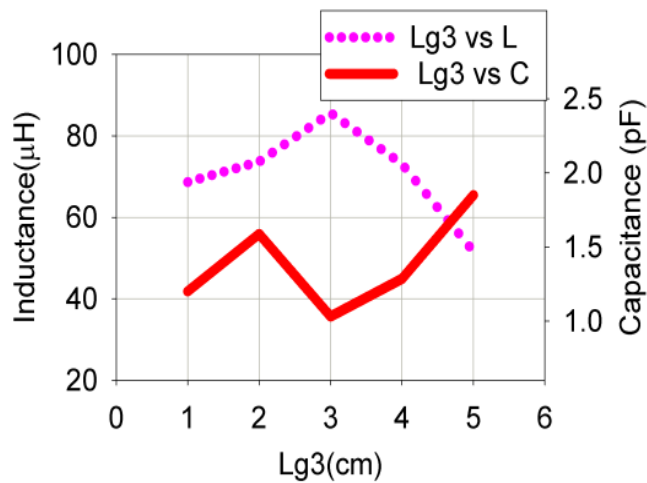
(b)

Fig 4.23 (a) Effect of L_{g3} on return loss of antenna. (b) Variation of reactive components with L_{g3}.

It can be inferred from parametric analysis that apart from length and number of meandering segments, the ground plane dimensions W_{g1}, W_{g2} and L_{g3} determines the resonant frequency. The radiating patch dimension L_3 has strong influence in widening the bandwidth of the antenna. All dimensions of the antenna contributes for improving the bandwidth of the antenna.

Although the height of Antenna 2 is acceptable for large aircrafts, for small aircrafts and helicopters, it is quite large. To fit in small aircrafts and helicopters, the

height of antenna should be further reduced. For this, the horizontal length of meander segment is increased. As the size of antenna decreases, the achievable bandwidth also decreases. To increase bandwidth of the antenna, loading techniques has to be considered. The design and development of a very compact printed monopole VHF antenna which attain wideband characteristics using resistance-inductor loading is discussed below.

4.2. R-L LOADED MEANDERED TOPLOADED PRINTED MONOPOLE ANTENNA (ANTENNA 3)

4.2.1. ANTENNA GEOMETRY

The schematic of the proposed antenna is shown in Fig 4.24 (a-b). The radiating patch of the antenna consists of meander line structure and a top loading structure. The top loading structure is gap coupled to meander line for improved impedance matching.

On ground plane, meander structure is incorporated along with the partial rectangular ground plane, symmetric with that of the meander line of the radiating patch for improved impedance matching. Top loading structure is also incorporated in ground plane for achieving frequency reduction.

The antenna was designed in an aerodynamic shape so as to reduce air drag. Edge feeding of 50Ω is used to excite the antenna. An aluminium base plate of rectangular shape was used for mounting the antenna. It holds the connector and acts as an interface to the mounting platform.

(a)   (b)
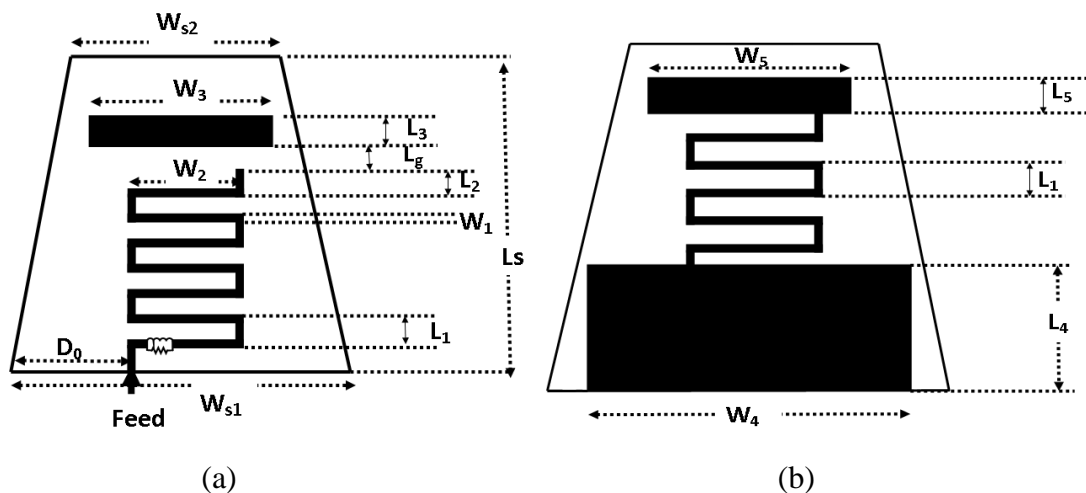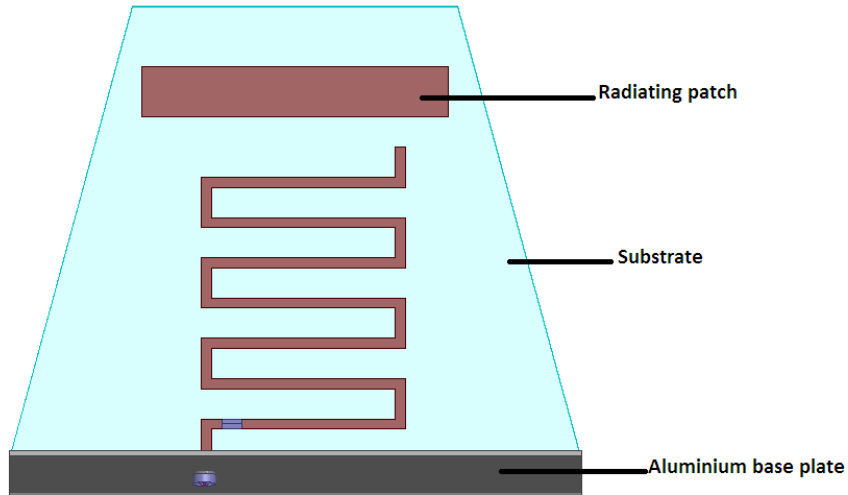
(c)

Fig 4.24. Structure of proposed antenna; (a) Radiating patch (b) Ground patch (c) 3D view

4.2.2. CHARACTERISTICS OF A TYPICAL STRUCTURE

The basic characteristics of a typical patch of this geometry is discussed in this section. The substrate used is FR4 glass epoxy of dielectric constant ε_r = 4.4 and thickness 0.16cm. The dimensions of the geometry are outlined in Table 4.2. The horizontal length of the meander line (W_2) is 10 cm; vertical length (L_1) is 2 cm and width (W_1) is 0.5cm.

Table 4.2. Dimensional details

Parameters	Ls	W_{S1}	W_{S2}	D_0	L_1	W_1	L_2	W_2
Value (cm)	23	28	17.5	9.5	2.5	0.5	2	10
Parameters	L_3	W_3	L_g	L_4	W_4	L_5	W_5	
Value (cm)	2	14	2	9	23.2	2	14	

4.2.2.a. Return loss

The return loss characteristics of this antenna is shown in Fig 4.25. The fundamental frequency of resonance of this antenna is 162MHz.
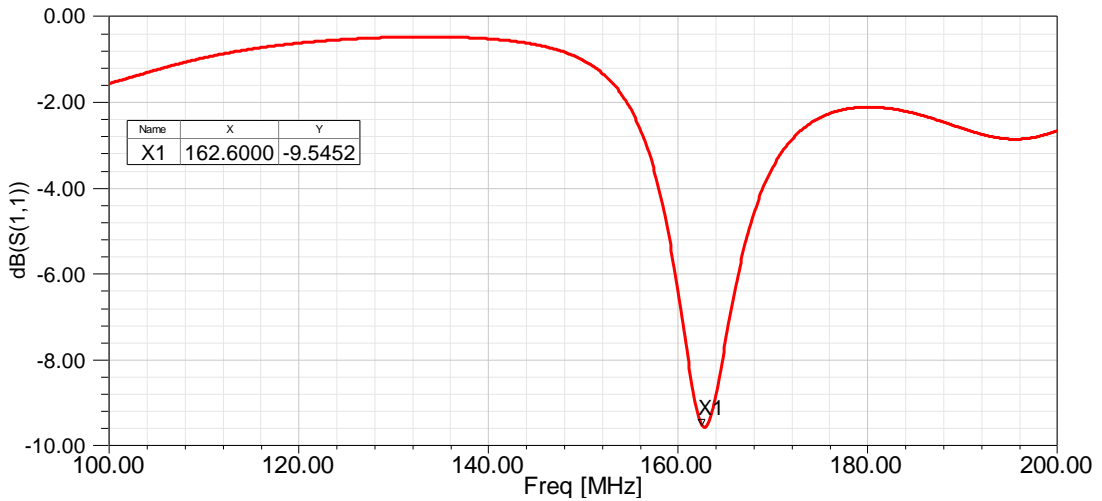
Fig 4.25 Return loss characteristics of Antenna 3

The variation of input impedance with frequency of Antenna 3 is plotted in Fig 4.26. It can be observed that the resistive component of the input impedance of this antenna is less and the reactive component is inductive at lower frequencies of the required band.
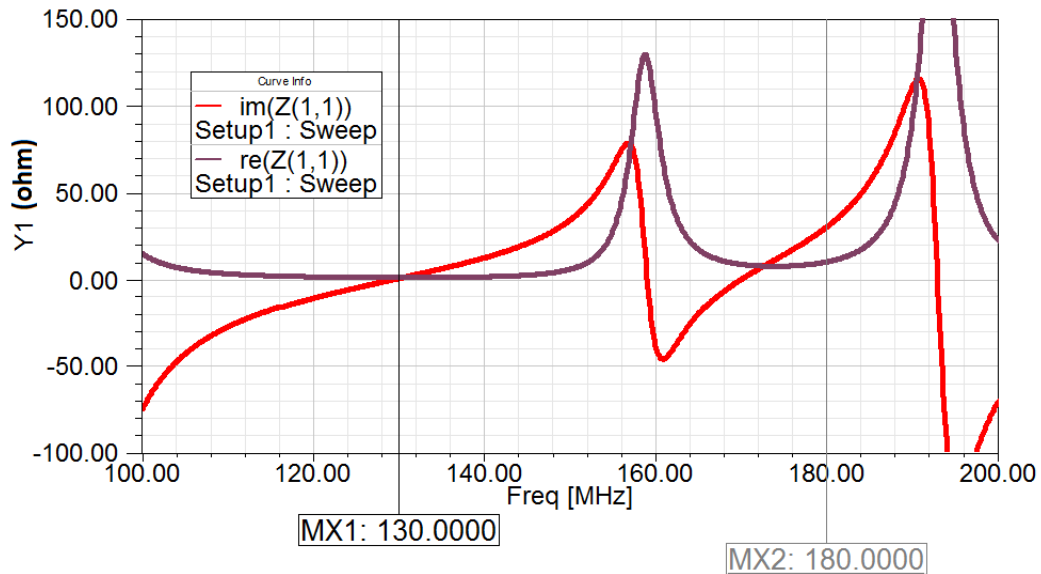
Fig 4.26 Variation of input impedance with frequency of Antenna 3

Since airborne applications demand wide bandwidth, the antenna need to operate over a wide frequency range. As the resistive component of the input impedance of this antenna is less, it is very difficult to match to a source whose output impedance is in order of 50ohms over this wideband. To increase the bandwidth of operation, resistive component of input impedance has to be increased. In order to

achieve this, without compromising its length or degrading azimuthal radiation pattern, a resistance loading technique was used on radiating patch. Adding an inductor parallel to resistor can increase the gain of antenna in lower frequencies of the band.

In order to fix the resistance value, a parametric analysis was carried out studying the effect of resistance on frequency response of antenna. It was observed that with the application of 15Ω resistance, the required bandwidth is obtained (Fig 4.27(a)).
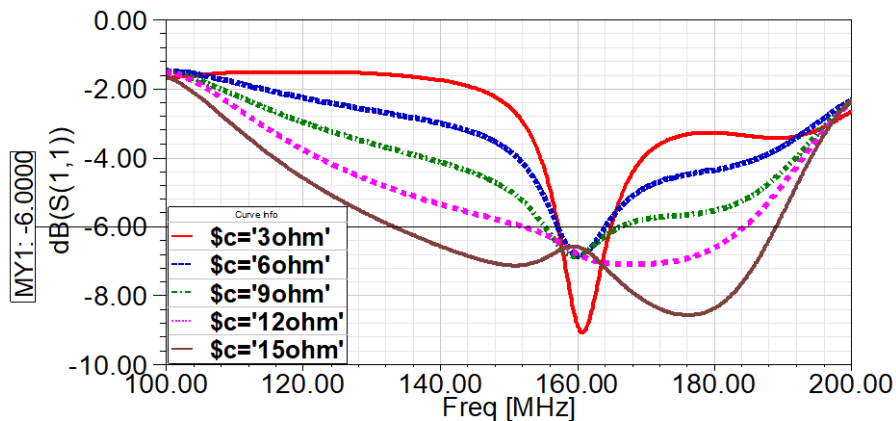
Fig 4.27 (a) Effect of resistor on the return loss of Antenna 3.

In order to fix the inductor value, parametric analysis was carried out studying the effect of inductance, parallel to 15Ω resistor, on bandwidth and gain of antenna. The inductance value is varied from 50nH to 200nH. It was observed that, the inductor increases the gain of the resistor loaded antenna in the lower frequencies of the band. Although, the gain of the antenna is better when the inductance is 50nH compared to 200nH, it decreases the bandwidth. Hence, the inductance value was fixed to 200nH as it gives better bandwidth and an improvement in gain of the antenna in lower frequency region.

The figure showing the effect of inductance on bandwidth of Antenna 3 is shown in Fig 4.27(b). The effect of inductor 200nH placed parallel to resistor on gain of antenna is plotted in Fig 4.27 (c).
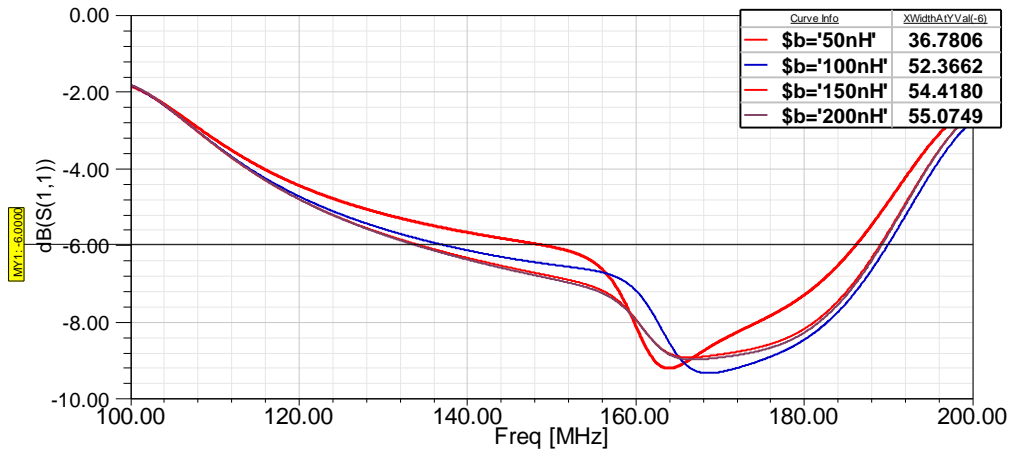
Fig 4.27 (b). Effect of inductor parallel to 15Ω resistor on bandwidth of Antenna 3

only resistor
with inductor parallel to resistor
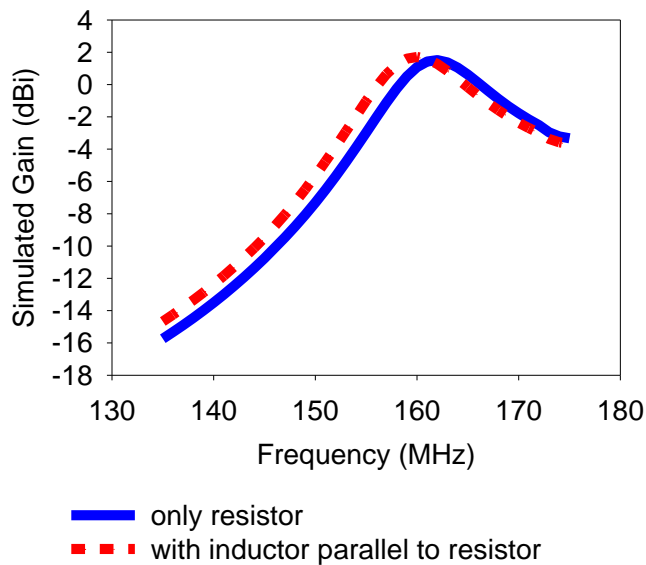
Fig 4.27(b) Simulated gain of Antenna 3 with resistance loading alone and with resistor inductor loading.

Thus, a parallel combination of lumped inductor of 200nH and resistor of 15Ω is connected in series to the radiating patch. The simulated return loss plot of the antenna with R-L loading is shown in Fig 4.28. The antenna exhibits a 3:1 VSWR bandwidth of 38% i.e. 58MHz ranging from 132MHz to 190MHz.
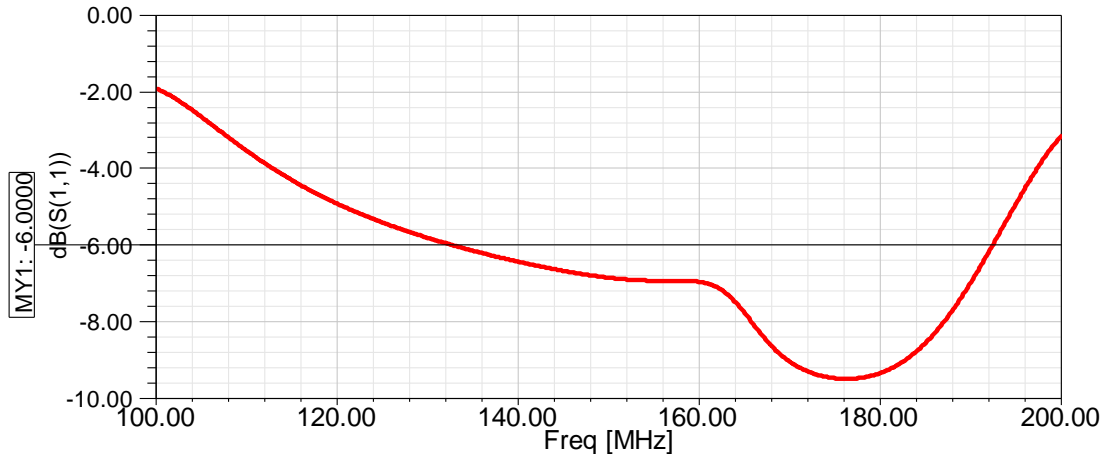
Fig 4.28. Return loss characteristics of R-L loaded meandered toploaded printed monopole antenna

4.2.2.b Surface Current distribution

The simulated surface current distribution on the radiating patch as well as on the ground plane of the antenna at center frequency (f_0=160 MHz) is shown in Fig 4.29 (a-b) respectively. It can be observed that surface current distribution shows a variation slightly greater than one half wavelength along the radiating patch at resonant frequency. The distribution of current on top loading of radiating patch is uniform. The ground plane meandering and ground top loading can be considered as a coupled line as its current is the image component of that on the radiating element.

(a)

(b)
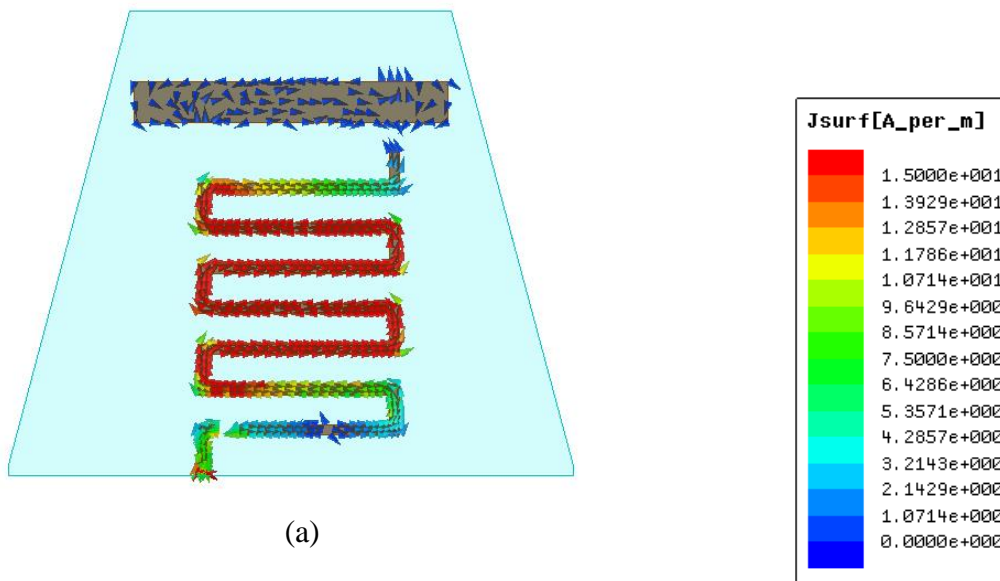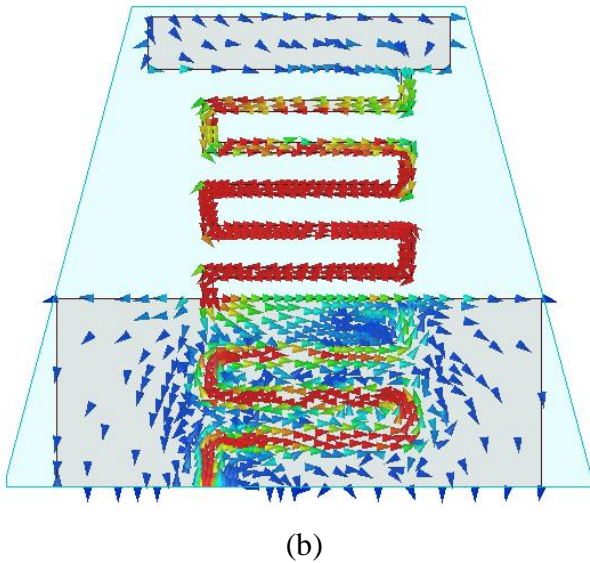
Fig 4.29. Simulated Current distribution at f_0 on (a) radiating patch (b) ground patch

4.2.2.c Gain, efficiency and radiation pattern

Simulated gain and efficiency of the antenna is shown in Fig 4.30. The gain of the antenna varies from -14dB to 1.5dB. Efficiency of the antenna varies from 20% to 77%. Efficiency of the antenna at lower frequency region is low (20%) due to resistor loading.
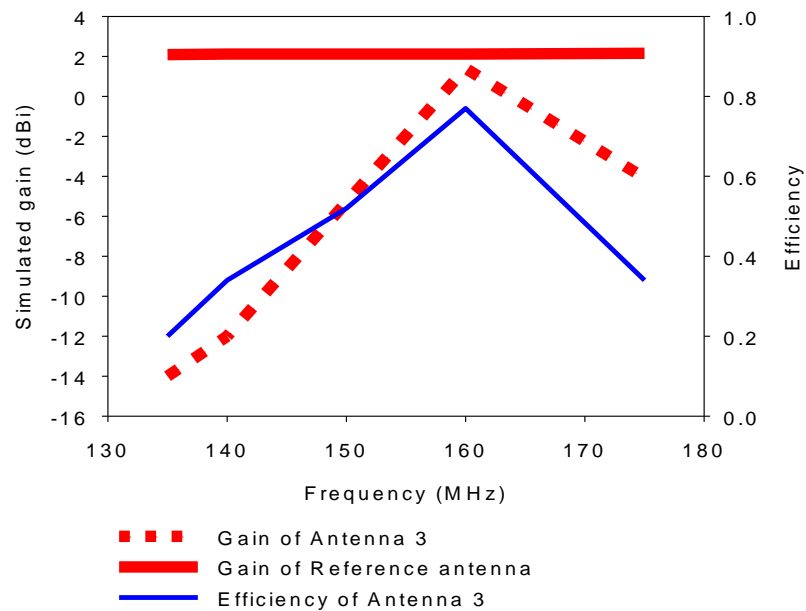
Fig 4.30 Simulated variation of gain and efficiency with frequency of R-L loaded meandered toploaded printed monopole antenna

The simulated radiation pattern of the antenna at f_0 is shown in Fig 4.31. The antenna shows omni directional radiation pattern at all frequencies within the band.
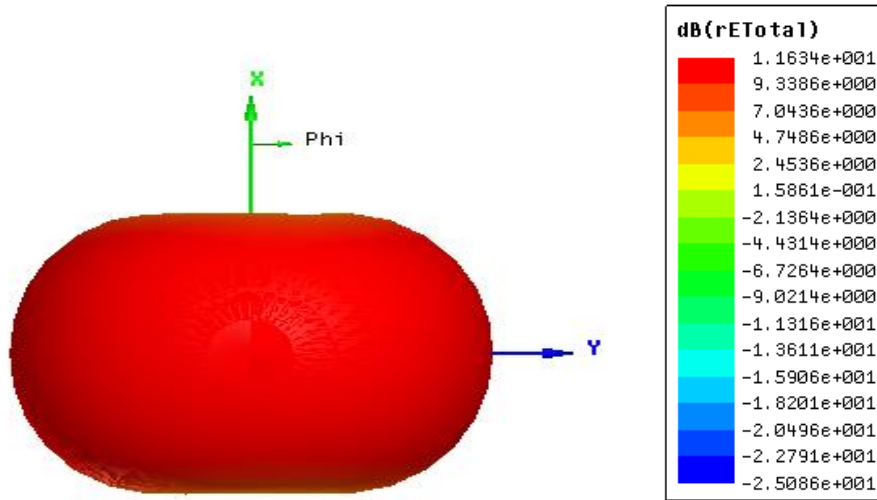
Fig 4.31 Simulated radiation pattern of R-L loaded meandered toploaded printed monopole antenna at f_0

4.2.3 PARAMETRIC ANALYSIS

A detailed parametric analysis was carried out in order to analyze the effect of each antenna dimension on the radiation characteristics of the antenna. To explain the variations in the frequency response of the antenna, the variations in the distributed reactive components are analyzed. The method used to calculate the distributed reactive component values are explained in Section 2.6.3.

(a) Effect of Top loading dimensions

The effect of top loading dimensions L_3, W_3, L_5 and W_5 on the frequency response of the antenna is studied.

The dimension L_3 is varied from 1cm to 2.5cm in steps of 0.5cm. The variations in the return loss characteristics of the antenna with L_3 is plotted in Fig 4.32. (a). The bandwidth of the antenna slightly increases on increase in L_3 till 2cm and then decreases. The variations in the distributed parameters with L_3 is plotted in Fig 4.32 (b). From figure it can be observed that increase in bandwidth is due to the increase in capacitive reactance. The distributed inductive reactance decreases with

increase in L_3 till 2.cm and then shows an uplift causing decrease in the bandwidth of the antenna.
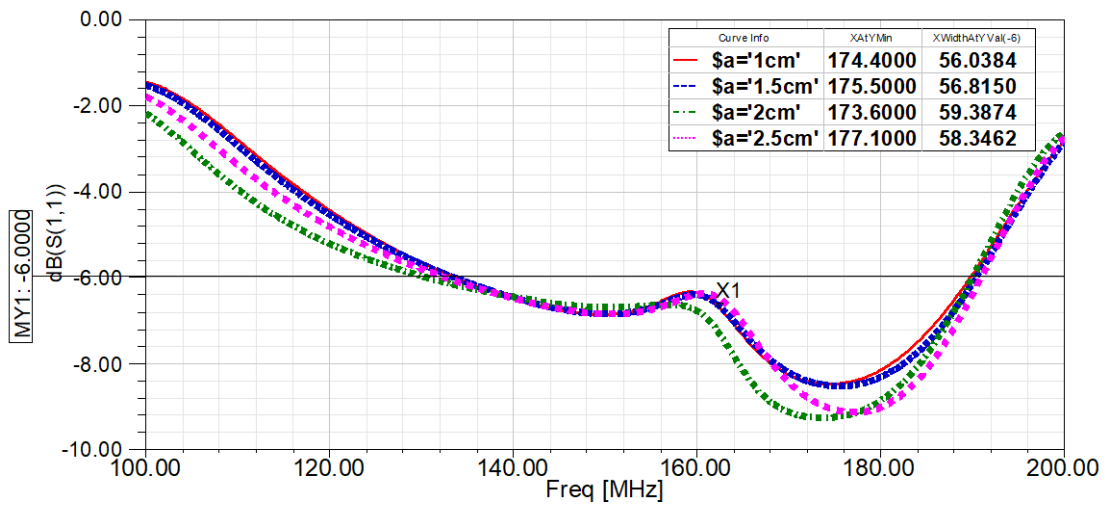
Fig 4.32 (a) Effect of L_3 on return loss characteristic of Antenna 3
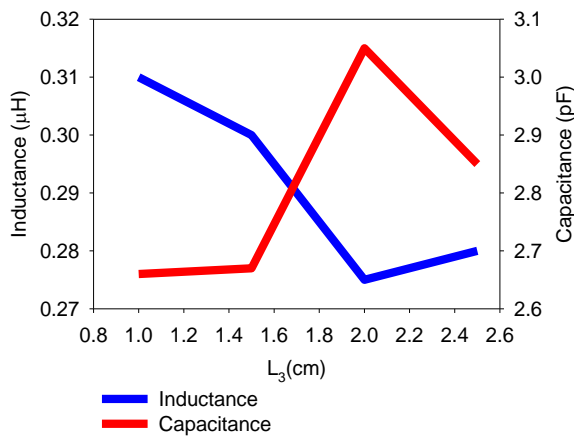
Fig 4.32 (b) Variation of distributed reactance with L_3

To study the effect of the top loading dimension W_3, it is varied from 1cm to 16cm. It is evident from the Fig 4.33 (a) that increase in W_3, improves the impedance matching at center frequencies, and thus increases the bandwidth of the antenna. It can be seen from Fig 4.33 (b) that inductive reactance decreases with increase in W_3 till 15cm and the capacitive reactance increases. Increase in W_3 beyond 15cm causes increase in distributed inductance causing decrease in bandwidth.
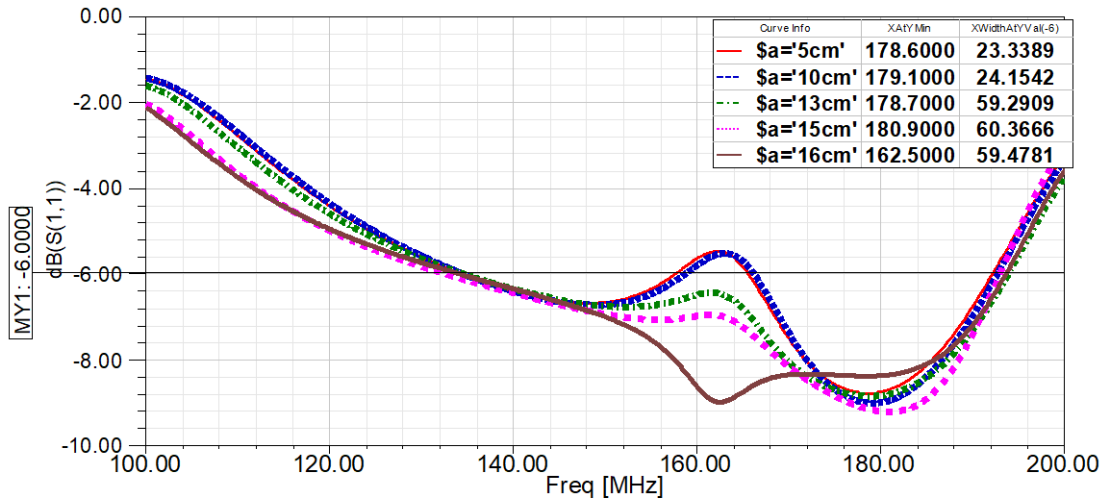
Fig 4.33 (a) Effect of W_3 on return loss characteristic of Antenna 3
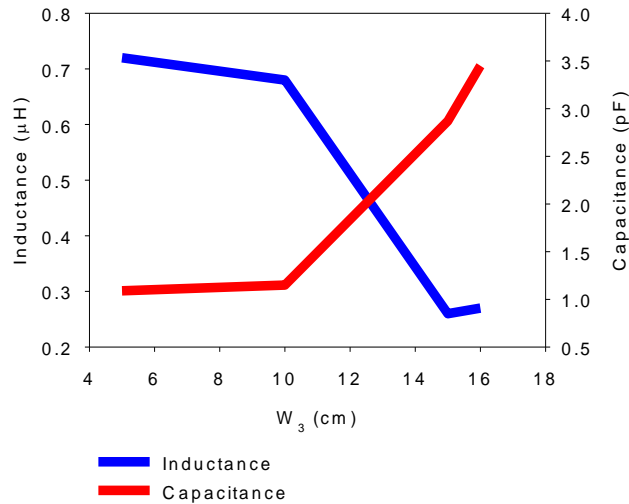
Fig 4.33 (b) Variation of distributed reactance with W_3

The effect of ground top loading length L_5 is studied and plotted in Fig 4.34 (a). L_5 was increased from 0.5cm to 2.5cm in step of 0.5cm. As L_5 increases the impedance matching at center frequency improves causing increase in bandwidth. It can be observed that $L_5 = 2$cm is the optimum value as it gives the maximum bandwidth. It can be observed from Fig 4.34 (b) that the distributed capacitance first decreases and then increases and then again decreases. The bandwidth of the antenna is effected by the change in distributed capacitance and it shows first a fall and then increase as L_5 reaches 2cm and again decline with further increase in L_5.
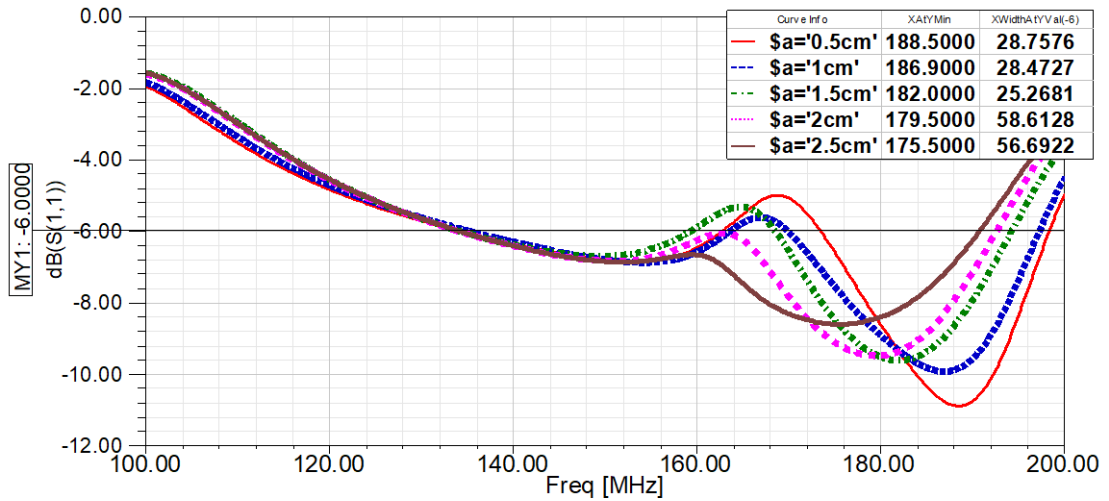
Fig 4.34 (a) Effect of L_5 on return loss characteristic of Antenna 3
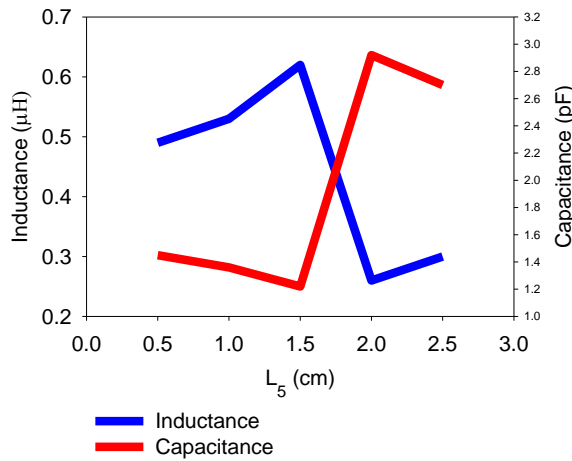
Fig 4.34 (b) Variation of distributed reactance with L_5

The effect of ground top loading width W_5 on the return loss of antenna is plotted in Fig 4.35 (a). W_5 is increased from 1cm to 7.5cm symmetrically to both sides from the center of the patch. It can be observed that the impedance matching at center frequencies improves with increase in W_5 and the bandwidth of the antenna increases. The variation in the distributed inductance and capacitance with W_5 is plotted in Fig 4.35 (b). It can be observed that the capacitive reactance shows a sharp increase at $W_5 = 14$cm causing a sharp increase in bandwidth. Hence $W_5 = 14$cm is chosen as optimum value.
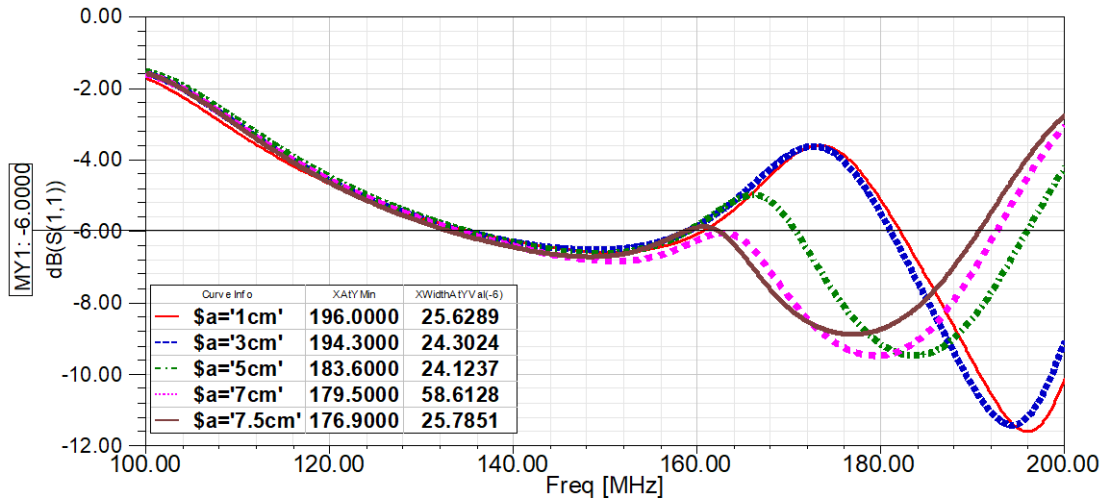
Fig 4.35 (a) Effect of W_5 on return loss characteristic of Antenna 3
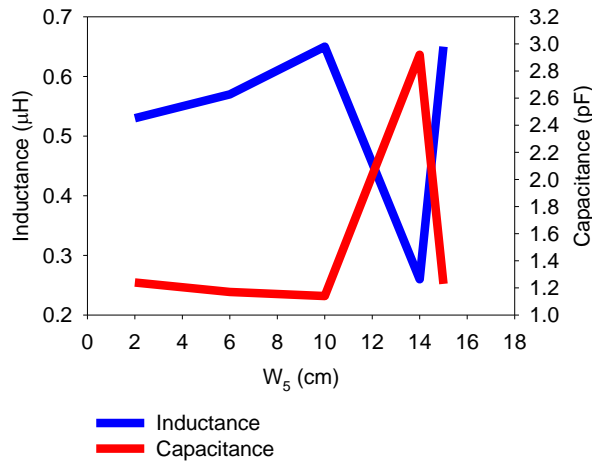
Fig 4.35 (b) Variation of distributed reactance with W_5

(b) Effect of ground plane dimensions L_4 and W_4

The length of the base rectangle of the ground plane is varied from 1cm to 10cm and its effect of on antenna performance is studied and plotted in Fig 4.36(a). The shift in the frequency towards higher side is due to the decrease in the surface current path with decrease in meander length. It can be observed from the Fig 4.36 (b) that inductive reactance remains almost steady till L_4= 9cm and then shows a sharp increase while capacitive reactance decreases as L_4 increases.

Curve Info	XAtY Min	X Width At Y Val(-6)
$a='1cm'	130.9000	34.3769
$a='3cm'	146.6000	35.6632
$a='5cm'	155.9000	45.7123
$a='7cm'	158.8000	57.7572
$a='9cm'	179.5000	58.6128
$a='10cm'	183.0000	24.6765
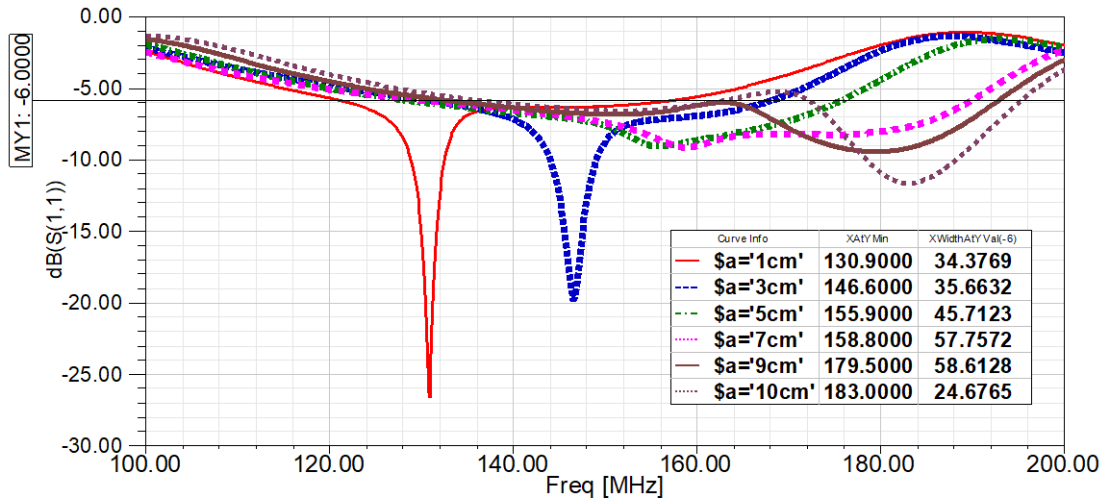
Fig 4.36 (a) Effect of L_4 on return loss characteristic of Antenna 3
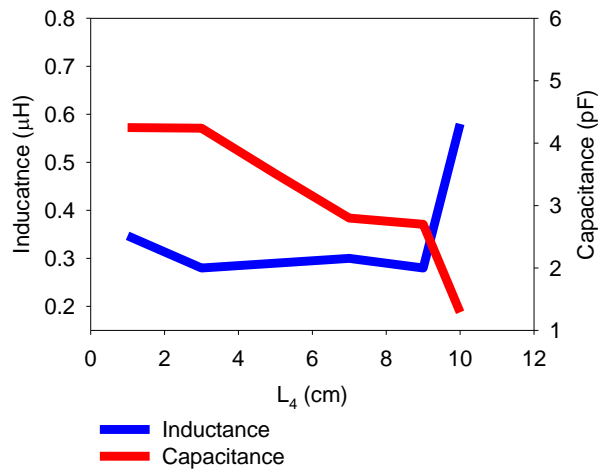
Fig 4.36 (b) Variation of distributed reactance with L_4

The effect of W_4 is analyzed by increasing it from 5cm to 11cm symmetrically to both sides from the center and the return loss characteristics of antenna is plotted in Fig 4.37 (a). It can be observed that the bandwidth of the antenna increases with W_4. From Fig 4.37 (b), it can be seen that the increase in bandwidth is due to the increase in capacitance with W_4.
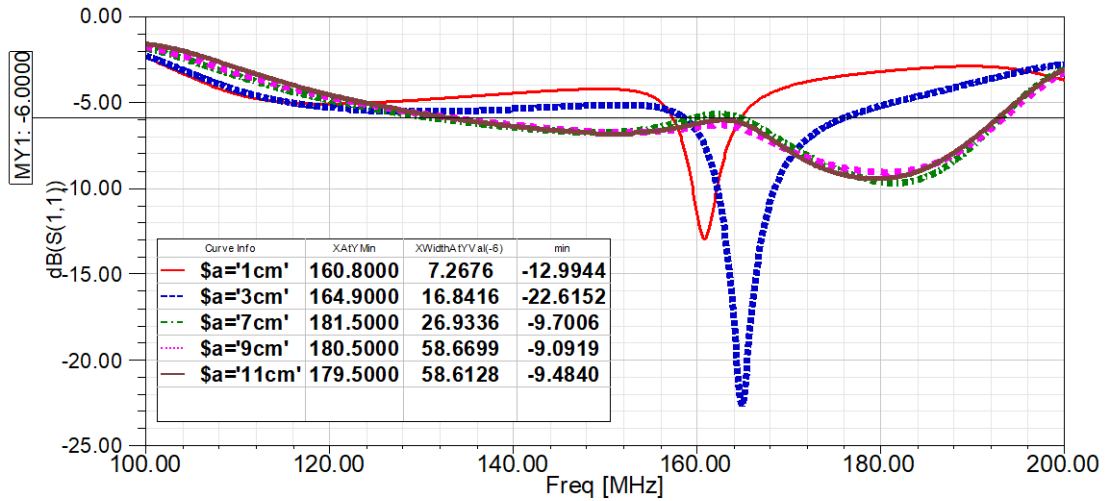
Fig 4.37 (a) Effect of W_4 on return loss characteristic of Antenna 3
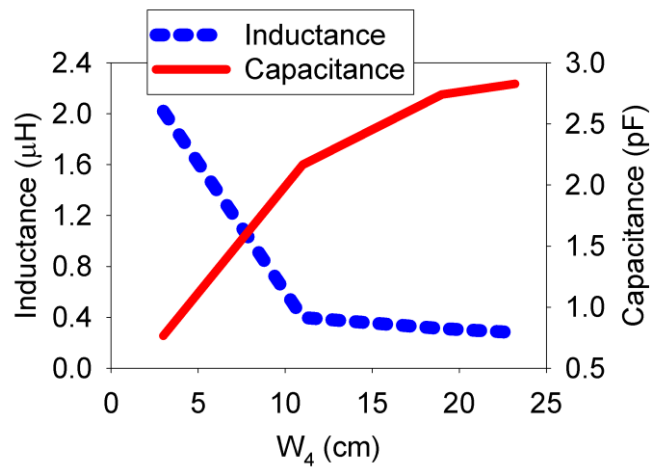
Fig 4.37(b) Variation of distributed reactance with W_4

The variation in frequency response of the antenna with variation in gap length L_g is studied and is plotted in Fig 4.38 (a). It can be observed that the impedance matching of the antenna at center frequencies improves with increase in L_g. From Fig 4.38 (b) it can be understood that the inductance decreases and capacitance increases as L_g increases from 0.5cm to 2cm, causing sharp increase in bandwidth. Further increase in L_g causes slight increase in the distributed inductance and decrease in distributed capacitance, decreasing bandwidth.
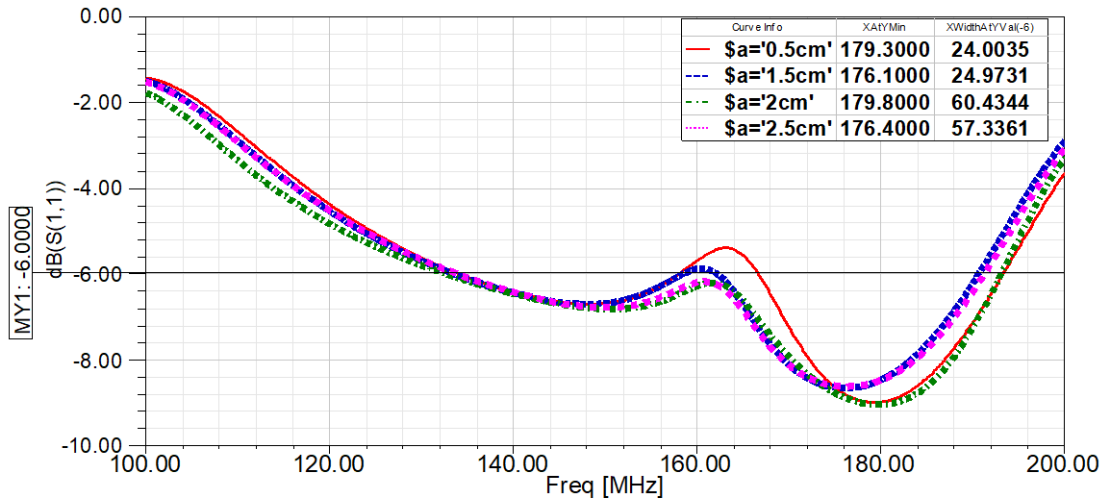
Fig 4.38 (a) Effect of L_g on return loss characteristic of Antenna 3
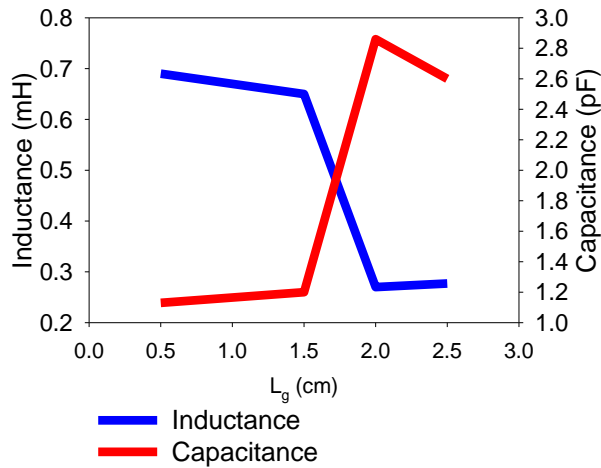
Fig 4.38 (b) Variation of distributed reactance with

4.2.4. ANTENNA FABRICATION

A meandered top loaded printed monopole antenna shown in Fig 4.24 was fabricated on FR4 substrate of dielectric constant 4.4 and thickness 0.16cm using photolithographic technique. The dimensions of the antenna are as shown in Table 4.2. A lumped resistor of 15Ω and an air core inductor of 200nH was connected parallel and was inserted into the meander line of radiating patch near the feed of the antenna.

The antenna was mounted on an aluminium base plate of dimensions 5cm X 28cm X 8cm. The aluminium base plate is used to hold the connector and also it acts as an interface between antenna and the mounting platform.

A 50Ω TNC connector is used to excite the antenna. The photograph of the fabricated antenna is shown in Fig 4.39.

Fig 4.39. Photograph of fabricated antenna

4.2.5 MEASURED RESULTS

The performance of the antenna was evaluated using E5071C Vector Network Analyzer. At first, the antenna was tested for its VSWR characteristics without any additional ground plane. The antenna was then mounted on a 1.2m diameter circular ground plane and the VSWR was measured. The measured VSWR is found to be less than 3 (S11 < -6 dB) over the referred frequency band in both the cases, although the presence of ground plane shows a slight shift in the frequency band towards lower side as shown in Fig 4.40. The effect of mounting ground plane on the printed monopole antenna is very less compared to conventional monopole antenna.
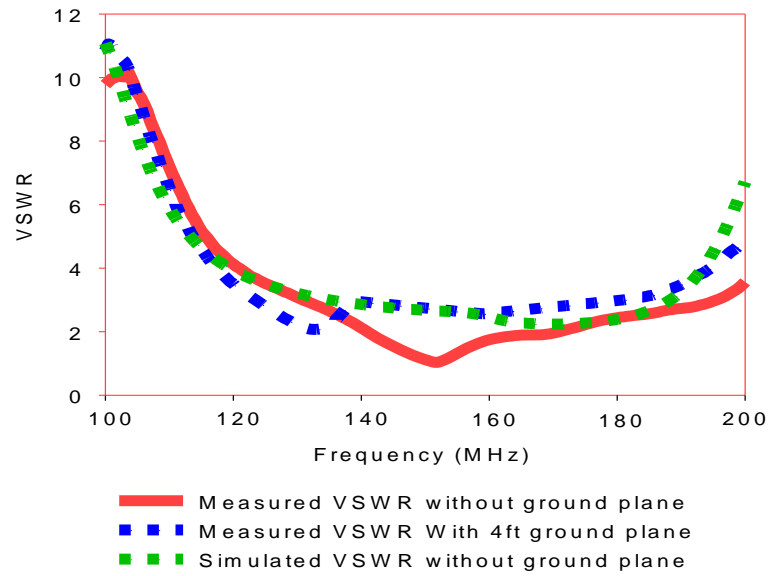
Fig 4.40 Measured VSWR of Antenna 3 with and without ground plane

The measured gain of the antenna with and without mounting ground plane is shown in Fig 4.41 and is compared with a conventional blade monopole antenna [37] and a basic printed strip monopole antenna. The gain increases in the lower frequency region when mounted on the ground plane due to improved impedance matching.
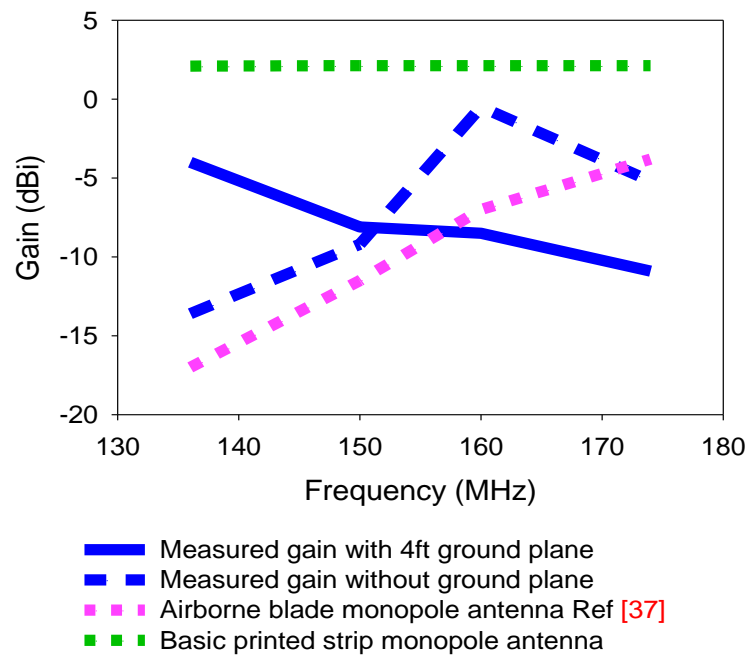
Fig 4.41 Measured Gain

The antenna was tested for its far field radiation characteristics in an open field. The measured H plane radiation pattern of the antenna with and without mounting ground plane at 136, 150 and 175 MHz is illustrated in Fig 4.42(a) and (b) respectively. It can be seen that the H plane radiation pattern of the proposed antenna is nearly omnidirectional at all frequencies.
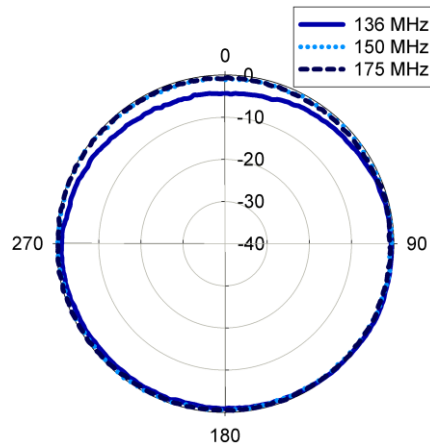
Fig 4.42 (a). Azimuth pattern with 4ft ground plane
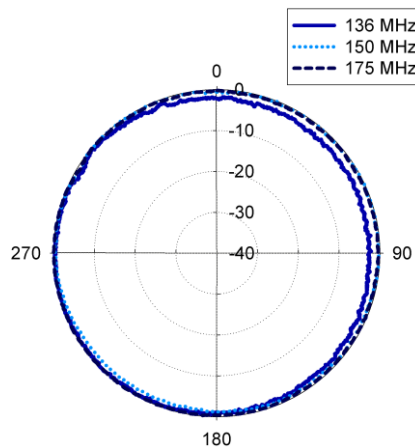
Fig 4.42 (b). Azimuth pattern without ground plane

The measured E plane radiation pattern of the antenna with and without mounting ground plane at 136, 150 and 175 MHz is illustrated in Fig 4.43 (a) and (b) respectively. The elevation pattern at the higher side of the frequency band resembles "figure-eight" pattern, and at lower frequency side, it is slightly distorted.
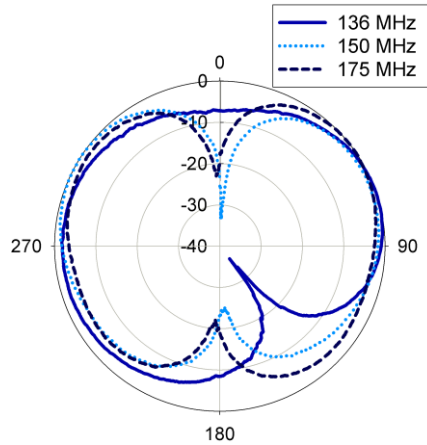
Fig 4.43 (a). Elevation pattern with 4ft ground plane
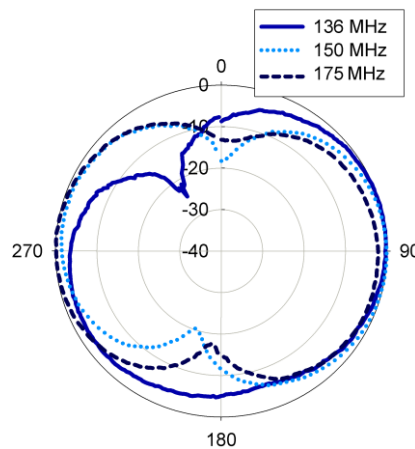
Fig 4.43 (b). Elevation pattern without ground plane

4.3. COMPARISON ON ANTENNAS IN EVOLUTION PROCESS

A comparison table of the characteristics of the antennas designed in the simulation process are tabulated in Table 4.3.

Table 4.3. Comparison on antenna characteristics

	Reference antenna	Antenna 1	Antenna 2	Antenna 3
Total height in cm	70	52	40	23
Height reduction in %	-	25	43	67
3:1 VSWR bandwidth (%)	22	27	23	38
Gain variation	2dBi	1.7dBi to 2dBi	0.8dBi to 1.8dBi	-14 dBi to -0.5dBi
Radiation pattern	Omni directional	Omni directional	Omni directional	Omni directional

4.4 SUITABILITY OF ANTENNA FOR AIRBORNE PLATFORM

The main features of this antenna - compact size and planar shape, light weight, wide bandwidth, omnidirectional radiation pattern and improved gain make it highly suitable for airborne applications. Also, the printed monopole configuration of the antenna make it apt choice for platform space constrained applications also.

The RL loaded meandered toploaded printed monopole antenna achieves 63% height reduction compared to conventional quarter wave planar monopole antenna and 67% compared to printed strip monopole antenna at lowest frequency of operation. The total height of the antenna is only 0.1λ at lowest frequency of operation. Also, the antenna is designed in planar aerodynamic shape – trapezoidal shape- so as to reduce air drag. These physical features meet the mechanical requirements of airborne antennas.

The antenna offers wide bandwidth in the VHF band (3:1 VSWR bandwidth of the antenna is 38% at center frequency). The radiation pattern of the antenna is omnidirectional at all frequencies within the band and exhibits vertical polarization when mounted vertically. The gain of the antenna varies from -14dBi to -1.5dBi within the band. These radiation characteristics makes this antenna apt for airborne VHF communication.

The printed monopole antenna configuration allows this antenna to mount in ground plane constrained positions. The substrate used for the fabrication of antenna (FR4) can tolerate wide temperature and pressure range and also is mechanically robust.

A comparison of this antenna was carried out with the airborne blade monopole antenna reported in literature operating in the band of 135MHz-175MHz and is tabulated in Table 4.4. The performance of the antenna is comparable to the conventional blade monopole antennas operating in VHF band with the added advantage of requiring minimal ground plane to mount on.

Table 4.4. Comparison of the antenna with the airborne antenna in literature

Characteristics	RL Loaded Meandered Toploaded Printed Monopole Antenna	Airborne blade monopole antenna Ref [37]
Height	23cm	18.8cm
Ground plane size	Antenna base plate (0.5cm × 29cm ×8cm)	1.2m diameter around the feed
3:1 VSWR bandwidth	132-190MHz	135-175MHz
Minimum gain over the frequency band	-14dBi	-17dBi
Maximum gain over the frequency band	-0.5dBi	-4dBi
Radiation pattern	Omnidirectional	Omnidirectional

4.5 CHAPTER SUMMARY

A wideband printed monopole antenna operating in VHF band has been developed and the results are presented. The antenna exhibits a 3:1 VSWR bandwidth of 38%. It achieves a height reduction of 67% compared to basic printed strip monopole antenna and 63% compared to quarter wavelength planar monopole antenna. The proposed VHF monopole antenna requires nil or minimal ground plane on the platform. The radiation characteristics measured with antenna alone as well as with antenna mounted on λ/2 diameter ground plane are presented.

5. Theoretical Investigations

This chapter presents the results of theoretical investigations on the printed monopole antennas presented in previous chapters. The design equation for the resonant frequency of an antenna structure provide a fast and simple way for the resonant frequency prediction compared to the complex simulation softwares. Hence, simple design equation are developed for calculating the resonant frequencies of the antenna structures – bifolded printed bent monopole antenna and RL loaded meandered top loaded printed monopole antenna - mentioned in chapters 3 and 4. The validity of these equations are established by comparing it with HFSS simulated results.

5.1. INTRODUCTION

A good insight to the antenna radiation mechanism can be obtained from the theoretical interpretations. The design equations for the resonant frequency of an antenna structure can be derived based on the parametric studies and surface current analysis. The calculated results using the formulated equations were compared with the corresponding HFSS simulated results. The theoretical predictions are found to be very close to these simulated results and thus establish the validity of design formulas.

5.2. DESIGN ASPECTS OF A PRINTED MONOPOLE ANTENNA

The design equations for a rectangular patch antenna based on cavity model is modified to derive the equation for the resonant frequency of the patches described in this thesis.

The derivation of the design equation of rectangular microstrip patch antenna involves the computation of relation between resonant frequency and its patch dimensions.

The derivation starts from the basic relation between frequency (f) and wavelength (λ) in vacuum.

$$f = \frac{c}{\lambda} \quad …(1)$$

Where,'c' is velocity of light in vacuum. It is known that, in a dielectric medium, the velocity of electromagnetic wave is modified as $c/\sqrt{\varepsilon_r}$ where, ε_r is the relative permittivity of the medium.

For the fundamental mode of resonance of rectangular microstrip antenna (TM_{010} mode), the length of the patch (L) corresponds to half wavelength at resonant frequency. Hence, the fundamental frequency (TM_{010} mode) of a standard rectangular microstrip antenna is calculated using the formula.

$$f_r = \frac{c}{2L\sqrt{\varepsilon_r}} \quad …(2)$$

For microstrip antennas, although most of the electric field lines resides in substrate, parts of some lines exist in air. Since some of the waves travel in the

substrate and some in air, an effective dielectric constant ε_{reff} is introduced to account for fringing and wave propagation in the microstrip line.

The effective dielectric constant of microstrip antenna is given by

$$\varepsilon_{reff} = \frac{\varepsilon_r + 1}{2} + \frac{\varepsilon_r - 1}{2}\left(1 + \frac{12h}{w}\right)^{\frac{-1}{2}} \qquad \dots(3)$$

Where 'h' is the thickness of the substrate, 'w' is the width of the patch and 'ε_r' is the substrate dielectric constant.

Because of the fringing effect, electrically the patch of the microstrip antenna looks greater than its physical dimensions. Hence, the length of the patch (L) in (2) is replaced by effective length of the patch (L_{eff}).

Thus the equation for calculating the fundamental frequency (TM_{010} mode) of a standard rectangular microstrip antenna is modified as

$$f_r = \frac{c}{2L_{eff}\sqrt{\varepsilon_{reff}}} \qquad \dots(4)$$

For most applications, the value of ε_{reff} will be closer to the value of the actual dielectric constant ε_r of the substrate [4].

But for printed monopole antennas, it is observed that the variation in the resonant frequencies of printed monopole antennas with the substrate dielectric constant is not by a factor of $\sqrt{\varepsilon_r}$ as observed in conventional microstrip antennas, but by a factor closer to unity. This is explained by taking the consideration that the printed monopole antenna can be viewed as a special case of microstrip antenna configuration, wherein the backing ground plane is located at infinity [152]. That is, it is assumed that beyond the printed monopole patch fabricated on a dielectric substrate, there exists a very thick air dielectric substrate ($\varepsilon_r = 1$). It makes the microstrip antenna configuration to look like as if it is fabricated on a thick substrate with ε_r closer to unity

Following this analogy, the factor *k,* whose value closer to unity can be thought of as having similar significance as $\sqrt{\varepsilon_{reff}}$.

$$\sqrt{\varepsilon_{r\text{eff}}} = k \qquad ...(5)$$

The methodology adopted to derive the design equation of the antennas mentioned in this thesis is as follows:

Fundamental mode excited by the printed monopole antennas are analysed by studying their surface current distribution. The number of half wave variations occurring along the length of patch is determined from this. The effective electrical length of patch L_{eff}, is determined by studying variation in resonant frequency with respect to different dimensional factors, by using parametric analysis method. The factors 2 and L_{eff} of (4) are then replaced by number of half wave variations along length of patch and effective electrical length of patch L_{eff} respectively.

The effective dielectric constant $\sqrt{\varepsilon_{r\text{eff}}}$ of (4) is replaced by the factor *k (5)*.

The resonant frequency of the antenna is then calculated using the relation

$$f_r = \frac{c}{\lambda \times k} \ .... \ (6)$$

where, λ = no. of half wave variations along the length of patch $\times L_{eff}$.

The design equation formulation of the bifolded printed bent monopole antenna and R-L loaded meandered toploaded printed monopole antenna are described below.

5.3. DESIGN EQUATION FORMULATION OF BIFOLDED PRINTED BENT MONOPOLE ANTENNA

Geometry of the antenna is shown in Fig 5.1. The standard printed bent monopole antenna is folded twice in order to achieve compactness. The radiating patch consists of four arms L_1, L_2, L_3 and L_4. The width of the radiating patch is W_1. The ground plane consists of an L shaped patch.
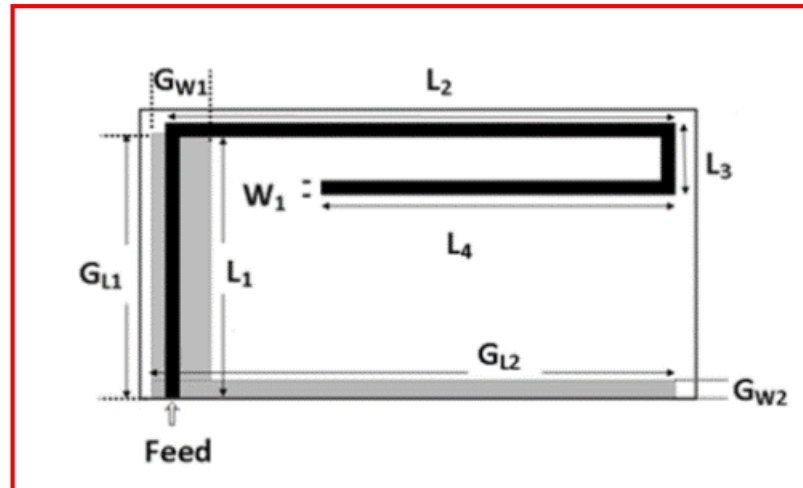
Fig 5.1 Bifolded printed bent monopole antenna

5.3.1. Surface Current Distribution

From the surface current distribution on the antenna structure at resonant frequency shown in Fig 5.2 (a), it can be observed that there is quarter wave variation in the surface current distribution along the radiating patch. From Fig 5.2 (b) it is understood that the surface current distribution along the ground patch is feeble and hence the contribution of ground patch towards the resonant frequency is less. Hence, it is inferred that the effective electrical length of the antenna is formed by the four arms of radiating patch L_1, L_2, L_3 and L_4 and it corresponds to quarter wavelength at resonant frequency.
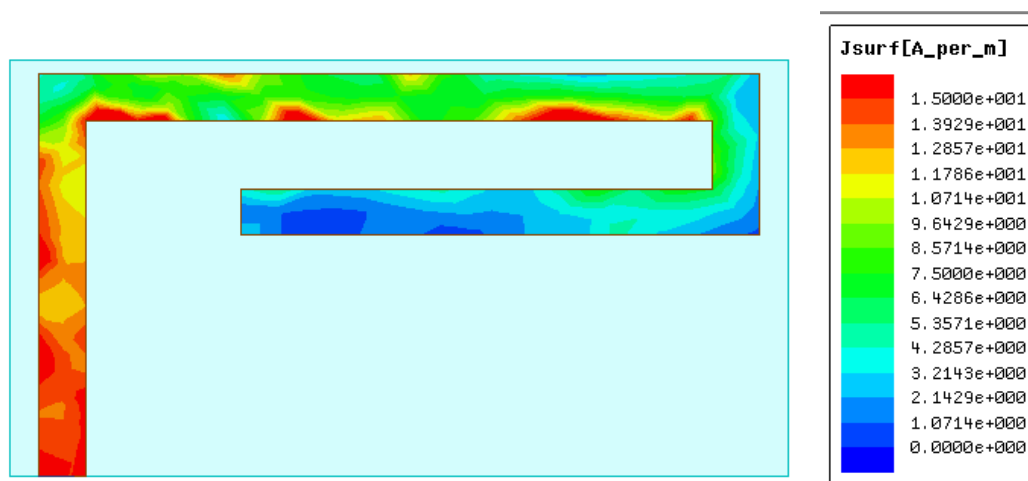
Fig 5.2(a) Surface current distribution along radiating patch
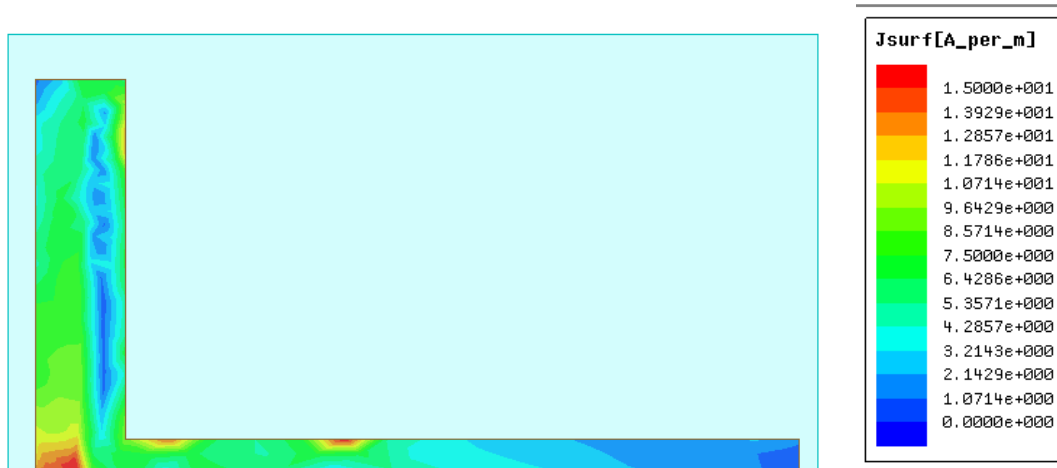
Fig 5.2(b) Surface current distribution along ground

5.3.2 Parametric Study

The dimensional factors affecting the resonant frequency are identified by carrying out intensive parametric study. The methodology followed in parametric study is to vary one parameter over a range keeping all other parameters fixed. Due to the structural limitations, the dimension L_1 is varied from 12cm to 14cm; L_2 is varied from 22cm to 25cm; L_3 is varied from 4.6cm to 7.6cm; L_4 is varied from 14cm to 18cm and W_1 is varied from 0.6cm to 2.4cm. The effect of L_1, L_2, L_3, L_4 and W_1 on the resonant frequency of the antenna is shown in Fig 5.3 (a-e).

It was evident from the parametric analysis that the length L_1, L_2, L_3 and L_4 contribute to the reduction of the resonant frequency. This is because increase in these dimensions increases the effective capacitance and inductance of the structure thereby decreases the resonant frequency. The contribution of L_2, L_3 and L_4 is found to be prominent in determining the resonant frequency than L_1. It was found that L_3 has noticeable effect on determining the resonant frequency compared to other parameters of the antenna. The effect of L_1 on the resonant frequency is comparatively less as it acts as a microstrip feed line to couple the RF power. As W_1 increases, the effective length of the antenna decreases, shifting the frequency to higher side.
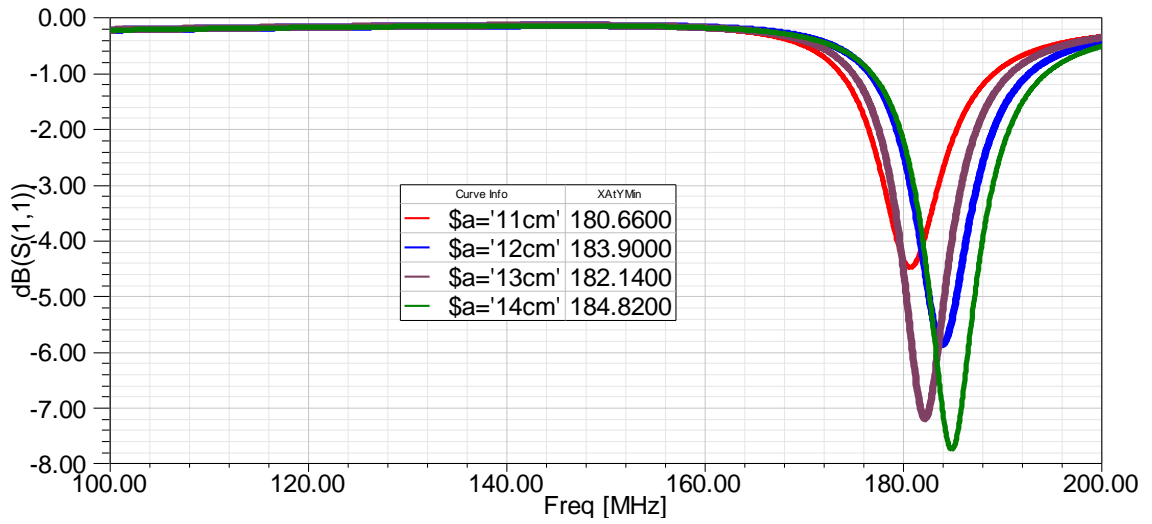
Fig 5.3 (a) Variation in frequency with L_1
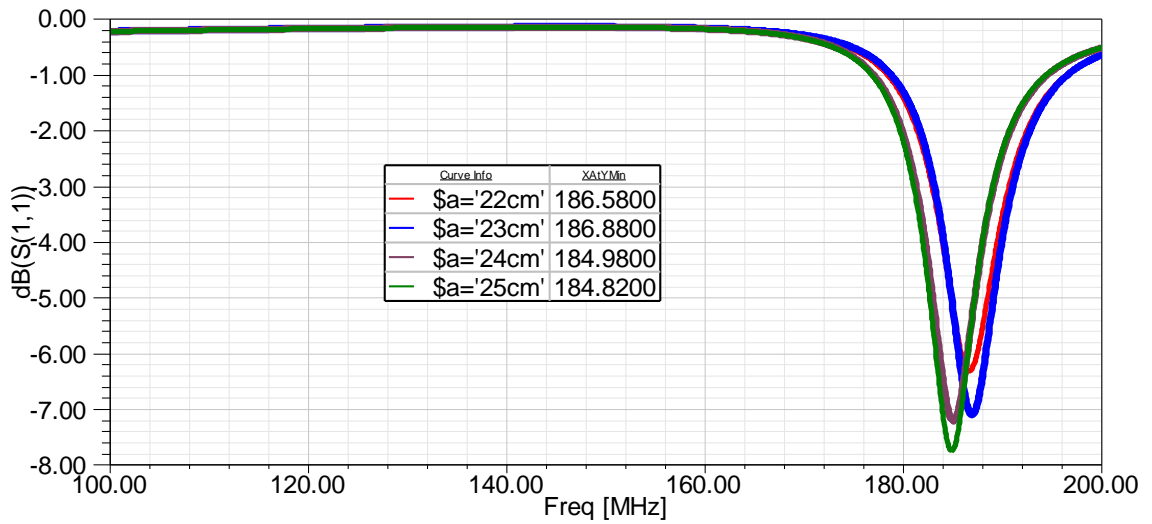
Fig 5.3 (b) Variation in frequency with L_2
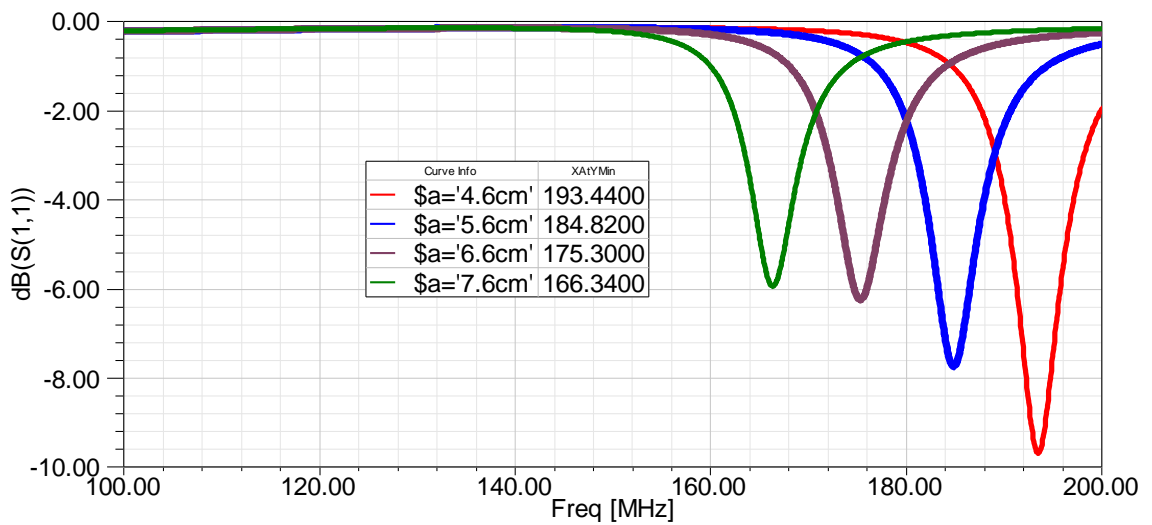
Fig 5.3 (c) Variation in frequency with L_3
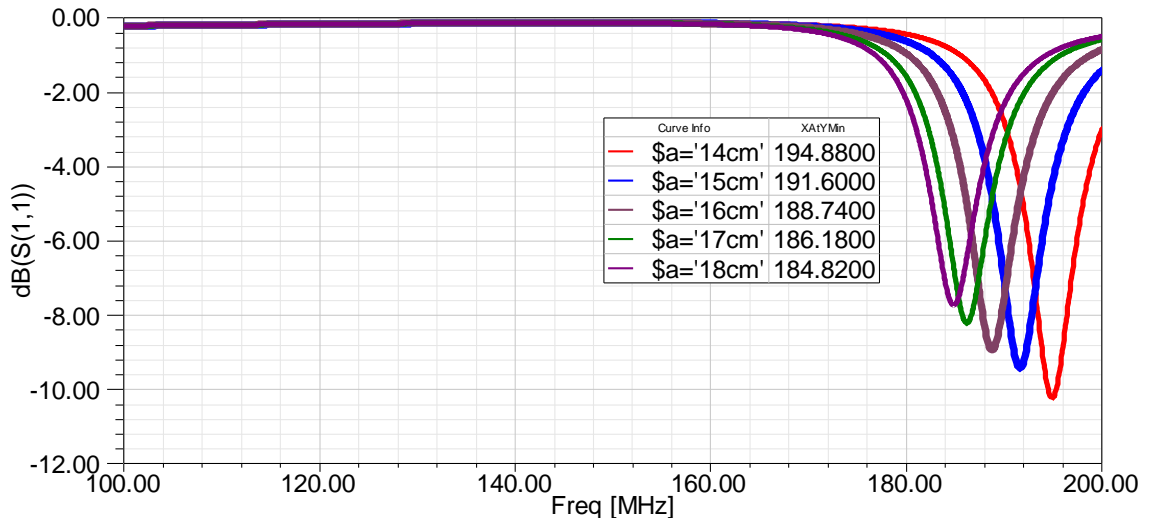
Fig 5.3 (d) Variation in frequency with L_4
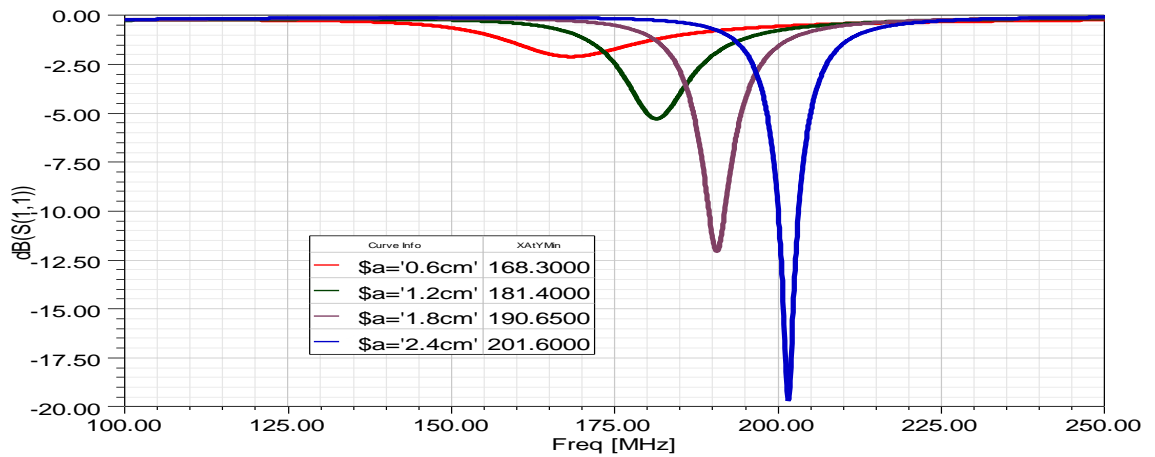
Fig 5.3 (e) Variation in frequency with W_1

The effect of dielectric constant on the resonant frequency is shown in Fig 5.4. It is observed that the substrate dielectric constant contribute to the reduction of resonant frequency of a printed monopole antenna by a factor closer to unity.

Curve Info	XAtYMin
$m='1'	202.1500
$m='2'	195.6500
$m='3'	190.9000
$m='4'	184.9500
$m='5'	181.7000
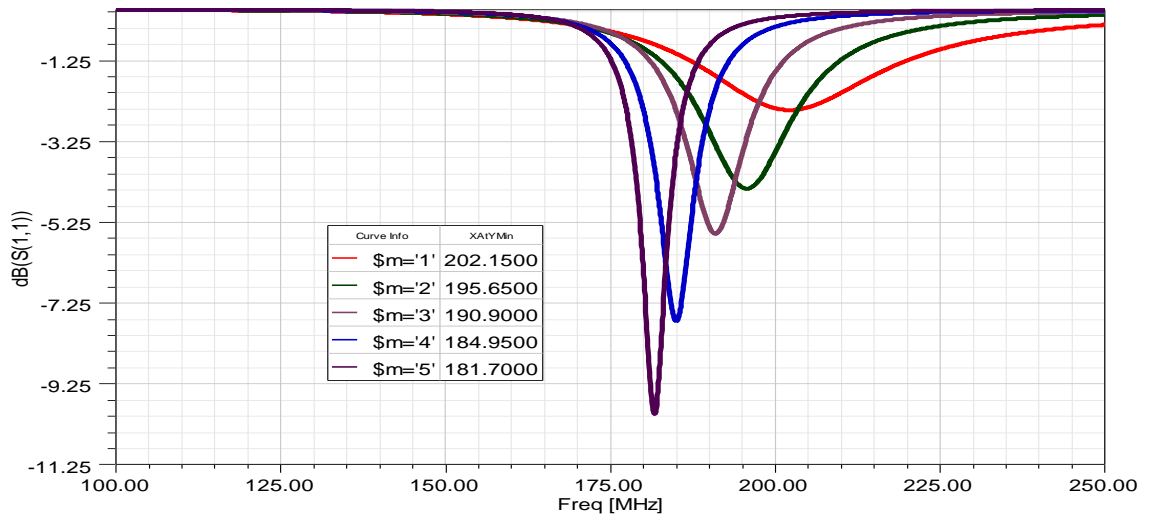
Fig 5.4 Variation in frequency with dielectric constant

The effect of resistor loading on antenna resonant frequency is shown in Fig 5.5. By loading the antenna with resistor, the impedance matching at the lower frequency region improves, increasing the bandwidth of the antenna. Since the shift in the resonant frequency due to resistor loading is very less; the effect of resistor is not considered in the design equation formulation

Curve Info	XAtYMin
$c='5ohm'	183.7000
$c='10ohm'	183.2000
$c='15ohm'	181.1000
$c='20ohm'	180.3500
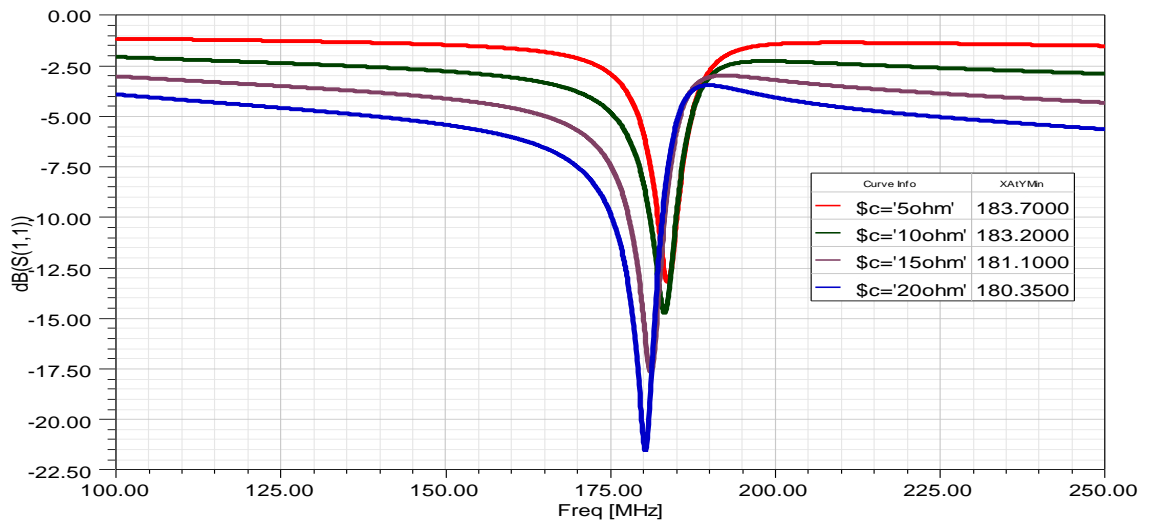
Fig 5.5 Variation in frequency with resistor value

5.3.3. Resonant frequency calculation

The standard equations for computing the resonant frequency of rectangular microstrip antenna given by equation (4) is modified to compute the resonant frequency of bifolded printed bent monopole antenna.

117

It is observed from the surface current distribution (Fig 5.2) that the effective electrical length of the antenna corresponds to quarter wavelength at resonant frequency. Hence factor 2 in equation (4) is replaced by 4.

The dimensions, L_1, L_2, L_3, L_4 and W_1 determine the effective electrical length of the patch, L_{eff}. By considering the effect of these dimensions from parametric study, the effective electrical length of the patch L_{eff} is calculated as

$$L_{eff} = 0.02L_1 + 0.5L_2 + 2.5L_3 + 0.7L_4 - 1.8W_1 \quad … (7)$$

As the substrate dielectric constant contributes to the resonant frequency determination by a factor closer to unity, the $\sqrt{\varepsilon_{reff}}$ in equation (4) is replaced by variable k.

Hence (4) for resonant frequency of rectangular microstrip antenna is modified as

$$fr = \frac{c}{4 \times L_{eff} \times k} \quad … (8)$$

5.3.4 Comparison between calculated and simulated results

The resonant frequency predicted by the derived equation was verified for different values of L_1, L_2, L_3, L_4 and W_1; varying one dimension at a time, keeping other dimensions constant. The calculated frequency was compared with the simulated result and the error was calculated. The validation of the equation was done by analyzing the equation for RT Duroid 5880 (ε_r=2.2) substrate.

The k value for FR4 substrate is determined as 1.1 and that of RT Duroid 5880 is determined as 1.008.

The resonant frequency calculation for variation L_1, L_2, L_3, L_4 and W_1 on FR4 substrate and RT Duroid substrate are tabulated in Table 5.1, 5.2, 5.3, 5.4 and 5.5 respectively. A percentage error less than 5% was obtained for both cases.

The plots corresponding to the frequency variation with different dimensions for Fr4 substrate and RT Duroid 5880 substrate are shown in Fig 5.6, 5.7, 5.8, 5.9 and 5.10 for comparison.

Table 5.1. Resonant frequency calculation for variation in L_1

(L_2=25cm; L_3 = 5.6cm; L_4=18cm, W_1=1.2cm)

L_1 (cm)	FR 4 substrate			RT Duroid 5880		
	Simulated Frequency (MHz)	Calculated Frequency (MHz)	% Error	Simulated Frequency (MHz)	Calculated Frequency (MHz)	% Error
14	184.8	183.1	0.9	195.3	199.9	2.3
13	182.1	183.2	0.6	196.2	200	1.9
12	183.9	183.3	0.3	196.6	200.1	1.7

Table 5.2. Resonant frequency calculation for variation in L_2

(L_1=14cm; L_3 = 5.6cm; L_4=18cm, W_1=1.2cm)

L_2 (cm)	FR 4 substrate			RT Duroid 5880		
	Simulated Frequency (MHz)	Calculated Frequency (MHz)	% Error	Simulated Frequency (MHz)	Calculated Frequency (MHz)	% Error
25	184.8	183.1	0.9	195.3	199.9	2.3
24	184.9	185.6	3.7	198.2	202.6	2.2
23	186.8	188.2	0.7	201.8	205.4	1.7
22	186.5	190.8	2.3	204.9	208.3	1.6

Table 5.3. Resonant frequency calculation for variation in L_3
(L_1=14cm; L_2 = 18cm; L_4=18cm, W_1=1.2cm)

L_3 (cm)	FR 4 substrate			RT Duroid 5880		
	Simulated Frequency (MHz)	Calculated Frequency (MHz)	% Error	Simulated Frequency (MHz)	Calculated Frequency (MHz)	% Error
4.6	193.4	196.3	1.4	205.2	214.3	4.4
5.6	184.8	183.1	0.9	195.3	199.9	2.3
6.6	175.3	171.6	2.1	187.3	187.3	0.0
7.6	166.3	161.5	2.8	179.1	176.2	1.6

Table 5.4. Resonant frequency calculation for FR4 substrate for variation in L_4

(L_1=14cm; L_2 = 18cm; L_3=5.6cm, W_1=1.2cm)

L_4 (cm)	FR 4 substrate			RT Duroid 5880		
	Simulated Frequency (MHz)	Calculated Frequency (MHz)	% Error	Simulated Frequency (MHz)	Calculated Frequency (MHz)	% Error
18	184.8	183.1	0.9	195.3	199.9	2.3
17	186.1	186.7	0.3	197.7	203.7	3.0
16	188.7	190.3	0.8	201.2	207.7	3.2
15	191.6	194.1	1.3	204.0	211.8	3.8
14	194.8	198.1	1.6	207.2	216.1	4.2

Table 5.5. Resonant frequency calculation for FR4 substrate for variation in W_1

(L_1=14cm; L_2 = 18cm; L_3=5.6cm, L_4=18cm)

W_1 (cm)	FR 4 substrate			RT Duroid 5880		
	Simulated Frequency (MHz)	Calculated Frequency (MHz)	% Error	Simulated Frequency (MHz)	Calculated Frequency (MHz)	% Error
1.2	181.4	183.1	0.9	195.3	199.9	2.3
1.8	190.6	188.6	1.0	204.6	205.8	0.5
2.4	201.6	194.4	3.5	215.4	212.2	1.4
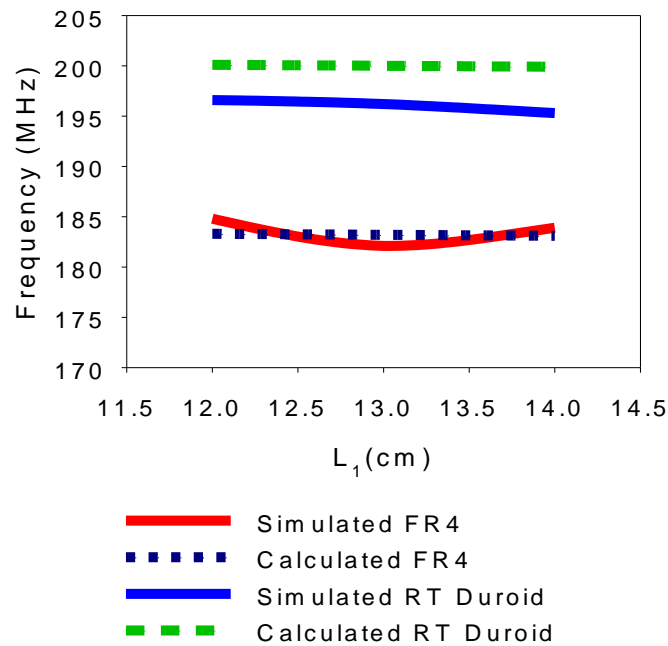
Fig 5.6 Simulated and calculated results for variation in L_1
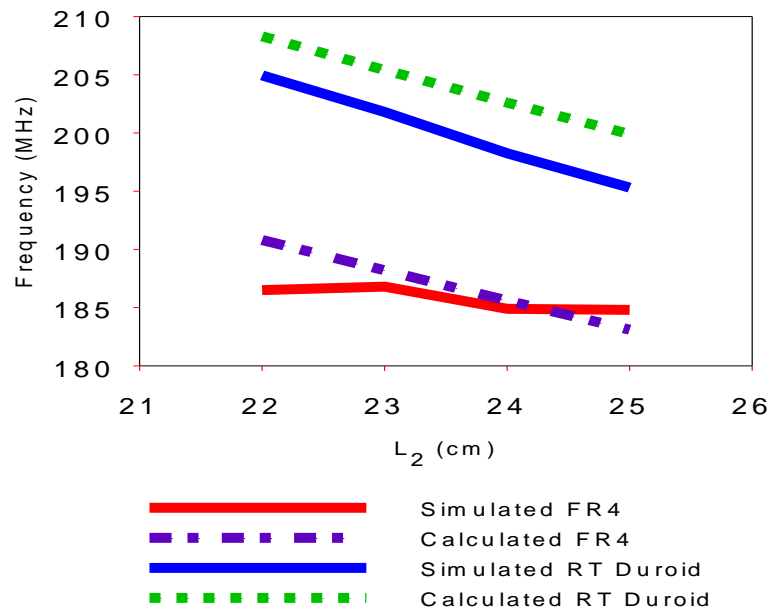
Fig 5.7 Simulated and calculated results for variation in L_2
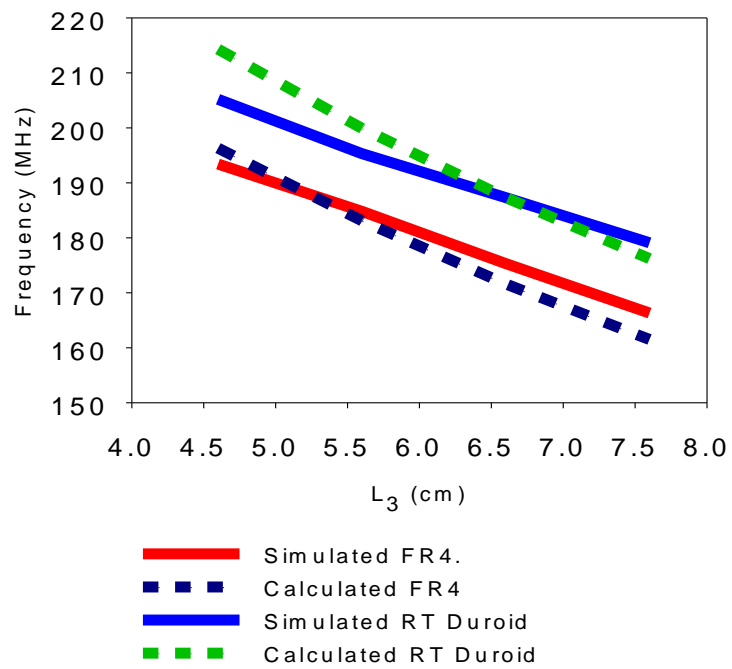
Fig 5.8 Simulated and calculated results for variation in L_3
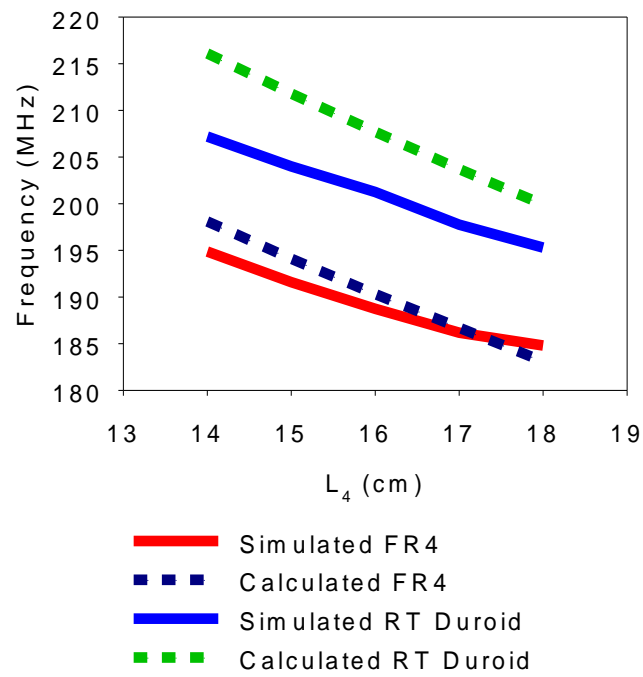
Fig 5.9 Simulated and calculated results for variation in L$_4$
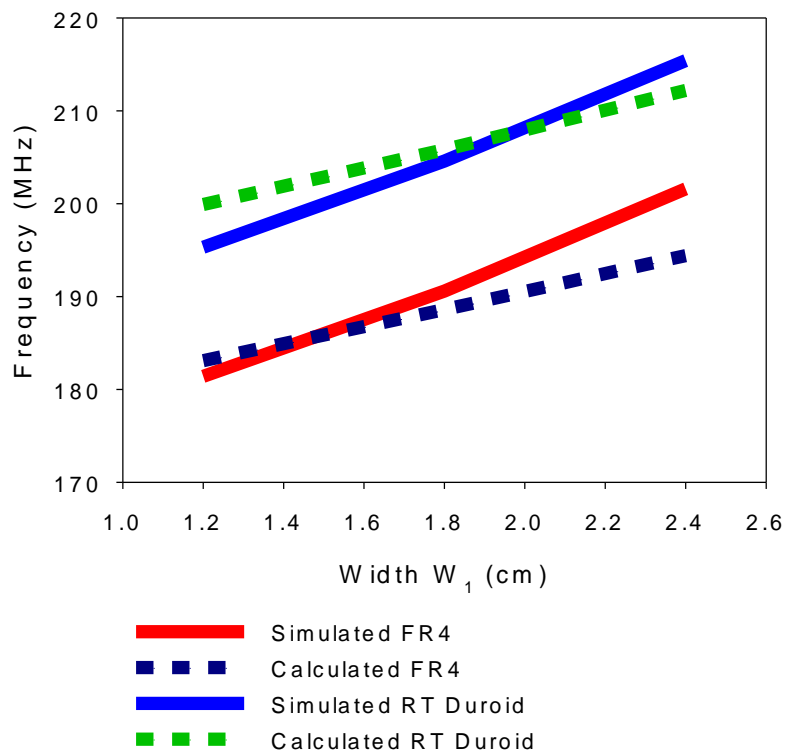
Fig 5.10. Simulated and calculated results for variation in W$_1$

5.4 DESIGN EQUATION FORMULATION FOR RL LOADED MEANDERED TOPLOADED PRINTED MONOPOLE ANTENNA

The schematic diagram of the antenna is shown in Fig 5.11. The radiating patch consists of a RL loaded meandering structure and a top loading which is gap coupled to meander line. The ground plane consists of a meander line and top loading structures implemented above the partial rectangular shaped ground. The meander line on ground plane is in symmetry with that of the meander line of the radiating patch for impedance matching.

(a)   (b)
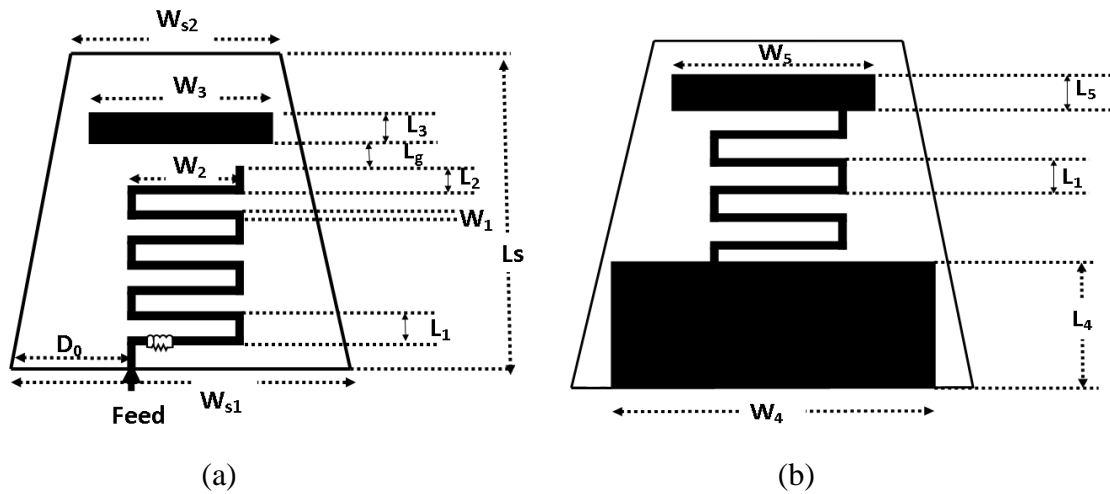
Fig 5.11. Geometry of RL loaded meandered toploaded printed monopole antenna; (a) Radiating patch (b) Ground patch

5.4.1 Surface current distribution

The surface current distribution at resonant frequency along the radiating patch and ground plane is shown in Fig 5.12 (a) and (b). From Fig 5.12 (a) it is understood that the current distribution on the radiating patch shows a variation slightly greater than one half wavelength at resonant frequency. It is observed from Fig 5.12 (b) that there is a strong coupling of current between the meanders of the radiating patch and ground patch and hence the ground plane dimensions also contribute to the effective length of the antenna. Since the variation in the surface current distribution along the radiating patch and ground patch are slightly greater than half wavelength at resonant frequency, the effective length of the patch is assumed approximately equal to half wavelength.

(a)

(b)
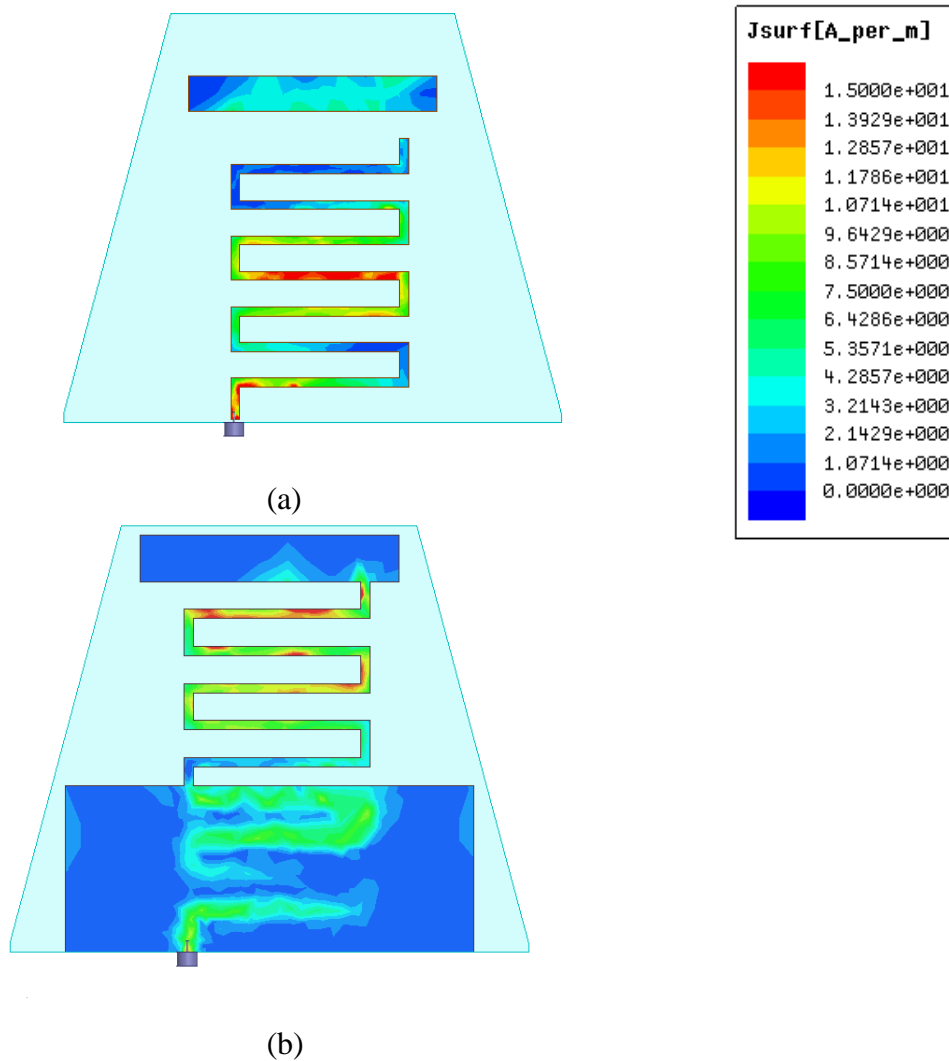
Fig 5.12. Simulated Current distribution on (a) radiating patch (b) ground patch

5.4.2 Parametric Study

To identify the factors affecting the resonant frequency of meandered top loaded printed monopole antenna, variation studies were carried out for all its dimensions.

a) Effect of meander line structure

To investigate on the effect of meander lines of radiating patch on antenna resonant frequency, a conventional printed meander line monopole antenna (Fig 5.13) was studied. The horizontal length of meander line segment is W_2 and vertical length of meander line segment is L_1 and the width of the meander line is W_1. N denotes the number of turns and total length of the monopole is denoted by $L = N \times L_1$.
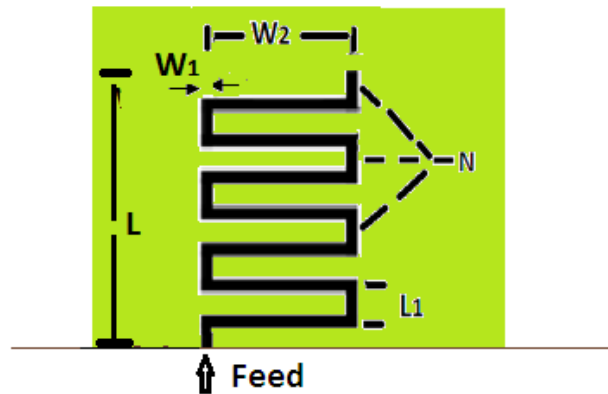
Fig 5.13. Structure of meander line antenna

The variation of frequency with the main factors of meander line; number of turns N and width of horizontal segment W_2; on the antenna resonant frequency are plotted in Fig 5.14 (a-b). It can be inferred from the figures that the effective length of meander line structure is more affected by W_2, and number of turns N.
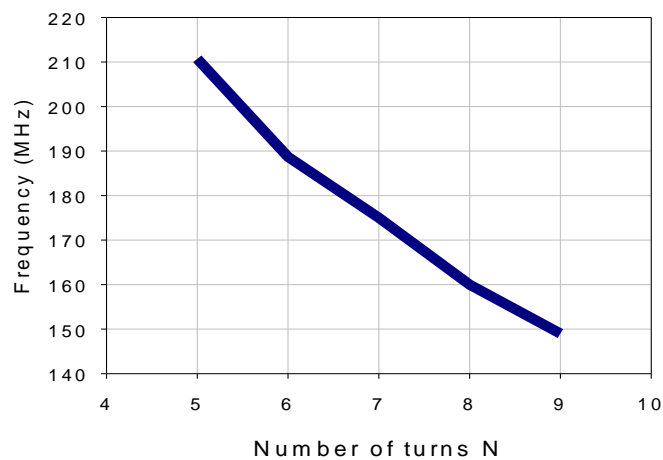
Fig 5.14 (a) Variation of frequency of meander line antenna with number of turns N ($W_2 = 10$cm)
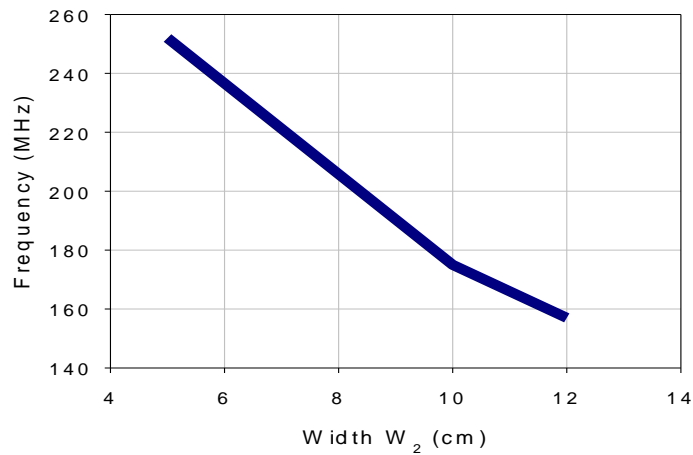
Fig 5.14 (b) Variation of frequency with length of the horizontal segment of meander line (N= 7)

From Fig 5.14 (a-b) it was inferred that the resonant frequency of meandered top loaded printed monopole antenna is greatly influenced by the meander line employed in the radiating patch. The resonant frequency is further reduced by the other structures employed in the antenna- top loading on radiating patch and ground plane, meander line employed in ground plane and the dimensions of rectangular partial ground plane. The meander line employed in the ground plane mainly serves to improve impedance matching and its contribution towards resonant frequency is less.

Parametric study was conducted to study the effect of the dimensions other than the meander lines of the RL loaded meandered top loaded printed monopole antenna on resonant frequency. The methodology followed in parametric study is to vary one parameter over a range keeping all other parameters fixed.

b) Effect of dielectric constant

The variation in resonant frequency with dielectric constant is shown in Fig 5.15 (a). It can be observed that the effect of dielectric constant on resonant frequency is very less and is by a factor closer to one.
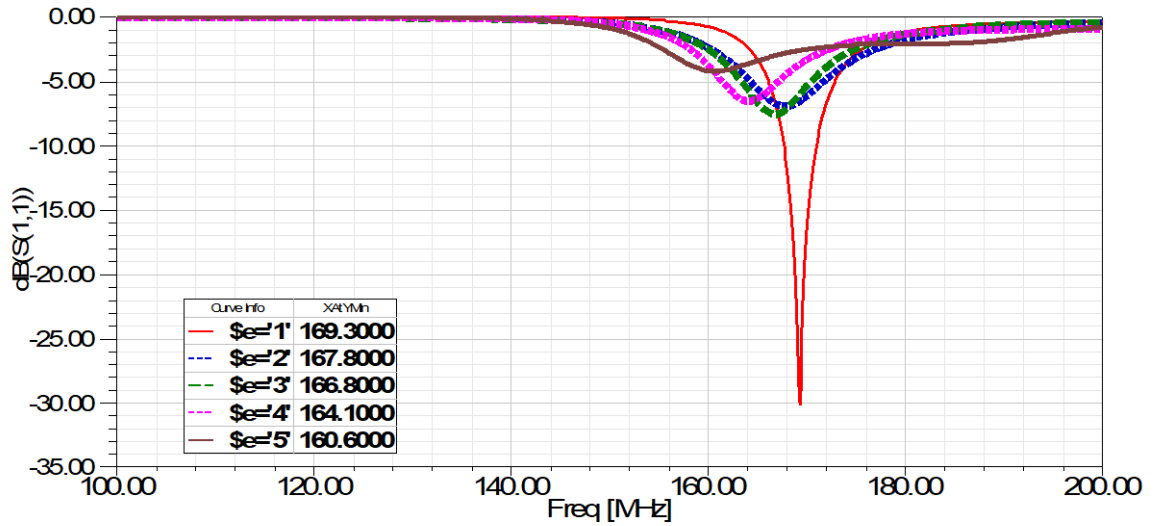
Fig 5.15(a) Variation of frequency with dielectric constant

c) Effect of radiating patch dimensions

The variation in resonant frequency with radiating patch dimensions is studied by varying the dimension L_g from 0.5cm to 2cm; L_3 from 0.5cm to 2.5cm; W_3 from 4cm to 16cm.

The variation in resonant frequency with patch dimensions L_g, L_3, and W_3 are plotted in Figures (Fig 5.15(b-d)).
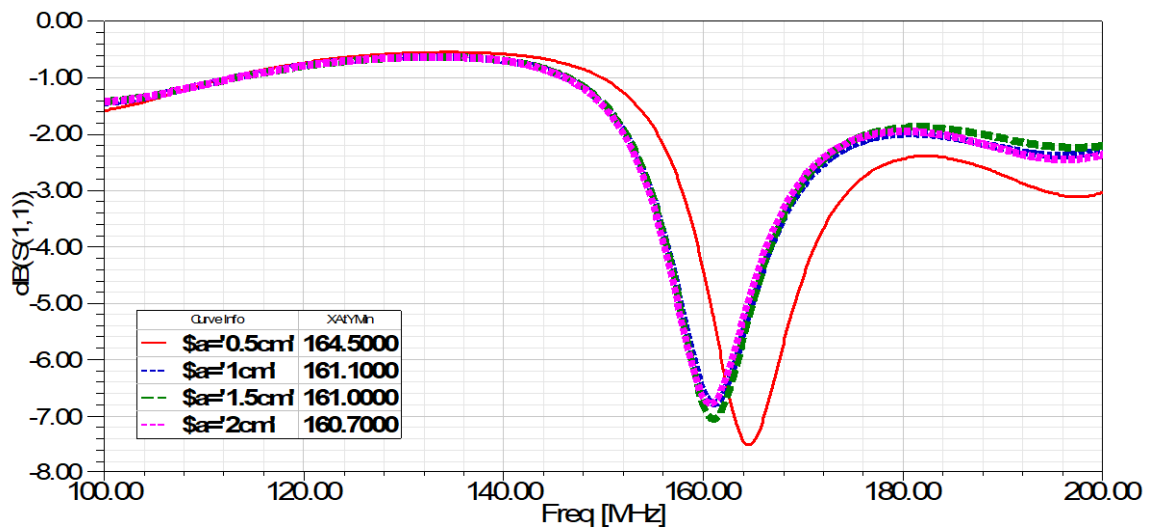
Fig 5.15 (b) Variation in frequency with L_g
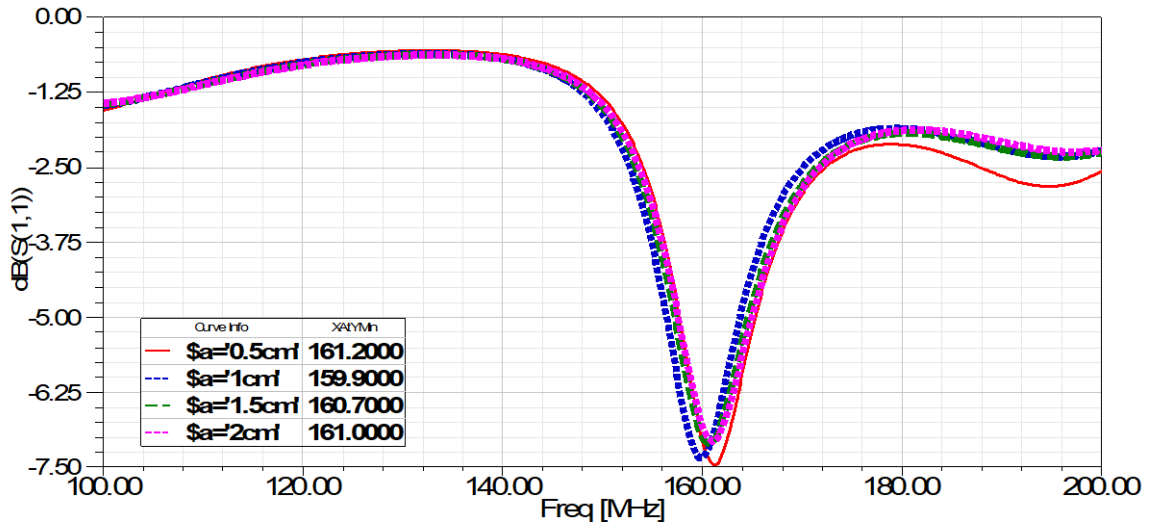
Fig 5.15 (c) Variation in frequency with L_3
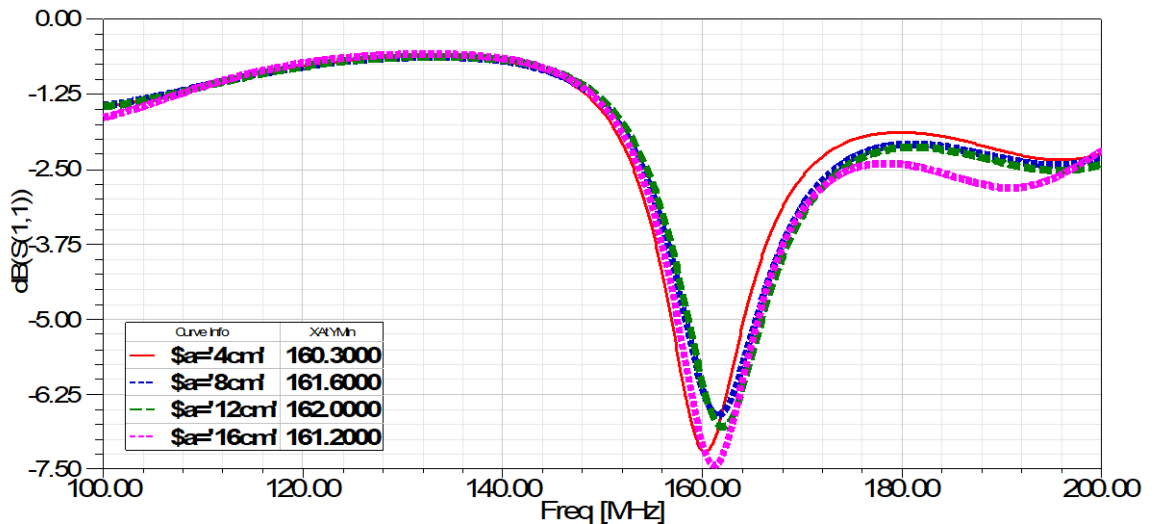
Fig 5.15 (d) Variation of frequency with W_3

d) Effect of ground plane dimensions

The effect of L_4 on resonant frequency is studied by varying it from 2cm to 8cm. The variation in frequency with W_4 is analyzed by varying it from 5cm to 11cm, symmetrically to both sides from the center. Frequency variation with L_5 is studied by varying it from 0.5cm to 2.5cm and W_5 is studied by varying it from 3cm to 15cm. The variation in frequency with dimensions L_4, W_4, L_5, and W_5 are plotted in Fig 5.15 (e-h)
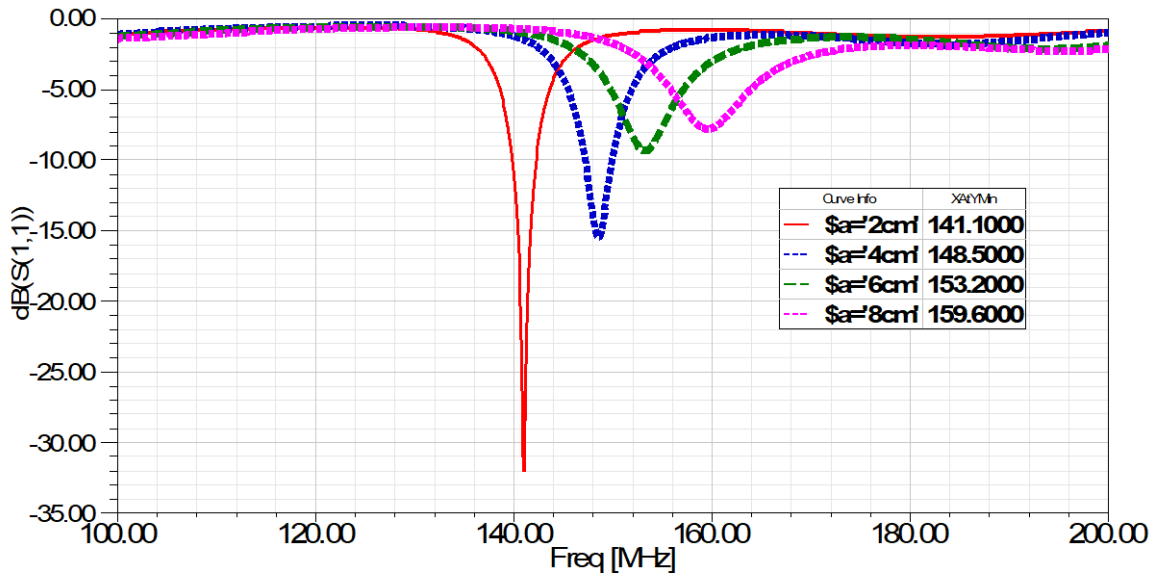
Fig 5.15 (e) Variation in frequency with L_4
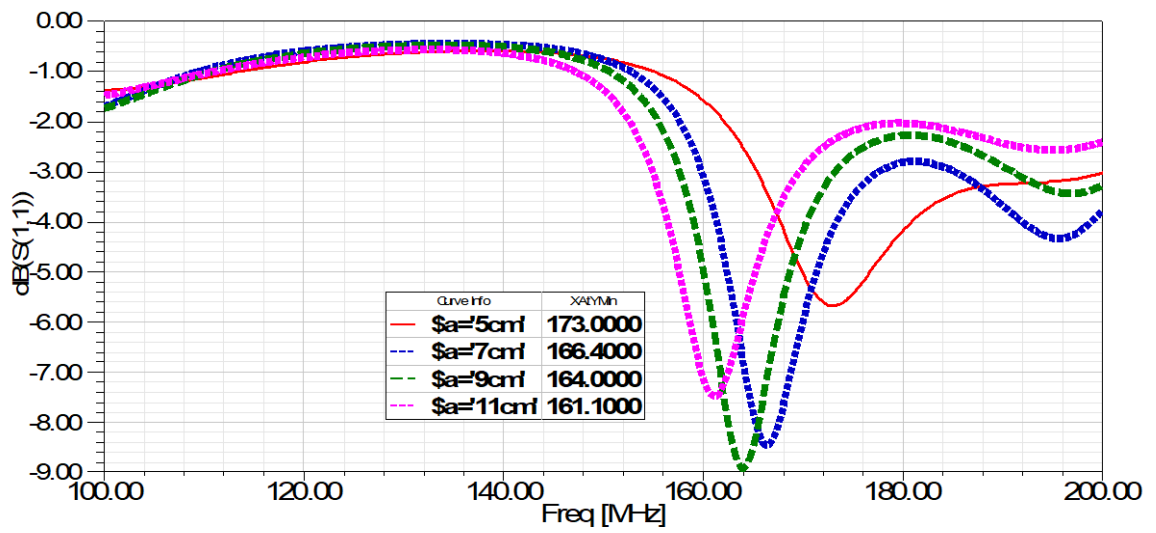
Fig 5.15 (f) Variation in frequency with W_4
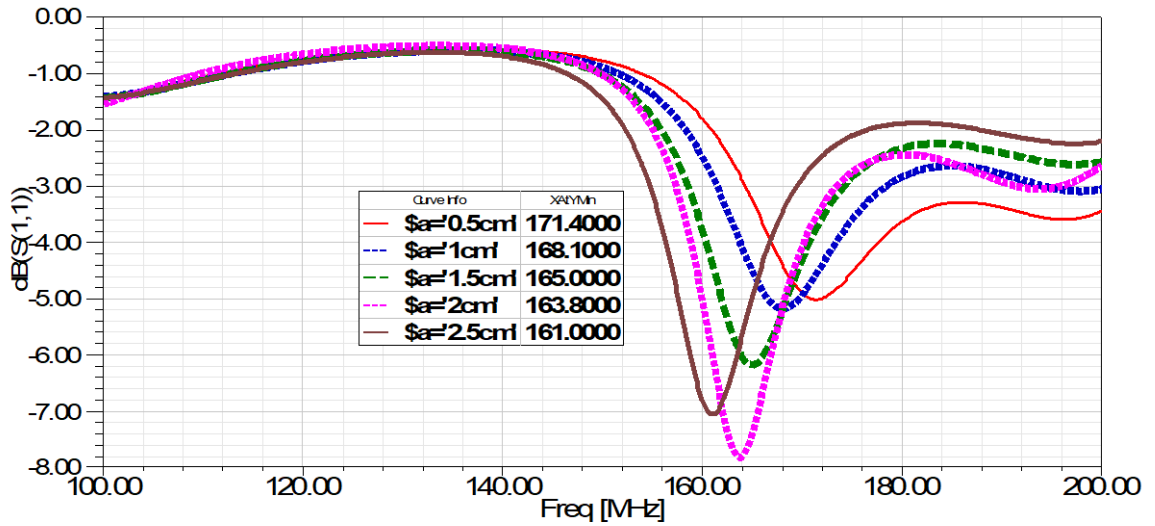
Fig 5.15 (g) Variation in frequency with L$_5$
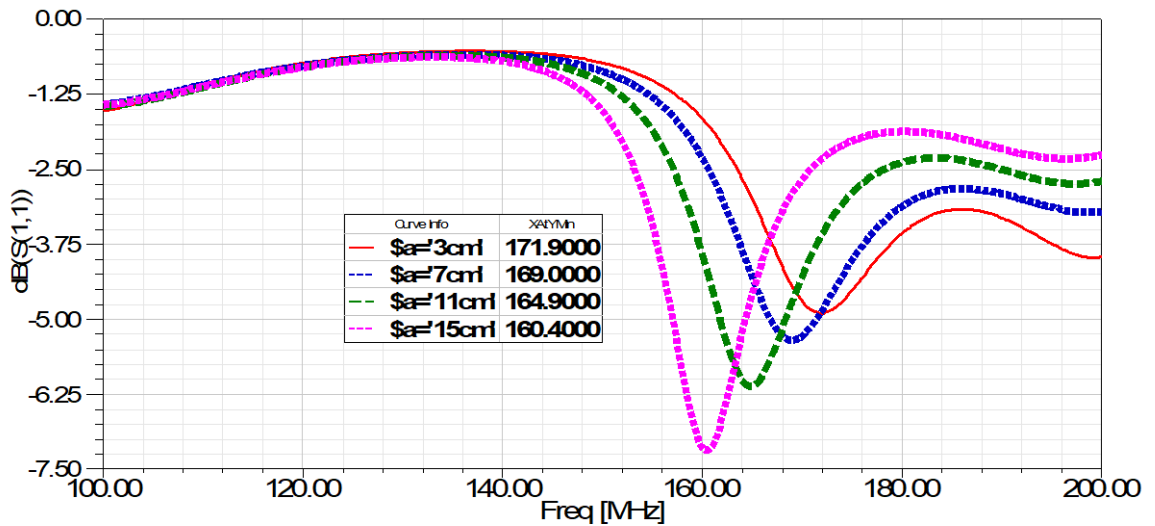
Fig 5.15 (h) Variation in frequency with W$_5$

Fig 5.15 Variation in frequency with different dimensional parameters of meandered top loaded printed monopole antenna

From the above figures, it is evident that W$_4$, L$_5$, and W$_5$ contribute significantly towards frequency reduction. The increase in dimensions L$_4$ increases the resonant frequency. It is obvious from the above figures that the effect of patch dimensions L$_g$ W$_3$, and L$_3$ on determining the resonant frequency is less compared to other dimensional parameters.

5.4.3. Resonant Frequency Calculation

To derive the resonant frequency of RL loaded meandered toploaded printed monopole antenna, a two-step procedure was adopted. First the relation between the resonant frequency and geometrical parameters of meander line structure alone (Fig 5.13) is derived. Then the relation for resonant frequency calculation of RL loaded meandered top loaded printed monopole antenna is derived by incorporating the effect of meander line and other dimensional parameters of the antenna.

It was inferred from the parametric study of meander line monopole structure that the effective electrical length of the meander antenna depends on number of turns N, width of horizontal segment W_2, width of the meander line W_1, and the total length of the antenna $L = N \times L_1$. From the parametric studies, the equation for calculating the effective length due to the basic meander line structure (L_M) in terms of geometrical parameters is derived as

$$L_M = 0.5 + 0.017W_2 + 0.05N + 0.004L + 0.045W_1 + 0.02NW_2 \text{ ... (9)}$$

Since the contribution of meander line employed in the radiating patch has significant effect on the resonant frequency of RL loaded meandered top loaded printed monopole antenna, equation (9) is used in the derivation of the design equation of this antenna. The notation L_M is used to denote the effective length due to meander line antenna on radiating patch. Further, it is inferred from the parametric study (Fig 5.15 (a-h)) that the resonant frequency is varied by the dimensions L_4, W_4, L_5, and W_5. It is also varied marginally by dimensions L_3, W_3 and L_g. The resonant frequency of the antenna is also slightly varied by the meander line on the ground patch. The notation L_G is used for denoting the effective length due to the meander line on the ground patch and is calculated from equation (9).

Based on the parametric studies, the effective length of this antenna in terms of geometrical parameters is estimated by the relation

$$L_{eff} = \frac{1}{3}(3L_M + 1.3W_4 + 3.5L_5 + 0.8W_5 - 6L_4 + 0.52L_3 + 0.3\ W_3 + 0.52L_g + 0.001L_G) \quad \text{.......(10)}$$

It is observed from the surface current distribution (Fig 5.12) that the effective electrical length of the antenna corresponds to half wavelength at resonant frequency.

132

As the substrate dielectric constant contributes to the resonant frequency determination by a factor closer to unity, the $\sqrt{\varepsilon_{reff}}$ in equation (4) is replaced by variable k.

Hence equation (4) for resonant frequency of rectangular microstrip antenna is modified as

$$fr = \frac{c}{\lambda} = \frac{c}{2 \times L_{eff} \times k} \quad \dots (11)$$

5.4.4 Comparison between calculated and simulated results

For examining the validity of these conclusions, the antenna was designed for various dimensional values and simulated using HFSS software. In order to establish the influence brought by each parameter, the methodology followed is – varying one parameter over a range keeping all other parameters fixed. The design was simulated for different substrates also- FR4 epoxy (ε_r=4.4), RT Duroid 5870 (ε_r=2.3) and air (ε_r=1.0006) were selected for this purpose. The value of k that corresponds to effective dielectric constant of FR4 is determined as 1.1 and that of RT Duroid is 1.08. The value of k for air is 1.

Table 5.6-5.12 described below shows the comparison between simulated and calculated values for different set of dimensional parameter. From the tabulated results it is obvious that the error is less than 5% for almost all cases. The plots corresponding to the different cases are shown in Fig 5.16-5.22 for comparison.

Table5.6. Variation of frequency with different dimensional values (L_g varied)

(h=0.16cm; L_3=2.5cm; W_3= 14cm; L_4=9cm; W_4=23.2cm; L_5=2cm; W_5=15cm)

L_g (cm)	FR4			RT Duroid 5870			Air		
	Simulated Frequency (MHz)	Calculated Frequency (MHz)	Error (%)	Simulated Frequency (MHz)	Calculated Frequency (MHz)	Error (%)	Simulated Frequency (MHz)	Calculated Frequency (MHz)	Error (%)
0.5	162.3	162.6	0.1	167.2	165.6	0.9	174.9	173.5	0.8
1	161.9	162.4	0.3	166.9	165.4	0.8	173.3	173.3	0.0
1.5	162.4	162.2	0.1	165.9	165.2	0.4	173.1	173.1	0.0
2	162.6	162.1	0.3	165	165.1	0.0	172.6	173	0.2

Table 5.7. Variation of frequency with different dimensional values (L_3 varied)

(h=0.16cm; L_g=1.5cm; W_3= 14cm; L_4=9cm; W_4=23.2cm; L_5=2cm; W_5=15cm)

L_3 (cm)	FR4 Substrate			RT Duroid 5870			Air		
	Simulated Frequency (MHz)	Calculated Frequency (MHz)	Error (%)	Simulated Frequency (MHz)	Calculated Frequency (MHz)	Error (%)	Simulated Frequency (MHz)	Calculated Frequency (MHz)	Error (%)
0.5	161.2	162.4	0.7	166.7	165.2	0.8	174	173.7	0.2
1	162.6	162.3	0.1	165	165.2	0.1	173.1	173.5	0.2
1.5	162.2	162.3	0.0	164.9	165.1	0.1	172.3	173.3	0.5
2	162.7	162.3	0.2	164.8	165.1	0.1	173.1	173.1	0

Table 5.8. Variation of frequency with different dimensional values (W_3 varied)

(h=0.16cm; L_g=1.5cm; L_3= 2.5cm; L_4=9cm; W_4=23.2cm; L_5=2cm; W_5=15cm)

W_3 (cm)	FR4 Substrate			RT Duroid 5870			Air		
	Simulated Frequency (MHz)	Calculated Frequency (MHz)	Error (%)	Simulated Frequency (MHz)	Calculated Frequency (MHz)	Error (%)	Simulated Frequency (MHz)	Calculated Frequency (MHz)	Error (%)
2	158.8	159.8	0.6	164.9	162.7	1.3	169.8	170.45	0.4
4	159	160.2	0.7	165.2	163.1	1.2	170	170.8	0.4
6	160.4	160.5	0.0	165.3	163.5	1.0	170.5	171.2	0.4
8	160.6	160.9	0.1	165.7	163.9	1.0	170.6	171.6	0.5
10	160.8	161.3	0.3	165.3	164.3	0.6	171.1	172	0.5
12	161.6	161.7	0.0	165.5	164.7	0.4	171.5	172.4	0.5
14	162	162.1	0.0	165	165.1	0.0	171.8	172.8	0.5

Table 5.9. Variation of frequency with different dimensional values (L_4 varied)

(h=0.16cm; L_g=1.5cm; L_3= 2.5cm; W_3=14cm; W_4=23.2cm; L_5=2cm; W_5=15cm)

L_4 (cm)	FR4 Substrate			RT Duroid 5870			Air		
	Simulated Frequency (MHz)	Calculated Frequency (MHz)	Error (%)	Simulated Frequency (MHz)	Calculated Frequency (MHz)	Error (%)	Simulated Frequency (MHz)	Calculated Frequency (MHz)	Error (%)
2	141.9	138.9	2.1	143.8	141.5	1.5	146.3	151.9	3.0
4	149.2	144.8	2.9	153.6	147.5	3.9	153.7	158.3	2.8
6	154.3	151.3	1.9	161.1	154.1	4.3	162	165.3	2.1
8	158.5	158.3	0.1	163.6	161.2	1.4	171.7	173.01	0.7

Table 5.10. Variation of frequency with different dimensional values (W$_4$ varied)
(h=0.16cm; L$_g$=1.5cm; L$_3$= 2.5cm; W$_3$=14cm; L$_4$=9cm; L$_5$=2cm; W$_5$=15cm)

W$_4$ (cm)	FR4 substrate			RT Duroid 5870			Air		
	Simulated Frequency (MHz)	Calculated Frequency (MHz)	Error (%)	Simulated Frequency (MHz)	Calculated Frequency (MHz)	Error (%)	Simulated Frequency (MHz)	Calculated Frequency (MHz)	Error (%)
12	174.8	172	1.6	183.6	175.2	4.5	184.3	184.0	0.14
14	173.6	170.1	2	180.5	173.3	3.9	181.1	182.1	0.5
16	171.4	168.3	1.8	178.2	171.4	3.8	183.2	180.2	1.6
18	167.2	166.5	0.4	175.2	169.6	3.1	178.3	178.3	0.0
20	166.4	164.8	0.9	171.6	167.8	2.2	176.5	176.5	0.0
22	163.8	163.1	0.4	168.4	166.1	1.3	174.7	174.7	0.0

Table 5.11. Variation of frequency with different dimensional values (L$_5$ varied)
(h=0.16cm; L$_g$=1.5cm; L$_3$= 2.5cm; W$_3$=14cm; L$_4$=9cm; W$_4$=23.2cm; W$_5$=15cm)

L$_5$ (cm)	FR4 substrate			RT Duroid 5870			Air		
	Simulated Frequency (MHz)	Calculated Frequency (MHz)	Error (%)	Simulated Frequency (MHz)	Calculated Frequency (MHz)	Error (%)	Simulated Frequency (MHz)	Calculated Frequency (MHz)	Error (%)
0.5	168.9	165.5	2	173.2	168.6	2.6	181.7	176.5	2.8
1	168	164.3	2.2	170.2	167.4	1.6	177.5	175.3	1.2
1.5	165.2	163.2	1.2	167.7	166.2	0.8	174.8	174.1	0.4
2	162.4	162.1	1.8	165	165.1	0.0	173.1	173.0	0.0

Table 5.12. Variation of frequency with different dimensional values (W$_5$ varied)
(h=0.16cm; L$_g$=1.5cm; L$_3$= 2.5cm; W$_3$=14cm; L$_4$=9cm; W$_4$=23.2cm; L$_5$=2cm)

W$_5$ (cm)	FR4 substrate			RT Duroid 5870			Air		
	Simulated Frequency (MHz)	Calculated Frequency (MHz)	Error (%)	Simulated Frequency (MHz)	Calculated Frequency (MHz)	Error (%)	Simulated Frequency (MHz)	Calculated Frequency (MHz)	Error (%)
7	171.4	166.3	2.9	173.4	169.4	2.3	182.2	177.9	2.4
9	169	165.2	2.2	171.6	168.3	1.9	179.6	176.8	1.5
11	167.2	164.1	1.8	171.3	167.2	2.3	178.1	175.7	1.3
13	164	163.1	0.5	167.1	166.1	0.5	175.2	174.6	0.3
15	162.4	162.1	0.1	165	165.1	0.0	173.1	173.5	0.2
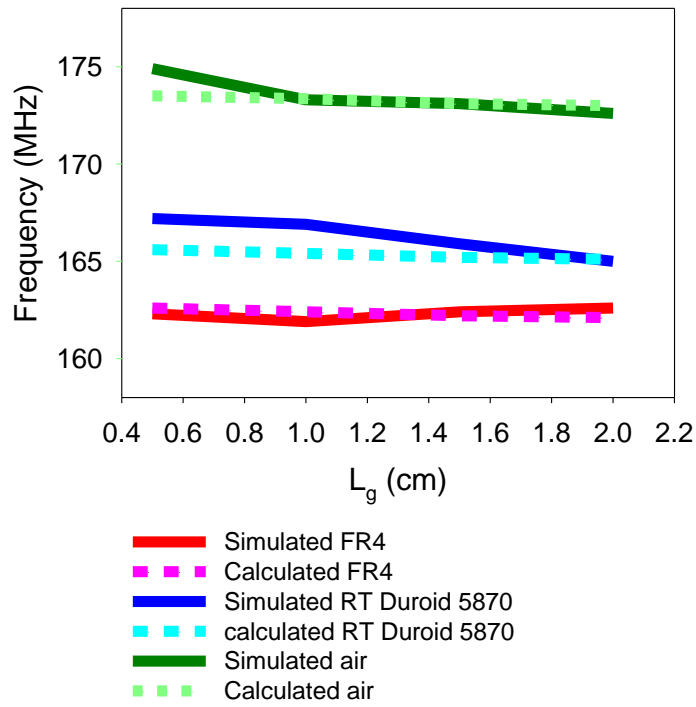
Fig 5.16. Comparison between theoretical and simulated result for various Lg values (h=0.16cm; L_5=2cm; L_3= 2.5cm; W_3=14cm; L_4=9cm; W_4=23.2cm; W_5=15cm)
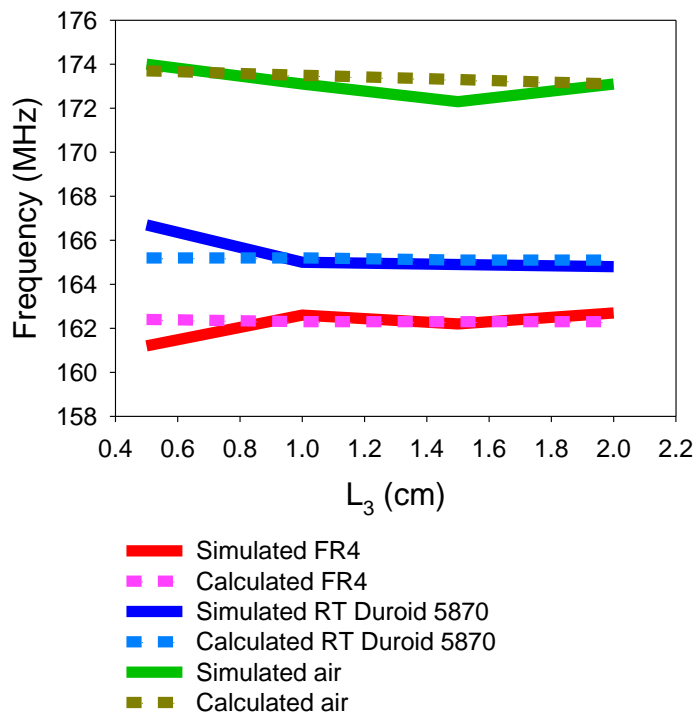
Fig 5.17. Comparison between theoretical and simulated result for various L_3 values (h=0.16cm; L_5=2cm; L_g= 1.5cm; W_3=14cm; L_4=9cm; W_4=23.2cm; W_5=15cm)
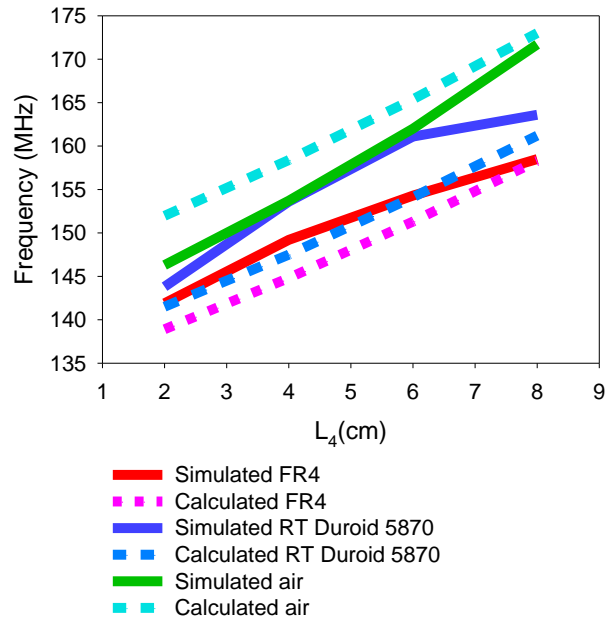
Fig 5.18. Comparison between theoretical and simulated result for various L_4 values (h=0.16cm; L_5=2cm; L_g= 1.5cm; W_3=14cm; L_3=2.5cm; W_4=23.2cm; W_5=15cm)
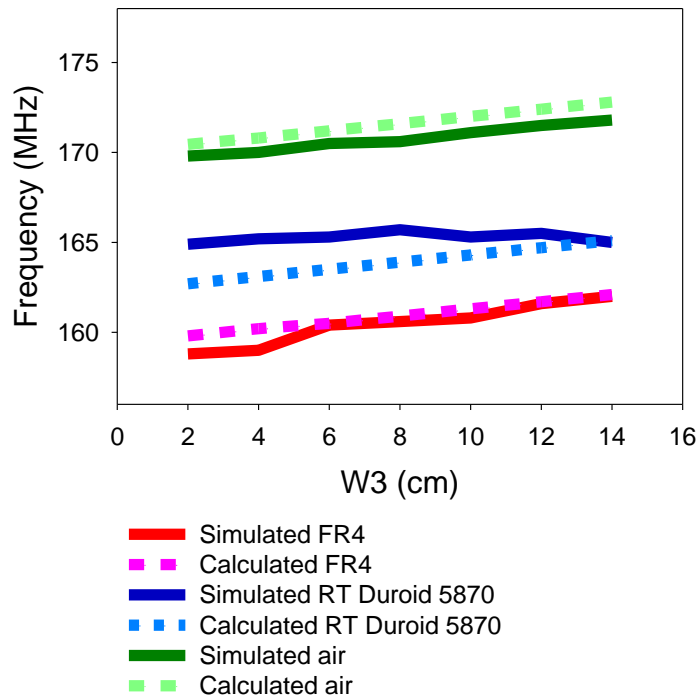
Fig 5.19. Comparison between theoretical and simulated result for various W_3 values (h=0.16cm; L_5=2cm; L_g= 1.5cm; L_3=2.5cm; L_4=9cm; W_4=23.2cm; W_5=15cm)
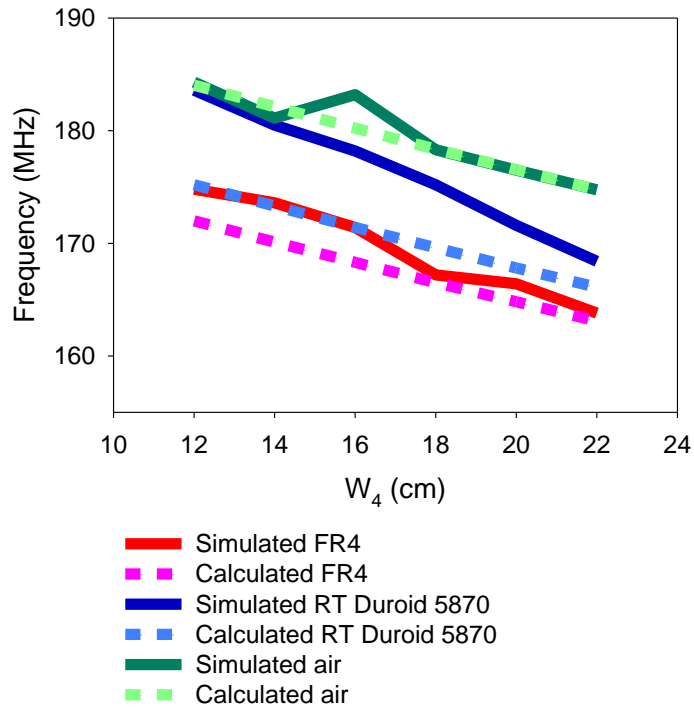
Fig 5.20. Comparison between theoretical and simulated result for various W_4 values (h=0.16cm; L_5=2cm; L_g= 1.5cm; L_3=2.5cm; L_4=9cm; W_3=14cm; W_5=15cm)
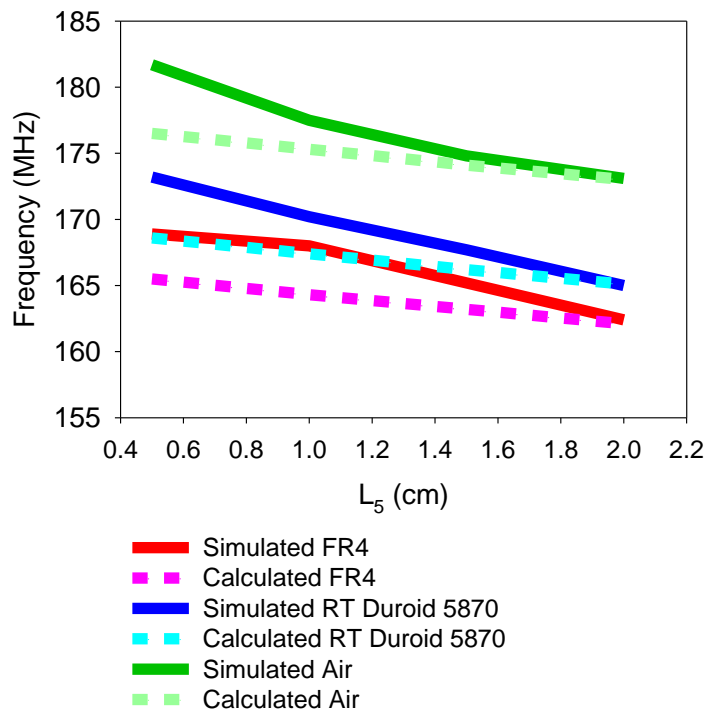
Fig 5.21. Comparison between theoretical and simulated result for various L_5 values (h=0.16cm; W_3=14cmcm; L_g= 1.5cm; L_3=2.5cm; L_4=9cm; W_4=23.2cm; W_5=15cm)
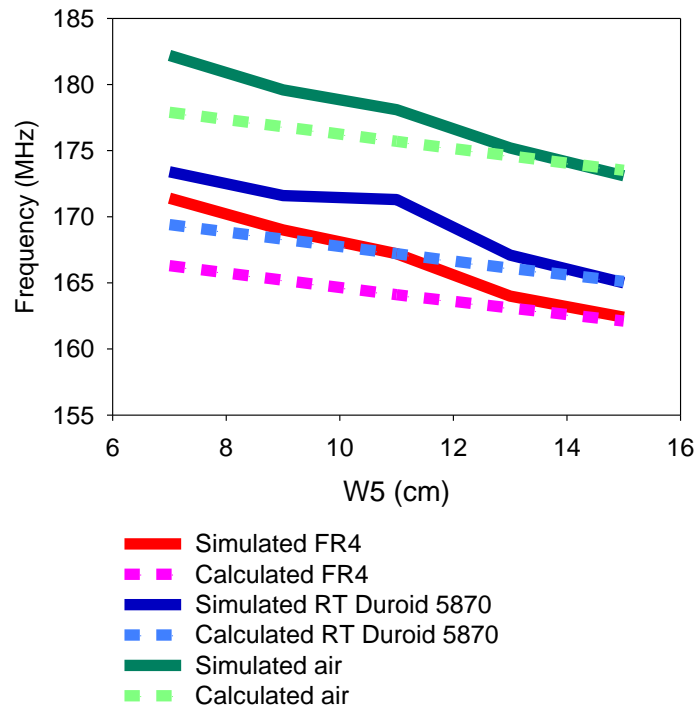
Fig 5.22. Comparison between theoretical and simulated result for various W_5 values (h=0.16cm; L_5=2cm; L_g= 1.5cm; L_3=2.5cm; L_4=9cm; W_4=23.2cm; W_3=14cm)

5.5. CHAPTER SUMMARY

Resonant frequency calculation of two antennas mentioned in chapter 3 and 4 are carried out in this chapter. The equations were validated for various set of dimensions and were compared with the HFSS simulated results. To further check the validity, simulations of this design was carried out for different substrate. The calculated values had good agreement with the simulated results. These simple relationships predict the resonant frequency accurately and it is a fast method for calculating the frequencies.

6. Conclusions

This chapter presents the summary of the inferences drawn from the experimental and theoretical investigations of the antennas- bifolded printed bent monopole antenna and RL loaded meandered toploaded printed monopole antenna developed for ground plane constrained airborne applications. It also highlights the achievements of the research work carried out. A few suggestions for future work in this field are also included.

6.1 INTRODUCTION

The simple planar shape, omnidirectional radiation pattern and wideband characteristics of planar monopole antennas makes them most preferred for airborne communications. As most of airborne communication utilizes HF/VHF band, the physical height of these antennas (conventionally $\lambda/4$ at lowest frequency of operation) are limited by the physical length, width and height of the aircraft. Hence airborne monopole antennas are subject to size reduction techniques for ensuring compactness. Another disadvantage of these antennas is the requirement of large ground plane to mount on, whose inadequacy may result in deteriorated radiation characteristics

To overcome the space constraints on mounting location in airborne platforms for conventional planar monopole antennas, printed monopole antennas are considered. Hence the main aim of the thesis was to design and develop wideband printed monopole antenna in VHF band suitable for mounting on ground plane constrained airborne platforms.

The investigations started with the literature study on the significance of ground plane on planar monopole antennas. Since printed monopole antennas does not require a backing ground plane to mount on, these antennas can be used to overcome the ground plane size constraints of conventional planar monopole antennas. A detailed study was carried out on printed monopole antennas, on its radiation characteristics and different configurations. There are only very few wideband printed monopole antennas reported in VHF band, and it was found that the size of these antennas are quite large for airborne applications. Hence, during this thesis work, emphasis was given to design VHF wideband printed monopole antenna suitable for airborne applications.

Two novel wideband printed monopole antennas were developed and analyzed during the course: Bifolded printed bent monopole antenna and RL loaded meandered top loaded printed monopole antenna.

The design aspects, based on the geometrical parameters of the antenna, were first investigated. The simulation studies were carried out to study the dependence of antenna radiation characteristics on the dimensional parameters. Surface current analysis was carried out to get an insight on the radiation mechanism of antenna. Optimum dimensions of the design were identified using parametric analysis and the

antenna was fabricated on FR4 substrate using photolithographic technique. Antennas were measured for its radiation characteristics using E5071C Vector Network Analyzer in open field.

The dimensions critically determining the resonant frequency were identified using parametric analysis. Based on the inferences from surface current analysis and parametric analysis, simple relations were deduced to design the antenna on any substrate for the desired frequency range of operation. The deduced geometry can act as a precursor to the final design optimized using any of the simulation softwares.

6.2 INFERENCES FROM EXPERIMENTAL AND THEORETICAL INVESTIGATIONS

6.2.1 Inferences from Bifolded printed bent monopole antenna

The bifolded printed bent monopole antenna is derived from the bent monopole antenna. The horizontal arm of the bent monopole antenna is folded twice in order to achieve compactness. The impedance matching of the antenna is achieved by modifying the partial ground plane of the conventional printed monopole antenna into L shape. Wideband characteristics of this antenna was achieved by resistance loading method.

Analysis on the surface current distribution on the radiating patch revealed that the effective length of the patch corresponds to quarter wavelength at fundamental frequency of resonance. The feeble intensity of current distribution on ground plane implies that there is negligible radiation from ground plane.

Parametric analysis of the antenna indicates that the resonant frequency of the antenna was determined by the total length of the arms of the radiating patch and its width. Bandwidth of the antenna is effected by the load resistance, width of the radiating patch and width of vertical portion of L shaped ground. The variation of frequency with respect to the substrate dielectric constant was lesser compared to microstrip antennas and found to be in a factor closer to unity. A decrease in bandwidth and increase in gain was observed with increase in substrate thickness.

As airborne monopole antennas are mounted on the skin of the platform, the effect of availability of large mounting ground plane for this antennas was also analyzed

using HFSS simulations. The studies reveals that the shift in frequency band due to the large ground plane is very less for this antenna compared to conventional planar monopole antenna. The antenna exhibits omnidirectional radiation pattern with increased null depth and improved gain when mounted on large mounting ground plane.

Measured results shows that the antenna offers a 3:1 VSWR bandwidth of 32%. The radiation pattern of the antenna is omnidirectional in azimuth plane but tilted due to the dominance of current along the horizontal arms of the radiating patch. Measured gain of the antenna varies from -17dBi to -8dBi in the frequency band.

Empirical equation to calculate the resonant frequency of the antenna was derived in terms of its geometrical parameters and is presented in chapter 5. The equation was verified for different substrates and different set of dimensions.

The highlights of this antenna is its wide bandwidth, reduced mounting ground plane and compactness. The antenna achieves a 3:1 VSWR bandwidth of 32%. The height reduction achieved by the antenna is 78% compared to basic printed strip monopole antenna and 73% compared to quarter wavelength planar monopole antenna at lowest frequency of operation. The overall size of this antenna is 0.065λ at lowest frequency of operation.

6.2.2. Inferences from RL loaded meandered top loaded printed monopole antenna

Another compact wideband antenna developed during this course is RL loaded meandered top loaded printed monopole antenna. The antenna was derived from the basic printed strip monopole antenna through step by step iterations, carried out to reduce the height of the antenna. Printed monopole antennas evolved in this iteration process are printed strip monopole antenna (Reference antenna), printed top loaded strip monopole antenna (Antenna 1), Meandered top loaded printed monopole antenna (Antenna 2) and RL loaded meandered top loaded printed monopole antenna (Antenna 3). The design and radiation characteristics of these antennas are discussed in Chapter 4. The main inferences from the studies are summarized below.

By analyzing the design of reference antenna, it was found that the optimum length of radiating strip of printed strip monopole antenna is 0.2λ above the partial

ground plane. The ground plane dimensions play an important role in determining the impedance matching and bandwidth of the antenna. The antenna exhibits a 3:1 VSWR bandwidth of 22% at center frequency. The radiation pattern of the antenna is omnidirectional at azimuth and simulated gain of the antenna is 2dBi. The height of the antenna is 0.32λ at lowest frequency of operation.

From the studies carried out on Antenna 1, it was understood that top loading the strip radiator can significantly reduce the antenna height. By implementing strip and top loading in the ground plane of this antenna, improved impedance matching and increased bandwidth is achieved. The antenna exhibits a 3:1 VSWR bandwidth of 27%. It exhibits omnidirectional radiation pattern in azimuth plane with a gain of 1.8dBi. Compared to printed strip monopole antenna, Antenna 1 achieves 25% height reduction. The height of the top loaded printed strip monopole antenna is 0.23λ at lowest frequency of operation.

Antenna 2 was derived from antenna 1 by meandering the strip employed on the radiating patch and ground plane. Meandering increases the length of surface current path thus increasing the effective length of the antenna. The meandering employed in ground plane in symmetry with that of the radiating patch improves impedance matching. Impedance matching was further improved by implementing a strip above the top loading of the radiating patch. The resultant antenna exhibits a 3:1 VSWR bandwidth of 23%. It exhibits omnidirectional radiation pattern in azimuth plane. The gain of the antenna varies from 0.8 to 1.8dBi within the frequency band. Antenna 2 achieves a height reduction of 43% compared to reference antenna. The overall size of this antenna is 0.18λ at lowest frequency of operation.

Antenna 3 was derived by increasing the length of horizontal arm of meander line of Antenna 2. The reduction of antenna dimension made it difficult to impedance match the antenna over a wide band of frequencies. This is because, at this reduced height, the input impedance undergoes rapid variation with frequency and the impedance at the feed end becomes highly capacitive. The resistive component of the input impedance of this antenna is increased by resistive loading and thus, the antenna achieved wideband characteristics. Adding an inductor parallel to the resistor improved the gain of the antenna at lower frequencies of the band.

From parametric analysis conducted on Antenna 3, it was inferred that the resonant frequency of the antenna is mainly determined by the meander line on the radiating patch. The ground plane top loading and partial ground plane dimensions also contributes to the resonant frequency of the antenna.

As skin of the platform acts as ground plane for these antennas when mounted on aircrafts, the effect of increased mounting ground plane availability was also analyzed. This was done by evaluating the radiation characteristics of this antenna mounted on 1.2m diameter ground plane. The measured results shows that the effect of large mounting ground plane is very little on frequency bandwidth of the antenna. Mounting the antenna on large ground plane improves the gain of the antenna in the lower frequency region. The radiation pattern of the antenna was found to be omnidirectional in azimuth plane at all frequencies within the band. The null depth of the radiation pattern was improved by mounting the antenna on large ground plane.

Empirical equation to calculate the resonant frequency of the antenna was derived in terms of its geometrical parameters and is presented in Chapter 5. The equation is verified for different substrates and for different set of dimensions.

The highlights of this antenna are: wide bandwidth, reduced ground plane, improved gain and compactness. Antenna 3 achieves a 3:1 VSWR bandwidth of 38% and the gain of the antenna varies from -14dBi to -1.5dBi within the band. It achieves a height reduction of 63% compared to conventional quarter wave monopole antenna at lowest frequency of operation and 67% compared to reference antenna. The overall size of the antenna is 0.1λ at lowest frequency of operation.

The key feature of the antennas presented in this thesis is that - the size, shape and radiation characteristics of these antennas are comparable to that of conventional blade monopole antennas used for airborne applications, with the added advantage of requiring minimal ground plane to mount on.

6.3 SUGGESTIONS FOR FUTURE WORK

The following are some of the prospects for future work:

The antennas presented in this thesis have sharp bends. Bandwidth enhancement of antennas by curving the bends of the radiator has been reported in literature. Research may be carried out to study the effect of curving the edges on the radiation characteristics of the antenna.

The resistance loading implemented in the antennas mentioned in this thesis for achieving the wideband characteristics reduces the gain of the antenna. Loading these antennas with a high permittivity superstrate layer for increasing its gain may be addressed in future.

The bifolded printed bent monopole antenna presented in this thesis radiates a tilted beam. The dimensions of ground plane of printed monopole antenna has a significant role in determining the radiation pattern of the antenna. Hence, investigations may be carried out in future to improve the radiation pattern by modifying the L shaped ground plane to U shape.

7. References

1. Dale Stacey (February 2008) Aeronautical Radio Communication Systems and Networks, Wiley.

2. V.C. Misra (2009) Recent Trends in Antennas for Electronic Warfare Applications DRDO Science Spectrum, March 2009, pp.114-119.

3. Melvin M. Weiner (2003), Monopole antennas, CRC Press 2003.

4. Balanis, C. A. (1996). Antenna Theory: Analysis and Design. 2nd Edition, New York, NY, USA.

5. Thereza Macnamara (2010) Introduction to Antenna Placement and installation, John Wiley and sons, UK

6. Burnside W.D., Marhefka R.J. (1988) Antennas on Aircraft, Ships, or Any Large, Complex Environment. In: Lo Y.T., Lee S.W. (eds) Antenna Handbook. Springer, Boston, MA

7. Calusdian, James (1998) Radiation Patterns of Antennas Installed On Aircraft, Master's Thesis, Naval Postgraduate School Monterey, California.

8. Hubregt J. Visser (2012) Antenna Theory and Applications, John Wiley & Sons Ltd

9. A.G. P. Boswell, (1997) "Guglielmo Marconi's antenna design," Tenth International Conference on Antennas and Propagation (Conf. Publ. No. 436), Edinburgh, pp. 546-549 vol.1.

10. Raymond Ricard C, Webb Wayne (1949) Radiation Resistances of Loaded Antennas, Journal of Applied Physics, Volume 20, Issue 4, p.328-330

11. R. Schildknecht, (1961) "Helical top-loading of electrically small monopole antennas," 1958 IRE International Convention Record, New York, NY, USA, pp. 86-86.

12. A.Gangi, S. Sensiper and G. Dunn, (1965) "The characteristics of electrically short, umbrella top-loaded antennas," in IEEE Transactions on Antennas and Propagation, vol. 13, no. 6, pp. 864-871

13. J. McVay and A. Hoorfar, (2007) "Miniaturization of top-loaded monopole antennas using Peano-curves," 2007 IEEE Radio and Wireless Symposium, Long Beach, CA, pp. 253-256.

14. C. Harrison,(1963) "Monopole with inductive loading," in IEEE Transactions on Antennas and Propagation, vol. 11, no. 4, pp. 394-400

15. R. K. Mongia, A. Ittipiboon, P. Bhartia and M. Cuhaci, (1993) "Electric-monopole antenna using a dielectric ring resonator," in Electronics Letters, vol. 29, no. 17, pp. 1530-1531.

16. A.Ikram and J. J. Laurin,(2016) Reducing the height of a monopole antenna by using magneto dielectric material, 2016 17th International Symposium on Antenna Technology and Applied Electromagnetics (ANTEM), Montreal, QC, 1-2.

17. Meinke, H and Gundlach, F.W, (1968), Taschenbuch der Hochfrequenztechnik, Springer-Verlag, Berlin, New York, 1968, pp. 531-535.

18. J. A. Evans and M. J. Ammann, (2004) The Effect of Element Width on the Impedance Bandwidth and Mode for the Rectangular Monopole Antenna, URSI International Symposium on Electromagnetic theory, Italy, 23-26 May, 582-584

19. H. Lebbar, M. Himdi and J. P. Daniel, (1994)"Analysis and size reduction of various printed monopoles with different shapes," in Electronics Letters, vol. 30, no. 21, pp. 1725-1726.

20. N. P. Agrawall, G. Kumar and K. P. Ray,(1998) "Wide-band planar monopole antennas," in IEEE Transactions on Antennas and Propagation, vol. 46, no. 2, pp. 294-295.

21. J. A. Evans and M. J. Amunann, (1999) "Planar trapezoidal and pentagonal monopoles with impedance bandwidths in excess of 10:1," IEEE Antennas and

Propagation Society International Symposium. 1999 Digest. Held in conjunction with: USNC/URSI National Radio Science Meeting (Cat. No.99CH37010), Orlando, FL, USA, pp. 1558-1561 vol.3.

22. Seong-YoupSuh, W. L. Stutzman and W. A. Davis, (2004) "A new ultrawideband printed monopole antenna: the planar inverted cone antenna (PICA)," in IEEE Transactions on Antennas and Propagation, vol. 52, no. 5, pp. 1361-1364.

23. J. Zhao, T. Peng, C. c. Chen and J. L. Volakis, (2009) "Low-profile ultra-wideband inverted-hat monopole antenna for 50 MHz-2 GHz operation," in Electronics Letters, vol. 45, no. 3, pp. 142-144.

24. Thomas, K. G. and Lenin, N. (2007), Ultra wideband printed monopole antenna. Microw. Opt. Technol. Lett., 49: 1082–1085. doi:10.1002/mop.22343

25. E. Lee, P. S. Hall and P. Gardner, (1999)"Compact wideband planar monopole antenna," in Electronics Letters, vol. 35, no. 25, pp. 2157-2158.

26. Ray, K. P., Anob, P. V., Kapur, R. and Kumar, G. (2001), Broadband planar rectangular monopole antennas. Microw. Opt. Technol. Lett., 28: 55–59.

27. Z. N. Chen, M. J. Ammann, M. Y. W. Chia and T. S. P. See, (2002) "Annular planar monopole antennas," in IEE Proceedings - Microwaves, Antennas and Propagation, vol. 149, no. 4, pp. 200-203.

28. B. Luadang, C. Phongcharoenpanich and S. Kawdungta,(2012) "A parasitic printed monopole antenna for a VHF mobile communication," 2012 IEEE Asia-Pacific Conference on Antennas and Propagation, Singapore, pp. 245-246.

29. B. A. Arand, R. Shamsaee and B. Yektakhah, (2013)"Design and fabrication of a broadband blade monopole antenna operating in 30 MHz–600 MHz frequency band," 2013 21st Iranian Conference on Electrical Engineering (ICEE), Mashhad, 1-3.

30. S.D.Ahirwar, C.Sairam, T.Khumanthem and C.N.Gaikwad (2006), "Broadband blade antenna covering 20-700 MHz", pp.202-207, Proc. ISM - IEEE 2006, Bangalore, India.

31. S. D. Ahirwar, C. Sairam and A. Kumar,(2009) "Broadband blade monopole antenna covering 100–2000 MHz frequency band," 2009 Applied Electromagnetics Conference (AEMC), Kolkata, pp. 1-4.

32. I. L. Morrow; G. P. Dingley; W. G. Whittow; A. Cooper (2009), "Wideband blade monopole antenna with sleeved coaxial feed," in 2009 Loughborough Antennas & Propagation Conference , vol., no., pp.789-792, 16-17 Nov. 2009

33. L. Scorrano; A. Manna; D. Spaziani; F. Trotta; P. Naglieri; M. Ferrari, (2015) "A novel ultra-wideband UHF low-profile monopole for UAV platforms," in 2015 International Symposium on Antennas and Propagation (ISAP) , vol., no., pp.1-3, 9-12 Nov.

34. Basaery, D., Razavi, S. M., Armaki, S. H. M. and Mehrpour, M. (2015), An ultra low-profile ultra wideband blade shape monopole antenna. Microw. Opt. Technol. Lett., 57: 1695–1699.

35. H. Tahmasbi; H. Aliakbarian, (2016) "Miniaturized printed Giuseppe-Peano fractal monopole blade antenna," in 2016 International Symposium on Electromagnetic Compatibility - EMC EUROPE , vol., no., pp.561-565, 5-9 Sept. 2016

36. Zill-e-Tooba; H. Raza; H. H. Mashhadi; A. Khan, (2016) "Design and fabrication of broadband planar monopole antenna operating in 1.2-6 GHz band," in 2016 13th International Bhurban Conference on Applied Sciences and Technology (IBCAST) , vol., no., pp.718-721, 12-16 Jan. 2016

37. Bandhakavi S. Deepak, Khumanthem Takeshore, Panakala R. Kumar, and Chandana Sairam (2017) Design of a wideband blade monopole antenna in 135-175MHz band, Progress In Electromagnetics Research Letters, Vol. 68, 25-32,

38. A.S. Meier and W. P. Summers,(1949)"Measured Impedance of Vertical Antennas over Finite Ground Planes," in Proceedings of the IRE, vol. 37, no. 6, pp. 609-616.

39. A.Leitner& R. D. Spence, (1950) Effect of a Circular Ground Plane on Antenna Radiation, J. Appl. Phys., Vol. 21, , p. 1001.

40. J. E. Storer, (1951)"The Impedance of an Antenna Over a Large Circular Screen, "J. Appl..Phys., Vol. 22, No. 8, p. 1058.

41. Sang- Bin Rhee (1967) Monopole antenna with a finite ground plane in the presence of an infinite ground, Supplemental technical report, Cooley Electronics Laboratory, the University of Michigan.

42. K. Iizuka,(1968)"An experimental study of a monopole over a grounded hemisphere," in IEEE Transactions on Antennas and Propagation, vol. 16, no. 6, pp. 764-766.

43. M. S. Smith and G. de Prunelé,(1981)"Crosspolarisation for monopole antennas on limited ground planes," in Electronics Letters, vol. 17, no. 18, pp. 653-656.

44. M. Weiner, (1987) "Monopole element at the center of a circular ground plane whose radius is small or comparable to a wavelength," in IEEE Transactions on Antennas and Propagation, vol. 35, no. 5, pp. 488-495, May 1987.

45. S. R. Best,(2006)"A Discussion on Small Antennas Operating with Small Finite Ground Planes," IEEE International Workshop on Antenna Technology Small Antennas and Novel Metamaterials, pp. 152-155.

46. Owais, Magnus Karlsson, and Shaofang Gong (2008) "Circular Monopole Antenna Stability with Regard to Ground Plane Size."International Symposium on Antennas and Propagation, Taipei, Taiwan, 27-30 October, 2008.

47. S. R. Best,(2009)"The Significance of Ground-Plane Size and Antenna Location in Establishing the Performance of Ground-Plane-Dependent Antennas," in IEEE Antennas and Propagation Magazine, vol. 51, no. 6, pp. 29-43.

48. H. Rmili, L. Aberbour and C. Craeye, (2010) "On the Radiation Resistance of a Planar Monopole Antenna with Reduced Groundplane," in IEEE Antennas and Wireless Propagation Letters, vol. 9, no. , pp. 732-736.

49. LusekeloKibona, (2013) Analysis of the Effects of Rectangular Ground Plane on Radiation Pattern of the Monopole Antenna, International Journal of Scientific and Research Publications, Volume 3, Issue 11.

50. G. H. Brown, R. F. Lewis and J. Epstein, (1937)"Ground Systems as a Factor in Antenna Efficiency," in Proceedings of the Institute of Radio Engineers, vol. 25, no. 6, pp. 753-787.

51. Wait, J.R. & Pope, W.A. (1955) Appl. Sci. Res. Vol 4: 177.

52. M. M. Weiner, S. Zamoscianyk and G. J. Burke, (1992)"Radiation efficiency and input impedance of monopole elements with radial-wire ground planes in proximity to earth," in Electronics Letters, vol. 28, no. 16, pp. 1550-1551, 30 July 1992.

53. Al Christman, Roger Radcliff (1990), Elevated monopole antennas: Effect of changes in radiator height and radial length, IEEE TRANSACTIONS ON BROADCASTING, VOL. 36, No. 4, 262-269.

54. Belrose, J.S.,(1997), Vertical monopoles with elevated radials: an up-date, Tenth International conference on antennas and propagation, Edinburg, 14 -17 April 1997.

55. James McLean, Marta Leuvano, and Heinrich Foltz, Reduced-size, folded ground plane for use with low-profile, broadband monopole antennas, Radio and Wireless Conference, 1-4 August 1999.

56. S. Lim, R. L. Rogers and H. Ling, (2005) Ground plane size reduction in monopole antennas for ground wave transmission, IEEE Antennas and Propagation Society International Symposium, 2005, Vol.1B, pp 406-409.

57. J. Michael Johnson and Yahya Rahmat-Samii, (1997) The tab monopole, IEEE Transactions on Antennas and Propagation, Vol. 45, No. 1, 187-188.

58. Kin-Lu Wong and Yi-Fang Lin,(1997) "Stripline-fed printed triangular monopole," in Electronics Letters, vol. 33, no. 17, pp. 1428-1429.

59. T. Dissanayake, K. Esselle and Y. Ge,(2004) "Broadband printed monopole antennas," 2004 10th International Symposium on Antenna Technology and Applied Electromagnetics and URSI Conference, Ottawa, Canada, 2004, pp. 1-3.

60. Choi, S. H., Park, J. K., Kim, S. K. and Park, J. Y. (2004), A new ultra-wideband antenna for UWB applications. Microw. Opt. Technol. Lett., 40: 399–401.

61. Wei Wang, Shun-Shi Zhong and Xian-Ling Liang,(2004) "A broadband CPW-fed arrowlike printed antenna," IEEE Antennas and Propagation Society Symposium, 2004., 2004, pp. 751-754 Vol.1

62. Jianxin Liang, C. C. Chiau, Xiaodong Chen and C. G. Parini,(2005) "Study of a printed circular disc monopole antenna for UWB systems," in IEEE Transactions on Antennas and Propagation, vol. 53, no. 11, pp. 3500-3504

63. L. Lizzi, R. Azaro, G. Oliveri and A. Massa,(2011) "Printed UWB Antenna Operating Over Multiple Mobile Wireless Standards," in IEEE Antennas and Wireless Propagation Letters, vol. 10, no. , pp. 1429-1432.

64. Jeongpyo Kim, Taeyeoul Yoon, Jaemoung Kim and Jaehoon Choi, (2005) "Design of an ultra wide-band printed monopole antenna using FDTD and genetic algorithm," in IEEE Microwave and Wireless Components Letters, vol. 15, no. 6, pp. 395-397.

65. Z. N. Low, J. H. Cheong and C. L. Law, (2005)"Low-cost PCB antenna for UWB applications," in IEEE Antennas and Wireless Propagation Letters, vol. 4, no. , pp. 237-239.

66. O. Ahmed and A. R. Sebak,(2008) "A Printed Monopole Antenna With Two Steps and a Circular Slot for UWB Applications," in IEEE Antennas and Wireless Propagation Letters, vol. 7, no. , pp. 411-413.

67. Z. Liu, H. Deng and X. He, (2008) "A New Band-Notched UWB Printed Monopole Antenna," 2008 Global Symposium on Millimeter Waves, Nanjing, 2008, pp. 291-294.

68. Liang, J., Chiau, C. C., Chen, X. and Parini, C. G. (2005), Printed circular ring monopole antennas. Microw. Opt. Technol. Lett., 45: 372–375.

69. Chang, D.-C., Liu, J.-C. and Liu, M.-Y. (2006), A novel tulip-shaped monopole antenna for UWB applications. Microw. Opt. Technol. Lett., 48: 307–312.

70. V. Shrivastava and Y. Ranga (2008)Ultra wide band CPW-fed printed pentagonal antenna with modified ground plane for UWB applications, IET Conference on Wireless, Mobile and Multimedia Networks, Mumbai, India, 11-12 January 2008 pp. 1 – 2

71. S. Cheng, P. Hallbjorner and A. Rydberg, (2008) "Printed Slot Planar Inverted Cone Antenna for Ultrawideband Applications," in IEEE Antennas and Wireless Propagation Letters, vol. 7, no. , pp. 18-21.

72. N. C. Azenui and H. Y. D. Yang, (2007) "A Printed Crescent Patch Antenna for Ultrawideband Applications," in IEEE Antennas and Wireless Propagation Letters, vol. 6, no. , pp. 113-116, 2007.

73. M. Gopikrishna, D. D. Krishna, C. K. Anandan, P. Mohanan and K. Vasudevan, (2009) "Design of a Compact Semi-Elliptic Monopole Slot Antenna for UWB Systems," in IEEE Transactions on Antennas and Propagation, vol. 57, no. 6, pp. 1834-1837.

74. M. Abdollahvand& G. R. Dadashzadeh, (2009)Compact Double-fed Dual Annular Ring Printed Monopole Antenna for UWB Application Journal of Electromagnetic Waves and Applications Vol. 23 ,Iss. 14-15.

75. J. H. Lu and C. H. Yeh, (2012) "Planar Broadband Arc-Shaped Monopole Antenna for UWB System," in IEEE Transactions on Antennas and Propagation, vol. 60, no. 7, pp. 3091-3095.

76. Gautam, A. K., Chandel, R. and Kr Kanaujia, B. (2013), A CPW-fed hexagonal-shape monopole-like UWB antenna. Microw. Opt. Technol. Lett., 55: 2582–2587.

77. C. Y. Huang and W. C. Hsia, (2005) "Planar elliptical antenna for ultra-wideband communications," in Electronics Letters, vol. 41, no. 6, pp. 296-297, 17 March 2005.

78. R. Azim, M. T. Islam and N. Misran, (2011) "Ground modified double-sided printed compact UWB antenna," in Electronics Letters, vol. 47, no. 1, pp. 9-11, January 6 2011.

79. Liang, X.-L., Zhong, S.-S. and Wang, W. (2006), UWB printed circular monopole antenna. Microw. Opt. Technol. Lett., 48: 1532–1534.

80. C. Hua, Y. Lu and T. Liu, (2016) "Printed UWB heart-shaped monopole antenna with band-notch reconfigurability," 2016 IEEE International Workshop on Electromagnetics: Applications and Student Innovation Competition (iWEM), Nanjing, 2016, pp. 1-3.

81. J. Liu, S. Zhong and K. P. Esselle, (2011) "A Printed Elliptical Monopole Antenna With Modified Feeding Structure for Bandwidth Enhancement," in IEEE Transactions on Antennas and Propagation, vol. 59, no. 2, pp. 667-670, Feb. 2011.

82. Jihak Jung, Wooyoung Choi and Jaehoon Choi, (2005) "A small wideband microstrip-fed monopole antenna," in IEEE Microwave and Wireless Components Letters, vol. 15, no. 10, pp. 703-705.

83. Melo, D. R., Kawakatsu, M. N., Nascimento, D. C. and Dmitriev, V. (2012), A planar monopole UWB antennas with rounded patch and ground plane possessing improved impedance matching. Microw. Opt. Technol. Lett., 54: 335–338.

84. W. C. Liu, C. M. Wu and Y. J. Tseng, (2011) "Parasitically Loaded CPW-Fed Monopole Antenna for Broadband Operation," in IEEE Transactions on Antennas and Propagation, vol. 59, no. 6, pp. 2415-2419, June 2011

85. S. K. Mishra, R. K. Gupta, A. R. Vaidya, and J. Mukherjee, (2011) "Printed fork shaped dual band monopole antenna for bluetooth and UWB applications with 5.5 GHz WLAN band notched characteristics," Progress In Electromagnetics Research C, Vol. 22, 195-210.

86. Shambavi, K. and Alex, Z. C. (2014), Fractal monopole antenna with electromagnetic bandgap structure for UWB applications. Microw. Opt. Technol. Lett., 56: 1872–1874.

87. Tasouji, Nasrin; Nourinia, Javad; Ghobadi, Changiz; Mirzamohammadi, FarnazA (2017) Novel UWB Monopole Antenna with Controllable Band-Notch Characteristics. Applied Computational Electromagnetics Society Journal . Jan2017, Vol. 32 Issue 1, pp68-73.

88. Santos, R. A., &Cerqueira S. Jr., Arismar. (2017). A low-profile and ultra-wideband printed antenna with a 176% bandwidth. Journal of Microwaves, Optoelectronics and Electromagnetic Applications, 16(1), 59-69.

89. J. R. Panda and R. S. Kshetrimayum, (2011) "A printed 2.4 GHz/5.8 GHz dual-band monopole antenna with a protruding stub in the ground plane for WLAN and RFID applications," Progress In Electromagnetics Research, Vol. 117, 425-434.

90. S. Mohammad Ali Nezhad and H. R. Hassani, (2010) "A Novel Triband E-Shaped Printed Monopole Antenna for MIMO Application," in IEEE Antennas and Wireless Propagation Letters, vol. 9, no. , pp. 576-579.

91. Song, Y., Jiao, Y.-C., Zhao, H., Zhang, Z., Weng, Z.-B. and Zhang, F.-S. (2008), Compact printed monopole antenna for multiband WLAN applications. Microw. Opt. Technol. Lett., 50: 365–367.

92. Yen-Liang Kuo and Kin-Lu Wong, (2003) "Printed double-T monopole antenna for 2.4/5.2 GHz dual-band WLAN operations," in IEEE Transactions on Antennas and Propagation, vol. 51, no. 9, pp. 2187-2192.

93. I-Fong Chen and Chia-Mei Peng, (2003) "Microstrip-fed dual-U-shaped printed monopole antenna for dual-band wireless communication applications," in Electronics Letters, vol. 39, no. 13, pp. 955-956.

94. Hua-Ming Chen and Yi-Fang Lin, (2003) "Printed monopole antenna for 2.4/5.2 GHz dual-band operation," IEEE Antennas and Propagation Society International Symposium. Digest. Held in conjunction with: USNC/CNC/URSI North American Radio Sci. Meeting (Cat. No.03CH37450), Columbus, OH, USA, 2003, pp. 60-63 vol.3.

95. Darvish, Masoumeh, and H. Reza Hassani.(2012) "Multiband printed monopole antenna with defected ground plane for GPS/WLAN/WiMAX applications." In Antennas and Propagation (EUCAP), 2012 6th European Conference on, pp. 1-4. IEEE.

96. Sun, X. L., Cheung, S. W. and Yuk, T. I. (2014), Frequency-reconfigurable dual-band monopole antenna for WiMAX wireless devices. Microw. Opt. Technol. Lett., 56: 49–55.

97. Verma, S. and Kumar, P. (2014), Printed inverted-L shaped monopole antenna with Parasitic Inverted-F element for dual band applications. Microw. Opt. Technol. Lett., 56: 1163–1167.

98. R. Q. Lee and Kue Chun, (2008) "Compact miniaturized antenna for 210 MHz RFID," 2008 IEEE Antennas and Propagation Society International Symposium, San Diego, CA, 2008, pp. 1-4.

99. Y. Zhang and I. Glover, Design of an ultrawideband VHF/UHF antenna for partial discharge detection,(2014) 2014 IEEE International Conference on Signal Processing, Communications and Computing (ICSPCC), Guilin, 2014, pp. 487-490.

100. A. Loutridis, M. John and M. J. Ammann, (2015) "Folded meander line antenna for wireless M-Bus in the VHF and UHF bands," in Electronics Letters, vol. 51, no. 15, pp. 1138-1140

101. YunfeiQiang, Wei Wang and Yufan Yao, (2016) "A printed ultra-wideband antenna with C-shaped ground plane for pattern stability," 2016 IEEE International Conference on Microwave and Millimeter Wave Technology (ICMMT), Beijing, 2016, pp. 749-751.

102. King, Ronold, C. Harrison, and D. Denton. (1960) "Transmission-line missile antennas." IRE Transactions on Antennas and Propagation 8, 88-90.

103. Adler, R., and E. Neely.(1974) "The bent monopole antenna." In Antennas and Propagation Society International Symposium, 1974, vol. 12, pp. 185-188.

104. Wong, Kin-Lu, Gwo-Yun Lee, and Tzung-Wern Chiou. (2003) "A low-profile planar monopole antenna for multiband operation of mobile handsets." IEEE Transactions on Antennas and Propagation 51, no. 1 : 121-125

105. Yang, Fan, and Yahya Rahmat-Samii. (2004)"Bent monopole antennas on EBG ground plane with reconfigurable radiation patterns." In Antennas and Propagation Society International Symposium, 2004. IEEE, vol. 2, pp. 1819-1822.

106. Oh, K., and K. Hirasawa. (2004) "A dual-band inverted-L-folded-antenna with a parasitic wire." In Antennas and Propagation Society International Symposium, 2004. IEEE, vol. 3, pp. 3131-3134.

107. Liu, W-C. (2005) "Wideband dual-frequency double inverted-L CPW-fed monopole antenna for WLAN application." IEE Proceedings-Microwaves, Antennas and Propagation 152, no. 6 pp 505-510.

108. Lin, Yu-De, and Pei-Ling Chi.(2005) "Tapered bent folded monopole for dual-band wireless local area network (WLAN) systems." IEEE Antennas and Wireless Propagation Letters 4, no. 1 pp 355-357.

109. L. Aberbour, C. Craeye and D. Vanhoenacker, (2006) "Miniature Bent Folded Planar Monopole Antenna," Loughborough Antennas and Propagation Conference Proceedings, pp. 61-64, April 2006.

110. Choi, H. S., S. H. Kim, K. H. Oh, and J. H. Jang. (2006) "Ultra-compact CPW-fed monopole antenna with double inverted-L strips for dual-band WLAN applications." In Antenna Technology Small Antennas and Novel Metamaterials, 2006 IEEE International Workshop on, pp. 72-75. IEEE, 2006

111. Panda, Jyoti R., and Rakhesh S. Kshetrimayum.(2009) "A printed inverted double L-shaped dual-band monopole antenna for RFID applications." In Applied Electromagnetics Conference (AEMC), 2009, pp. 1-3. IEEE.

112. Kashiwagi, Ippei, Masaki Nishio, Shuichi Obayashi, Hiroki Shoki, and Tasuku Morooka.(2010) "Dual-band Bent-folded-monopole Antenna." In Antennas and Propagation Society International Symposium (APSURSI), 2010 IEEE, pp. 1-4. IEEE.

113. Iigusa, Kyoichi, and Hiroshi Harada. (2012) "Bandwidth Enhancement of bent monopole antenna by closely locating a slotted plate." In Antennas and Propagation Society International Symposium (APSURSI), 2012 IEEE, pp. 1-2. IEEE.

114. Iigusa, Kyoichi, Fumihide Kojima, and Hiroyuki Yano. (2015) "Bandwidth enhancement of a bent planar monopole antenna by ground plate extension." In Antennas and Propagation & USNC/URSI National Radio Science Meeting, 2015 IEEE International Symposium on, pp. 1942-1943. IEEE.

115. Jalil Rashed and Chen-To Tai, (1982)"A new Class of Wire Antennas", IEEE/AP-S Symposium, May 24-28.

116. JalilRashed and Chen-To Tai, (1982) "A new Class of Wire Antennas", IEEE/AP-S Symposium, May 24-28, 1982

117. J. Wong and H. King,(1986) "Height-reduced meander zigzag monopoles with broad-band characteristics," in IEEE Transactions on Antennas and Propagation, vol. 34, no. 5, pp. 716-717.

118. M. Ali, S. S. Stuchly and K. Caputa, (1995) "A wideband dual meander sleeve antenna," IEEE Antennas and Propagation Society International Symposium. 1995 Digest, Newport Beach, CA, USA, 1995, vol.2 pp. 1124-1127

119. Horng-Dean Chen, (2002) "Compact CPW-fed dual-frequency monopole antenna," in Electronics Letters, vol. 38, no. 25, pp. 1622-1624

120. W. C. Liu, (2004) "Broadband dual-frequency meandered CPW-fed monopole antenna," in Electronics Letters, vol. 40, no. 21, pp. 1319-1320.

121. Yun-Ho Lee, Jong-Ho Jung, HosungChoo and Ikmo Park, (2005) "A multiple meander strip monopole antenna for ultra wideband communication," 2005 IEEE Antennas and Propagation Society International Symposium, vol. 3A, pp. 532-535.

122. S. C. Kim, S. H. Lee and Y. S. Kim, (2008) "Multi-band monopole antenna using meander structure for handheld terminals," in Electronics Letters, vol. 44, no. 5, pp. 331-332.

123. R. Sujith, S. Mridula, C. K. Aanandan, K. Vasudevan and P. Mohanan, (2011) "Compact coplanar waveguide fed ground meandered antenna for wireless application," 2011 XXXth URSI General Assembly and Scientific Symposium, Istanbul, pp. 1-4

124. Z. Liang, H. Jiang and Y. Long, (2012) "Simulation and design of multi-band planar meandered monopole antenna for mobile phone application," 2012 International Conference on Microwave and Millimeter Wave Technology (ICMMT), Shenzhen, pp. 1-4

125. M. S. Hashmi and D. Sharma,(2015)"A meandered rectangular monopole antenna for quad-band applications," 2015 IEEE MTT-S International Microwave and RF Conference (IMaRC), Hyderabad, pp. 61-63.

126. E. Seeley, J. Burns and K. Welton, (1958) "Cap-loaded folded antenna," 1958 IRE International Convention Record, New York, NY, USA, pp. 133-138.

127. J. W. Lee, K. K. Kang, Choon-Sik Cho and Jaeheung Kim, (2006) "An enhancement of input impedance bandwidth of circular-disc loaded monopole antenna with horizontal and vertical parasitic strips," 2006 Asia-Pacific Microwave Conference, Yokohama, pp. 1960-1963

128. Li Jian-Ying and GanYeow-Beng, (2006) "Characteristics of broadband top-load open-sleeve monopole," 2006 IEEE Antennas and Propagation Society International Symposium, Albuquerque, NM, pp. 635-638

129. T. Noro and Y. Kazama, (2006) "Low Profile and Wide bandwidth Characteristics of Top Loaded Monopole Antenna with Shorting Post," IEEE International Workshop on Antenna Technology Small Antennas and Novel Metamaterials, 2006., pp. 108-111

130. J. McVay and A. Hoorfar, (2007) "Miniaturization of top-loaded monopole antennas using Peano-curves," 2007 IEEE Radio and Wireless Symposium, Long Beach, CA, pp. 253-256.

131. E. Ghafari and D. N. Aloi, (2012) "Top-loaded UWB monopole antenna for automotive applications," Proceedings of the 2012 IEEE International Symposium on Antennas and Propagation, Chicago, IL, pp. 1-2.

132. L. Akhoondzadeh-Asl, J. Hill, J. J. Laurin and M. Riel, (2013) "Novel Low Profile Wideband Monopole Antenna for Avionics Applications," in IEEE Transactions on Antennas and Propagation, vol. 61, no. 11, pp. 5766-5770.

133. Taeyoung Yang, W. A. Davis and W. L. Stutzman, (2005) "Small, planar, ultra-wideband antennas with top-loading," 2005 IEEE Antennas and Propagation Society International Symposium, vol. 2A, pp. 479-482.

134. 'An Introduction to HFSS: Fundamental principles, concept and Use' (2009) retrieved from http://www.ansys.com/products/electronics/ansys-hfss

135. http://www.keysight.com/en/pdx-x202270-pn-E5071C/ena-vector-network-analyzer

136. John D. Kraus (1988), Antennas Mc. Graw Hill International, second edition.

137. Munson R.E (1974), Conformal microstrip antennas and microstrip phased arrays, IEEE Trans. Antennas Propag, Vol. AP-22, 1974, pp 74-78

138. A Sudhakar (2010) "Circuits and networks analysis and synthesis" Tata McGraw Hill IInd edition

139. M. J. Ammann and M. John, (2005) "Optimum design of the printed strip monopole," in IEEE Antennas and Propagation Magazine, vol. 47, no. 6, pp. 59-61.

140. Kin-Lu Wong and Yi-Fang Lin,(1997) "Stripline-fed printed triangular monopole," in Electronics Letters, vol. 33, no. 17, pp. 1428-1429.

141. Chih-Yu Huang, Jian-Yi Wu, Cheng-Fu Yang and Kin-Lu Wong (1998) Gain Enhanced Compact Broadband Microstrip Antenna, Electronics Letters Vol. 34 No. 2, 138-139

142. Wenquan Cao, Bangning Zhang, Tongbin Yu, and Hongbin Li (2010) A Single-Feed Broadband Circular Polarized Rectangular Microstrip Antenna With Chip-Resistor Loading IEEE Antennas And Wireless Propagation Letters, VOL. 9, 1065-1069

143. Halpern, B & Mittra, R. (1985). Broadband whip antennas for use in HF communication. 763 - 767.

144. Best, S.R. (2005), "The Performance Properties of Electrically Small Resonant Multiple arm Folded Wire Antennas," Antennas and Propagation Magazine, IEEE, vol.47, no.4, pp.13- 27.

145. K.P. Ray, (2008) Design Aspects of Printed Monopole Antennas for Ultra-Wide Band Applications, International Journal of Antennas and Propagation, Volume 2008, Article ID 713858, 8 pages.

146. R.A.Burberry (1992) VHF and UHF Antennas Peter Peregrinus Ltd., London, United Kingdom

147. H. D. Foltz, J. S. McLean and G. Crook,(1998) "Disk-loaded monopoles with parallel strip elements," in IEEE Transactions on Antennas and Propagation, vol. 46, no. 12, pp. 1894-1896.

148. Ju, D. K., T. H. Oh, J. M. Woo, and S. Y. Hong, (2007) "Double rectangular meander line loop monopole antenna for miniaturisation and bandwidth," Electronics Letters, Vol. 43, No. 16, 846–848.

149. Jung, J., H. Lee, and Y. Lim,(2007) "Modified meander line monopole antenna for broadband operation," Electronics Letters, Vol. 43, No. 22.

150. Noguchi, K., M. Mizusawa, T. Yamaguchi, and Y. Okumura, (1997) "Increasing the bandwidth of a meander line antenna consisting of two strips," in IEEE 1997 Digest Antennas and Propagation Society International Symposium, 2198–2201.

151. Jun Fan, Zhenya Lei , YongjunXie, and Mingyuan Man (2014) "Bandwidth Enhancement for Low Frequency Meander Line Antenna" Progress In Electromagnetics Research C, Vol. 51, 169–177.

152. K. P. Ray, P. V. Anob, R. Kapur, and G. Kumar, (2001)"Broadband planar rectangular monopole antennas," Microwave and Optical Technology Letters, vol. 28, no. 1, pp. 55–59.

Compact Collapsible Wideband VHF Monopole Antenna

For collapsible antenna applications, simple wire antennas of narrow bandwidth are commonly used. In this section, a wideband collapsible monopole antenna operating in VHF band is presented. The antenna has a simple structure, consisting of multiple wire elements, bound together in a flat wide strip, and all joined at their base using a conductor. The proposed antenna exhibits 3:1 VSWR bandwidth ($S_{11}<-6dB$) of 25%. The height reduction achieved by the proposed antenna is 20% compared to a conventional quarter wave monopole antenna.

I. INTRODUCTION

Transmitting antennas with a collapsed, compact configuration that could be released or extended to an operational state, when desired can have many applications [A1]. Examples for such applications include emergency locator beacons, communication satellites, sonobuoys etc. In applications like sonobuoy, wire monopole antennas are used for RF link which use sea water as its infinite ground plane. Wire monopoles are narrow bandwidth devices and there is a requirement of wideband transmitting antennas with collapsible property for sonobuoy application.

Several methods are discussed in the literature for increasing the bandwidth of monopole antennas [A2]. Different loading techniques can be used for increasing the bandwidth of wire monopole antennas in cost of efficiency [A3]. The bandwidth of wire monopoles can also be improved by increasing the diameter of the wire or by using a fan of wires, all of equal length connected at their ends [A4]. The thickness of the wire cannot be increased in order to keep the cross sectional area minimum for low wind resistance. Radio amateurs have constructed an antenna by connecting several wires of different length at the ends for achieving a 6 band antenna [A5]. Replacing thick wire by a planar element also results in wide bandwidth performance [A6]. But a planar disk type monopole radiator cannot be used for collapsible antenna requirements. Hence, in this paper, a wideband wire antenna is proposed for sonobuoy application by using a strip of multiple wires, all bound together in a planar configuration and connected at their base using a conductor. The proposed antenna uses no matching circuits and hence noises due to matching circuits can be avoided.

II. ANTENNA DESIGN

Planar monopole radiators have increased bandwidth than the wire monopole antennas of same length due to its increased surface area. Hence to attain a wideband collapsible antenna, a planar configuration was investigated using multiple wires. The length of the proposed monopole antenna is 44cm. The diameter of copper wire is 0.05cm. A parametric analysis was performed for the antenna with length as 44cm and spacing between the copper wire elements as 0.05cm to examine the impact of number of wire elements on the antenna's bandwidth. A comparison table is shown varying the number of wire elements (TABLE A1). It was found to exhibit an increase in bandwidth of antenna at the center frequency f_0, as the number of wire elements increased.

TABLE AI Effect of number of wire elements on bandwidth of antenna

Number of wire elements	3:1 VSWR Bandwidth in MHz at f_0
2	32
4	33
8	35
16	42

Hence, a ribbon cable was selected and the proposed monopole antenna was constructed using 16 elements of insulated copper wire bounded together in a planar configuration. The diameter of each wire element is 0.05cm and the spacing between the elements is 0.05cm. All wire elements are joined at their base using a copper wire and fed at the middle point of the strip by a TNC connector of 50Ω. The antenna was mounted on a λ/4 ground plane for primary investigation. The schematic of the proposed monopole antenna is shown in Fig A1. The dark portion of the figure shows the copper wire elements.
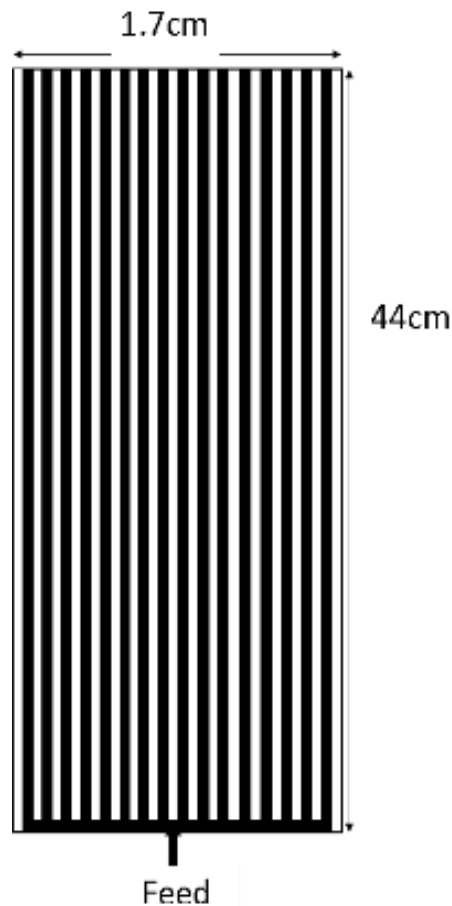
Fig. A1. Schematic of the proposed monopole antenna

III. RESULTS AND ANALYSIS

The proposed wire monopole antenna was measured for its VSWR characteristics using N9342C Agilent handheld spectrum analyzer. The antenna shows a 3:1 VSWR bandwidth of 38MHz in the VHF band. Simulated and measured return loss characteristics are shown in Fig. A2. Simulated gain of the antenna is -1dB to 0.5dB in the increasing band of frequency. The radiation pattern of the antenna is omnidirectional. Simulated radiation patterns at center frequency f_0 MHz are shown in Fig. A3. The $\lambda/4$ wavelength at lowest frequency of operation corresponds to 55cm. The proposed monopole antenna has achieved a height reduction of 20% compared to conventional quarter wave monopole antenna.
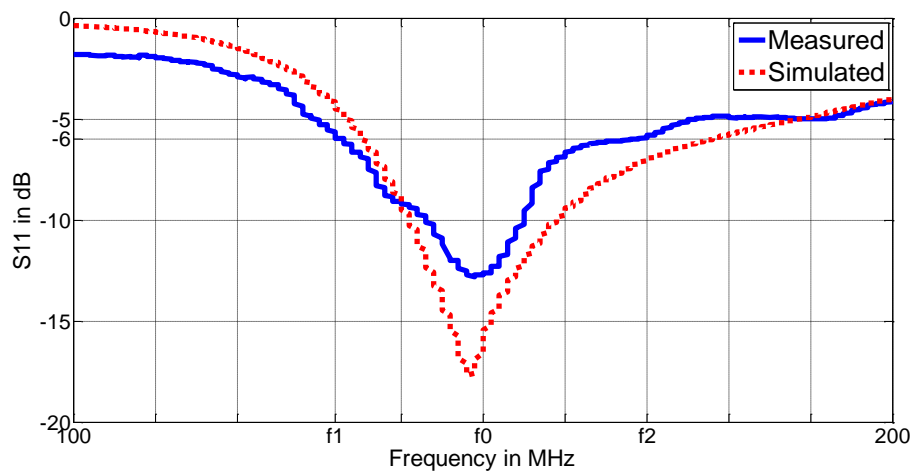
Fig. A2. Simulated and measured return loss characteristics of proposed antenna
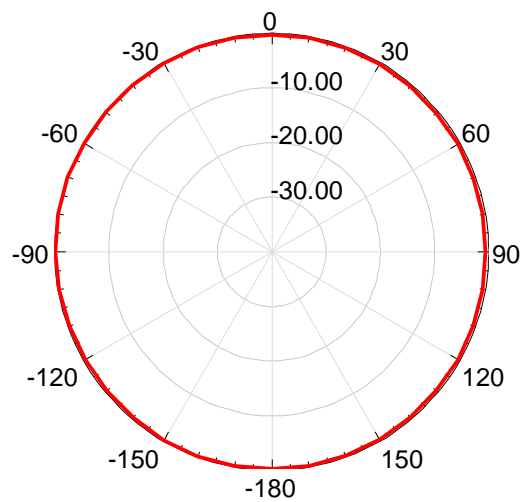
Fig. A3a. Simulated azimuth radiation pattern at f_0 MHz
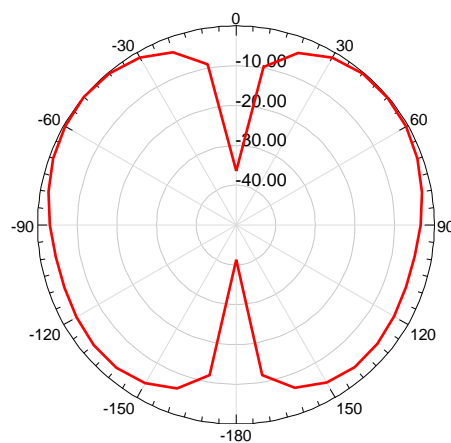
Fig. A3b. Simulated elevation radiation pattern at f_0 MHZ

IV. CONCLUSION

A wideband collapsible VHF antenna is constructed and analyzed. Antenna shows a 3:1 VSWR bandwidth of 25%. Simulation studies show that the radiation pattern of the proposed antenna is omnidirectional and the gain of the antenna varies from -1dB to 0.5dB in the increasing band of frequency. The antenna uses no matching circuit and hence the noise due to matching circuits can be avoided. Hence the proposed antenna could replace wire antenna with narrow bandwidth which are conventionally used in sonobuoy.

REFERENCES

[A1] Edward A. Wojtowicz, Bryn Mawr, "Collapsible antenna assembly.*"* . U.S. Patent 4,593,290A : issued June 3, 1986

[A2] Chuan Peng; Chunlan Lu; Yingsong Zhang, "A UHF wide bandwidth Omni-directional wire antenna based on Genetic-Algorithms", International Conference on Wireless Communications and Signal Processing (WCSP), 2010 pp 1-3, DOI: 10.1109/WCSP.2010.5633450

[A3] Boag, A., A. Boag, E. Michielssen, and R. Mittra, "Design of electrically loaded wire antenna using genetic algorithms," IEEE Transactions on Antennas and Propagation, Vol. 44, No. 5, 687– 695, May 1996

[A4] W. Edson "Broadband trapped multiple-wire antennas", Society International Symposium on Antennas and Propagation, Volume: 19, Pages: 586 – 589, 1981. DOI: 10.1109/APS.1981.1148473

[A5] Raynor Bob, "6 band wire antenna" http://www.eham.net/articles/21407

[A6] Narayan Prasad Agrawall, Girish Kumar, and K. P. Ray "Wide-band planar monopole antennas" IEEE Transactions On Antennas And Propagation. Volume: 46, Issue: 2, pp. 294-295, February 1998, DOI: 10.1109/8.660976

Publications

International Journals:

1. Mary Rani Abraham, Sona O. Kundukulam and C.K. Aanandan, An airborne VHF Printed Monopole Antenna for Platform Constrained Applications, Progress in Electromagnetics Research M, Vol.78 (2019) 103-113.

2. Mary Rani Abraham and Sona O. Kundukulam, "Design and Analysis of a Wideband Printed Monopole VHF Antenna for Airborne Applications" International Journal of Applied Engineering Research (IJAER) Vol.13, No.14, (2018) pp 11428-11435.

3. Mary Rani Abraham and Sona O. Kundukulam, "Empirical Relation for Designing a Bifolded Printed Bent Monopole Antenna" International Journal of Applied Engineering Research (IJAER) Volume 13, Number 12 (2018) pp. 10707-10713

4. Mary Rani Abraham, Sona O. Kundukulam and C.K. Aanandan, Compact Printed Monopole Antenna For Airborne Applications, International Journal of Electronics and Communication Engineering and Technology, 8(2), 2017, pp. 129–135.

International Conferences:

1. Mary Rani Abraham, Abdul Wahab, Sona O. Kundukulam, U.Ganesan "Compact Collapsible Wideband VHF Antenna" International Symposium on Antennas and Propagation (APSYM'16), pp 240-243, 15-17 December 2016.
   (Published in IEEE Xplore)

2. Mary Rani Abraham, Sona O. Kundukulam "Wideband Printed Monopole VHF Antenna" Proceedings of 2015 IEEE International Conference on Computing and Network Communications (CoCoNet'15), pp 845-849, 16-19 December 2015.
   (Published in IEEE Xplore)

3. Mary Rani Abraham, Sona O. Kundukulam, Abdul Wahab, U.Ganesan "Wideband Printed Monopole Antenna for Airborne Applications" Proceedings of International Symposium on Antennas and Propagation (APSYM'14), pp 240-243, 17-19 December 2014.

4. Ansha K. K., Mary Rani Abraham, Sameer Babu T. P. "Demonstration of a Wireless Communication System using SDR Platform", Proceedings of International Symposium on Antennas and Propagation (APSYM'14), 17-19 December 2014.

Monograph

1. Sona O. Kundukulam and Mary Rani Abraham "RF Fundamentals and System Design"- Basics of Sonar System Vol.8, NPOL Training Series, Naval Physical and Oceanographic Laboratory Kochi, January 2015.

Research Report

1. Mary Rani Abraham, Sona O. Kundukulam, Abdul Wahab, U.Ganesan, "Theory and Analysis of Homing System", Research Report, Naval Physical and Oceanographic Laboratory Kochi, January 2015.

Resume

MARY RANI ABRAHAM
Vallikattukuzhiyil
Chittadi P.O, Palakkad,
Kerala, India.
Mob: +91-9961702810
Email: maryraniabraham@gmail.com

Objective:

To pursue research activities in the field of electromagnetics and antennas

Experience:

- Worked as Research Fellow (RF Project) in Naval Physical And Oceanographic Laboratory, Defense Research and Development Organization, Kochi (August 2013 to August 2017)
- Worked as Project Assistant for General Electricals (GE) consultancy project in Department of Electronics, CUSAT (February 2012 to November 2012)

Technical Skills:

- Experience in using HP 8510C Vector Network Analyzer, Spectrum Analyzer, Anechoic chamber etc.
- Experience in Antenna and RF/Microwave circuit design tools like HFSS, CST.
- Hands-on experience in building of antenna prototypes using photolithography and CNC Machine, and antenna experimental work.
- Experience in the design and development of microstrip antennas
- MATLAB
- Documentation- MS Office

Scholarly Works and Services

- Actively engaged in organizing various events and workshops
- Attended various National and International conferences and presented research papers

Projects undertaken:

1. Study on the effect of ground plane on the performance of VHF monopole antenna and analysis on interelement spacing for homing operation.
2. Design and implementation of wideband VHF ribbon antenna
3. Simulation and design of coaxial waveguide

4. Design, fabrication and analysis of U slot patch antenna for dual frequency operation

Education:

❖ Ph. D. in Microwave Electronics
  Cochin University of Science and Technology
  Thesis submitted in October 2018

❖ M.Sc Electronics
  Specialization: Microwave Electronics
  Cochin University of Science and Technology,
  Kerala, India
  Score: CGPA 8.46, First class with Distinction (2011)

❖ B.Sc Physics
  Mercy College, Palakkad.
  Calicut University
  Kerala, India
  Score: 96.8% First class with Distinction (2009)

Awards Obtained:

❖ UGC NET in June 2012

Personal:

Date of Birth   : 17-08-1988
Sex   : Female
Nationality   : Indian
Languages known   : English, Malayalam, Hindi
Marital Status   : Married

References:

1) Dr. Sona O. Kundukulam
   Scientist,
   NPOL, Kochi, Kerala, India
   Ph: 9744857257
   Email: sonalitto@yahoo.com

2) Prof. (Dr.)C.K. Aanandan
   Dept of Electronics
   CUSAT, Cochin
   Ph: 9447667267
   e-mail: aanandan@gmail.com